

**Fast detection of protein-protein interactions with an
automated FRET-based system on the flow cytometer**

Dissertation

zur
Erlangung des Doktorgrades (Dr. rer. nat.)
der
Mathematisch-Naturwissenschaftlichen Fakultät
der
Rheinischen Friedrich-Wilhems-Universität Bonn

vorgelegt von

Kerstin von Kolontaj

aus Bensberg

Bonn, August 2017

Angefertigt mit genehmigung der Mathematisch-
Naturwissenschaftlichen Fakultät der Rheinischen Friedrich-
Wilhelms-Universität Bonn.

1. Gutachter: Prof. Dr. med. Eicke Latz

2. Gutachter: Prof. Dr. rer. nat. Joachim L. Schultze

Tag der mündlichen Prüfung: 01.03.2018

Erscheinungsjahr: 2018

Ein Teil der vorgelegten Arbeit wurde in folgender Originalpublikation veröffentlicht:

von Kolontaj, K., Horvath, G. L., Latz, E. & Büscher, M. Automated nanoscale flow cytometry for assessing protein-protein interactions. *Cytometry A* **89, 835-843, doi:10.1002/cyto.a.22937 (2016)**

Table of contents

Restriction note	X
List of figures	XI
List of Tables.....	XII
List of Formula.....	XII
Abbreviations	XIII
1. Zusammenfassung	1
1. Summary	3
2. Introduction	2
2.1 FRET	2
2.2 FRET Efficiency calculation	3
2.3 The human immune system	6
2.4 T cells and T cell activation	7
2.4.1 Structural rearrangements in the IS	9
2.4.2 CD3 clustering immunodeficiencies.....	11
2.4.3 Lipid rafts.....	11
2.4.4 <i>Staphylococcal</i> enterotoxin B	13
2.5 Immune checkpoint inhibition	13
2.5.1 PD-1 and CD3 colocalization	14
2.5.1 Pharmaceutical use immune checkpoint inhibition modulators.....	15
2.6 Flow cytometry	16
2.6.1 Fluorochromes	17
2.6.2 Express mode and post processing parser	18
2.7 Objectives of the study	18
3. Material.....	20
3.1 Cells.....	20
3.2 Instruments.....	20
3.3 Reagents	20
3.4 Antibodies and antibody conjugates	22
3.5 Consumables, others	22

3.6 Statistical Analysis.....	23
3.7 Software.....	23
4. Methods.....	24
4.1 Cell isolation and cultivation	24
4.1.1 PBMC isolation	24
4.1.2 T cell isolation	25
4.1.3 Freezing and thawing of cells.....	25
4.1.4 MDA-MB-231 cultivation	25
4.2 T cell activation and SEB blocking.....	26
4.2.1 Activation protocol for T cells with SEB.....	26
4.2.2 Activation protocol for PBMC with TransAct Kit.....	26
4.2.3 Cytokine secretion assay.....	26
4.2.4 Calcium influx measurements.....	27
4.3 Fluorochrome conjugation	27
4.4 Staining protocols	28
4.5 Lipid raft integrity manipulation.....	28
4.6 Confocal laser scanning microscopy and sample preparation.....	29
4.6.1 Colocalization analysis at the confocal microscope	29
4.7 Flow cytometry.....	30
4.7.1 Gating strategy.....	31
4.8. The FRET Express Mode workflow	32
4.8.1 Import function	34
4.8.2 Default settings	34
4.8.3 Automatic gating.....	35
4.8.4 FRET calculation	36
4.8.5 Acquisition page.....	36
4.8.6 Analysis pages	37
4.8.7 The FRET efficiency histogram.....	38
4.8.8 FRET Post Processing Parser	38
4.9 Validation of the FRET Express Mode.....	39

5. Results.....	41
5.1 Validation of the FRET program with FRET calibration beads.....	41
5.2. CD3-CD4 interaction	42
5.2.1 CD3-CD4 FRET	42
5.2.2 CD3-CD4 CLSM colocalization and correlation	43
5.3. CD3 homoclustering	46
5.3.1 CD3 homoclustering FRET.....	46
5.3.2 Cytokine secretion	47
5.3.3 Calcium Influx versus FRET efficiency as activation marker	48
5.3.4 CD3 clustering as diagnostic tool for immunodeficiencies.....	48
5.3.5 Lipid raft disruption.....	49
5.3.6 Long term dynamic rearrangement of the CD3 coreceptor	52
5.4 Immune checkpoint inhibition	55
5.4.1 PD-1 expression on T cells	55
5.4.2 PD-L1 and PD-L2 expression on antigen presenting tumor cell lines.....	56
5.4.3 T cell isolation and its effect on FRET efficiency.....	57
5.4.4 PD-1 CD3 FRET and PD-L blocking.....	58
5.4.5 Impaired signaling on T cell lines	59
5.4.6 Downscale of the PD-1 CD3 FRET assay for a screening approach	60
6. Discussion.....	63
6.1 FRET analysis program validation.....	63
6.2 CD3 and CD4 interaction	63
6.2.1 Colocalization on the confocal laser scanning microscope	64
6.3 CD3 homoclustering FRET.....	65
6.3.1 CD3 homoclustering versus T cell activation measurements.....	65
6.3.2 CD3 clustering as a diagnostic marker	66
6.3.3 Lipid raft manipulation.....	67
6.3.4 CD3 homoclustering and long-term dynamic rearrangements.....	68
6.4 Immune checkpoint inhibition	70

6.4.1 PD-1 CD3 FRET and isolated T cells.....	70
6.4.2 PD-1 CD3 FRET and PD-L blocking.....	71
6.4.3 Downscale of the PD-1 CD3 FRET for screening purposes	73
6.5 Conclusions.....	75
7. Acknowledgements.....	76
8. References	77
9. Appendix	86
9.1 The FRET Express Mode Script	86
9.2 The FRET Express Mode Post Paser Script	121

Restriction note

I declare that I am the sole author of this submitted dissertation and that I did not make use of any sources or help apart from those specifically referred to. Experimental data or material collected from or produced by other persons is made easily identifiable. I also declare that I did not apply for permission to enter the examination procedure at another institution and that the dissertation is neither presented to any other faculty, nor used in its current or any other form in another examination.

.....

Place, Date

.....

Kerstin von Kolontaj

List of figures

Figure 1: Emission spectra in FRET.....	4
Figure 2: Activation of T helper cells.....	9
Figure 3: Structural rearrangements in the immunological synapse.....	10
Figure 4: TCR and CD3 receptor organization on lipid rafts in the immunological synapse....	12
Figure 5: PD-1 colocalizes with the CD3 coreceptor in a ligand-dependent manner.....	15
Figure 6: Energy states of an electron.....	17
Figure 7: Gating strategy.	32
Figure 8: Work flow of the automatic FRET calculation program.....	33
Figure 9: The FRET Express Mode Program.	38
Figure 10: Workflow of the FRET Post Processing Parser.	39
Figure 11: Validation of the FRET Express Mode program..	40
Figure 12: Increasing amount of acceptor to donor fluorescent molecule ratios.....	41
Figure 13: Validation of the FRET Express Mode using the Pearson correlation.....	42
Figure 14: FRET Efficiency for CD3 and CD4 coreceptor clustering	43
Figure 15: Comparison between the colocalization coefficient.	44
Figure 16: Confocal images of CD3-FITC (green) and CD4-APC (red).....	44
Figure 17: Colocalization controls.	45
Figure 18: T cell inhibition by SEB superantigen blocking antibody.	46
Figure 19: Cytokine secretion of activated T cells.....	47
Figure 20: Time course measurement of FRET efficiency	48
Figure 21: Detection of different immunodeficiencies in patients using FRET	49
Figure 22: Mean fluorescence intensity of VioBlue, FITC and VioGreen	50
Figure 23: FRET efficiency after T cell stimulation via SEB and bCD or cholesterol treatment	51
Figure 24: FRET efficiency after 0-3h treatment of T cells.....	51
Figure 25: Long-term changes in FRET efficiency.....	53
Figure 26: PD-1 expression on T cells after SEB stimulation.....	55
Figure 27: PD-L1 and PD-L2 expression on different tumor cell lines..	56
Figure 28: FRET efficiency for CD3 and PD-1 clustering.....	57
Figure 29: Blocking of PD-L1 and PD-L2	58
Figure 30: FRET efficiency for the CD3-PD-1 interaction on Jurkat cells	59

Figure 31: FRET efficiency for CD3-PD-1 interaction on HuT-78 cells.....	60
Figure 32: FRET efficiency for CD3 and PD-1 clustering in the downscaled screening approach.....	61
Figure 33: Confocal analysis of CD3 and PD-1 colocalization.	62
Figure 34: Model for dynamic rearrangement of the CD3 coreceptor on lipid rafts	69

List of Tables

Table 1: Optical configuration of the MACSQuant VYB.	30
Table 2: Optical configuration of the MACSQuant Analyzer 10.....	31

List of Formula

Equation 1: Förster radius	2
Equation 2: FRET Efficiency	3
Equation 3: Measured intensities for donor, acceptor and FRET and the contributions from other intensities.	4
Equation 4: Spectral correction factors for FRET donors and acceptors.	5
Equation 5: Scaling factor alpha.....	5
Equation 6: Equation for A	5
Equation 7: Simplified equation for A.....	6
Equation 8: Equation for the FRET efficiency as sensitized emission signal.....	6

Abbreviations

%	per cent
°C	degree Celsius
µg	microgram
µl	microliter
µm	micrometer
A	acceptor
APC (cell)	antigen presenting cell
APC (dye)	allophycocyanin
BSA	bovine serum albumin
Ca ²⁺	calcium ions
CD	cluster of differentiation
CFP	cyan fluorescent protein
Cl ⁻	chloride
CRISPR	clustered regularly interspaced short palindromic repeats
CSV	comma separated value
Cy	cyanine
D	donor
DAG	diacylglycerol
E	FRET efficiency
e.g.	exempli gratia
EDTA	ethylenediaminetetraacetic acid
etc.	et cetera
F	FRET
FCM	flow cytometer
FDA	Food and Drug Administration
FITC	fluoresceinisoithiocyanat
FRET	Förster resonance energy transfer
FSC	forward scatter
F _x	background-corrected intensity

Fyn	fibroblast yes-related non-receptor kinase
g	relative centrifugal force due to gravity
GTP	guanosine-5'-triphosphate
h	hours
I	Intensity
ICAM1	intercellular Adhesion Molecule 1
IgG	immunoglobulin G
IL	interleukin
IL	interleukin
IP3	inositoltriphosphate
IS	immunological synapse
ITAM	immunoreceptor tyrosine-based activation motif
kDa	kilo dalton
Lck	lymphocyte kinase
LFA1	lymphocyte function-associated antigen 1
M	Molar
MACS	magnetic activated cell sorting
MAP	mitogen-activated protein
MEMS	micro-electro mechanical systems
mg	milligram
MHC	major histocompatibility complex
MHCp	peptide MHC complex
min	minute(s)
ml	milli liter
mM	milli molar
MTOC	microtubule organization center
NaCl ₃	sodium azide
NFAT	nuclear factor of activated T cells
NF-κB	nuclear factor 'κ-light chain enhancer' of activated B cells
ng	nanogram
nm	nanometer
PBMC	peripheral blood mononuclear cell

PBS	phosphate buffered saline
PE	phycoerythrin
PerCP	peridinin chlorophyll
PIP2	phosphatidylinositol-4,5 biphosphate
PK-C	protein kinase C
PKC Θ	protein kinase C Θ
PLC γ	phospholipase γ
PMA	phorbol ester myristate acetate
PMT	photo multiplier tube
R	Förster radius
r	colocalization coefficient
Ras	rat sarcoma
Scr	sarcoma-associated kinase
SEB	<i>Staphylococcal</i> enterotoxin B
SSC	sideward scatter
TCR	T cell receptor
TNF	tumor necrosis factor
YFP	yellow fluorescent protein
ZAP70	Z-associated protein of 70 kDa

1. Zusammenfassung

Protein-Protein-Interaktionen spielen eine Schlüsselfunktion in fast allen biologischen Prozessen. Dennoch sind konventionelle Methoden, um diese Interaktionen nachzuweisen, wie beispielsweise das Hefe-Zwei-Hybrid System, üblicherweise sehr aufwendig und kompliziert. Häufig werden Protein-Protein-Interaktionen auch mithilfe des Förster Resonanz Energietransfers (FRET) vor allem bei der Konfokalmikroskopie gemessen. Diese Methode produziert allerdings riesige Datenmengen und verlangt dazu viel Fachwissen.

Um diese Einschränkungen zu überwinden, wurde hier eine Methode entwickelt, mit der sich Protein-Protein-Interaktionen automatisch und auf Einzelzellbasis mit Hilfe der Durchflusszytometrie am MACSQuant Durchflusszytometer nachweisen lassen, da hier die FRET-Effizienz automatisch berechnet wird. Änderungen im Status der Protein-Protein-Interaktionen werden durch relative Änderungen in der Intensität der FRET Donor- und Akzeptorfluorochrome erfasst, wodurch sich der Wert der FRET-Effizienz ändert. So können Protein-Protein-Interaktionen sehr einfach auch auf hohen Zellzahlen in äußerst geringer Zeit und in Hochdurchsatzscreenings gemessen werden.

In der vorliegenden Arbeit konnte gezeigt werden, dass die CD3 und CD4 Korezeptoren auf der T Zell-Oberfläche nach der Aktivierung mit SEB interagieren. Hier stieg die FRET-Effizienz nach der T Zell Aktivierung deutlich an. Weiterhin konnte auch die Clusterbildung des CD3 Rezeptors durch das automatisierte Messen der FRET-Effizienz nachgewiesen werden. Auch wenn das FRET-Fluorochromenpaar gewechselt wurde, waren die Messergebnisse vergleichbar. Der Nachweis der T Zell Aktivierung gelang mit der FRET-Analyse sogar schneller als durch die Messung des Anstiegs an intrazellulären Kalziumionen als Standard-Aktivierungsmarker. Daher wurde auch getestet, ob auf Blutproben von immundefizienten Patienten, die in der Clusterbildung ihres CD3-Rezeptors aus verschiedenen Gründen eingeschränkt waren, diesen Defekt nachgewiesen werden konnte. Tatsächlich konnte hier im Vergleich zu gesunden Spendern kein Anstieg in der FRET-Effizienz nach T-Zell Aktivierung gemessen werden. Aus diesem Grund könnte die automatisierte FRET-Analyse auch im klinischen Alltag zum Nachweis von speziellen Immundefekten verwendet werden.

Mit Hilfe der CD3-Clustering FRET-Analyse konnte außerdem den Einfluss der Integrität der Lipid Rafts auf das Clustervermögen des CD3 Korezeptors nachgewiesen werden. Wurden

die Lipid Rafts mit Hilfe verschiedener Chemikalien modifiziert, nahm die FRET-Effizienz nach T Zell Aktivierung verglichen zu unbehandelten Zellen ab.

Weiterhin konnten die automatisierte FRET Analyse auch genutzt werden, um Immun-Checkpoint-Inhibition auf T Zellen zu bestätigen. Dafür wurde mittels FRET die Interaktion der CD3 und PD-1 Rezeptoren nach einer längeren T Zell-Stimulation gemessen: hier stieg die FRET-Effizienz deutlich an. Dieser Anstieg konnte jedoch verhindert werden, indem blockierende Antikörper, die gegen die Liganden des PD-1-Rezeptors gerichtet sind, verwendet wurden. Diese Antikörper unterbinden die Kostimulation, die für die antigenpräsentierende Zelle essentiell ist, um sich der Erkennung des Immunsystems erfolgreich zu entziehen. Folglich ist die automatisierte FRET-Analyse auch eine leistungsstarke Methode, um im Hochdurchsatzverfahren nach pharmakologisch aktiven Wirkstoffen, die diese Checkpoint Inhibition unterbinden, zu screenen.

1. Summary

Although protein-protein interactions play a major role in almost all biological functions, those interactions cannot easily be analysed, especially not on single cell level and with regard to dynamic changes in protein arrangement. Conventional investigation methods, like the yeast two-hybrid system are highly time consuming. Förster resonance energy transfer (FRET) is commonly used to identify protein-protein interactions via confocal microscopy. However, this requires expert knowledge and produces high amounts of data.

In order to overcome those limitations, a program was developed that automatically measures and calculates the FRET efficiency on cell by cell basis on the MACSQuant flow cytometer. Changes in protein-protein interactions can be assessed via relative signal changes of the donor and acceptor fluorochromes, causing a change in FRET efficiency. This allows for the identification of protein-protein interactions on large cell numbers in a minimum of time, in high throughput screenings and is easy to use.

In this study, it could be shown that interaction of the CD3 and CD4 coreceptors can be measured on the T cell's surface after activation via an increase in FRET efficiency. Furthermore, also the homoclustering of the CD3 coreceptor could be detected using the automatic FRET measurement. Even when the FRET fluorochrome pair was changed, the results were highly comparable. For this experiment, the increase in FRET efficiency was even faster than the increase in intracellular calcium that is used as the standard activation marker. For that reason, this automatic assay had been used to test blood samples of patients that are suffering from severe immunodeficiencies and are compromised for different reasons in their ability of CD3 clustering. Indeed, here no increase in FRET efficiency could be measured compared to healthy blood donors. Therefore, the automatic FRET program can easily be used in clinical settings for the determination of certain immunodeficiencies in patients.

Moreover, using the CD3 homoclustering FRET assay, the impact on lipid raft integrity on the clustering of CD3 could be detected. If the lipid rafts were manipulated, the CD3 receptor could not cluster effectively after T cell stimulation, leading to a decreased FRET efficiency compared to untreated T cells.

The automatic FRET assay could also be used to determine the checkpoint inhibition in T cells. For that purpose, the interaction of CD3 and the PD-1 receptor was measured after a

prolonged T cell stimulation leading to an increased FRET efficiency. That increase could be inhibited by applying blocking antibodies that are directed against the PD-1 ligands, prohibiting the co-stimulation that is essential for a successful immune escape. Therefore, this method is also a powerful tool allowing for high throughput screenings for pharmacologically active compounds.

2. Introduction

2.1 FRET

Usually in flow cytometry, the overall fluorescent signal of a single cell is measured. This provides information on the presence or expression level of a certain target molecule on the cell. However, no information can be derived on the special distribution of this molecule or its interactions with other molecules of interest. Still, protein-protein interactions play a major role in almost all biological functions. To overcome the limitation in spatial resolution, the Förster resonance energy transfer (FRET) between two fluorescent molecules can be determined on a flow cytometer.

In 1948, Theodor Förster described a process in which a fluorescent donor molecule in an excited state transfers its energy via nonradiative dipole-dipole interactions to a neighboring acceptor molecule¹. However, FRET requires an overlap of the emission spectra of the donor with the acceptor excitation spectra². The efficiency of the energy transfer is strongly distance depended. The energy transfer (E) decreases with the power of six with an increase of distance between the donor and acceptor, as described by the Förster radius R:

$$E = \frac{1}{\{1 + (R/R_0)^6\}}$$

Equation 1: Förster radius

Therefore, the energy transfer can usually not occur for distances larger than 10 nm². As the range of 10 nm is the dimension in which protein-protein interactions normally occur, this makes FRET an important tool to measure protein-protein interactions. For that reason, FRET is also known as a 'spectroscopic ruler'³ and already found many applications in microscopy and flow cytometry^{4,5}.

As a results of the energy transfer leads to a reduction of donor fluorescence intensity is reduced and therefore an increase in acceptor fluorescence emission can be measured when excited with the FRET donor wavelength⁶.

There are still some major constraints in the application of the FRET system. Traditionally, FRET signals were measured via microscopy⁷. However, this produces high amounts of data

and requires expert knowledge for the subsequent data analysis. Furthermore, as a consequence of the spectral overlap between donor and acceptor, the spillover in the respective channels makes the measurement of a clear FRET signal more complex. For that reason, numerous controls have to be included in the experiment and complex calculations are required in order to exclude measurement artifacts. To enable the analysis of large cell numbers, a FRET analysis program had been previously developed. However, it only allows for a computer-based post-measurement analysis.

Besides, in all FRET applications the size of fluorophores has to be considered, because steric effects of large and bulky fluorophores might inhibit a successful energy transfer. For that reason, not observing a FRET effect does not necessarily indicate for no molecular interactions to take place⁸.

2.2 FRET Efficiency calculation

FRET efficiency describes the rate of absorbed photons that are transferred non-radiatively from the donor molecule to the acceptor:

$$E = \frac{k_{ET}}{k_f + k_{ET} + \sum k_i}$$

Equation 2: FRET Efficiency

Here, k_{ET} describes the rate of energy transfer, k_f the radiative decay rate and k_i the sum of other de-excitation rates⁴. If energy transfer occurs, the quantum yield of the donor will become smaller and thus donor fluorescence intensity will decrease. As this energy is transferred to the acceptor molecule, this leads to an increase in the amount of acceptor molecules in an excited state and therefore to an increase in acceptor fluorescence intensity. However, these differences can often not be clearly distinguished via optical evaluations in diagrams and should therefore be calculated as FRET efficiency.

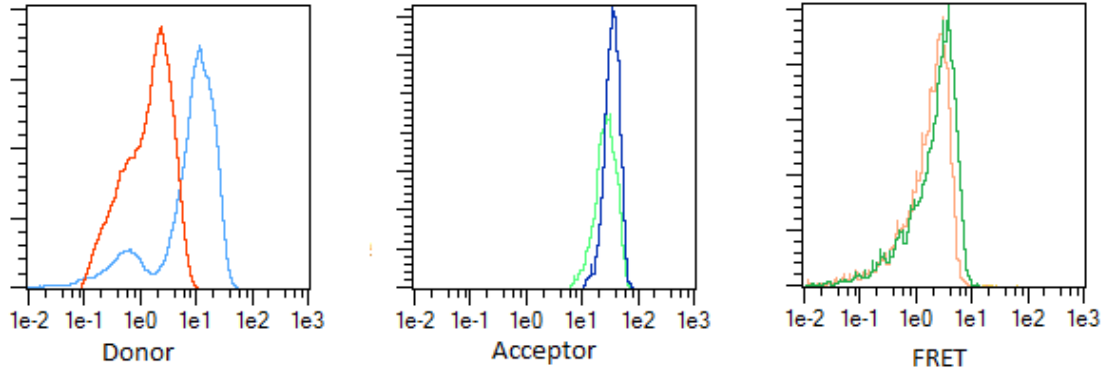


Figure 1: Emission spectra in FRET. The donor intensity is decreased (red) in FRET double stainings in comparison to single stainings (light blue), whereas the acceptor intensity is increasing (blue) compared to single stainings (green). In addition, the signal in the FRET channel is increased by FRET (green), compared to non-FRET samples (pink).

Here, we calculated the FRET efficiency according to published and established calculations^{4,9,10} on background corrected raw fluorescence intensities on cell-by-cell basis¹¹. As the fluorescence spectra of donor and acceptor are overlapping, these signals cannot be separated by optical filters.

To determine the contribution of donor and acceptor the in respective signals, each of the three measured intensities (I_1 , I_2 and I_3) will also have direct contributions from the donor and acceptor intensities (I_D and I_A , respectively) as well as the energy transferred intensity ($I_D * E$):

$$\begin{aligned}
 I_1(\lambda_{excD}, \lambda_{emD}) &= I_D(1-E) + I_A S_4 + \frac{S_4}{S_2} I_D E \alpha \\
 I_2(\lambda_{excD}, \lambda_{emA}) &= I_D(1-E) S_1 + I_A S_2 + I_D E \alpha \\
 I_3(\lambda_{excA}, \lambda_{emA}) &= I_D(1-E) S_3 + I_A + \frac{S_3}{S_1} I_D E \alpha
 \end{aligned}$$

Equation 3: Measured intensities for donor, acceptor and FRET and the contributions from other intensities.

Using these intensities, the spectral correction factors (S_1 , S_2 , S_3 and S_4) that account for the spectral contributions to each of the channel can be determined. The factors can be calculated on single-fluorophore labeled samples using the following equation:

$$S_1 = \frac{I_2^D}{I_1^D} \text{ and } S_3 = \frac{I_3^D}{I_1^D} \text{ for donors, and}$$

$$S_2 = \frac{I_2^A}{I_3^A} \text{ and } S_4 = \frac{I_1^A}{I_3^A} \text{ for acceptors.}$$

Equation 4: Spectral correction factors for FRET donors and acceptors.

Furthermore, the alpha factor as a scaling factor for the relative detection efficiency has to be determined using single labeled samples. The alpha factor normalizes for the conversion of a donor fluorophore excitation that gets emitted by an acceptor fluorophore, and can be determined empirically using this formula:

$$\alpha = \frac{I_2^A}{I_1^D} \frac{F^D}{F^A} \frac{b^D}{b^A} \frac{\epsilon_{excD}^D}{\epsilon_{excD}^A}$$

Equation 5: Scaling factor alpha

Here, F is the fluorophore to antibody labeling ratio, b the average amount of bound antibody (it is assumed to be identical for donor only and acceptor only labeled samples) and ϵ is the extinction coefficient of the fluorophores excited at the maximum donor excitation wavelength.

When A is substituted with $A = E / (1 - E)$, the equation set can be solved to:

$$A = \frac{E}{1-E} = \frac{1}{\alpha} \frac{S_1 S_2 [I_2(1-S_3 S_4) - I_1(S_1 - S_2 S_3) - I_3(S_2 - S_4 S_1)]}{(S_1 - S_2 S_3)(I_1 S_2 - I_2 S_1)}$$

Equation 6: Equation for A

Normally in biological systems the correction factors S_3 and S_4 are approaching 0, and also in our system we found that both factors were <0.01 . For that reason, we could use a simplified equation derived from Equation 6: Equation for A to calculate the FRET efficiency:

$$A = \frac{E}{1-E} = \frac{1}{\alpha} \frac{I_2 - I_1 S_1 - I_3 S_3}{I_1} = \frac{1}{\alpha} \frac{SE}{QUE}$$

Equation 7: Simplified equation for A

The FRET efficiency is determined here as a pure sensitized emission signal (SE) that is normalized to the total donor signal as converted to the acceptor emission¹²:

$$E = \frac{A}{1+A} = \frac{SE}{\alpha \cdot QUE + SE}$$

Equation 8: Equation for the FRET efficiency as sensitized emission signal

2.3 The human immune system

The human body is constantly exposed to microorganisms like bacteria, viruses, fungi or parasites that can potentially be disease-causing to the organism. The substances that the immune system is recognizing is referred to as antigens, as those substances were primarily discovered to stimulate the antibody generation. Antigens may not only consist of proteins or polysaccharides, but can also be comprised of metals, chemicals or even drugs.¹³

Several mechanisms have evolved to protect the body very efficiently from most of the diseases¹⁴. Those mechanisms, called the immune response, can be further subdivided into two different approaches of defense.

The first line of defense, the innate immunity, is a germline-encoded general but unspecific immune response. It is instantly available as soon as a pathogen is recognized via its specific pattern, but does not protect in a long-lasting manner. Here, the pathogens are destroyed by different immune cell types immediately before they can even infect the organism and cause a disease¹⁵.

The adaptive immune response is highly specific against the pathogens¹⁶. It called adaptive because it is constantly developing during a human's life during encountered infections. In the case of infection, it might take days until the specific immune response of the adaptive immune has developed. Yet, this immune response is highly efficient in eliminating the pathogen via very specific antigen receptors on the cell surface. The adaptive immune

response is also able to form an immunological memory against pathogens that it had once encountered, leading to a long-term immunity against that pathogen¹⁷. However, the adaptive immune response needs to be initiated via the innate immune system to form the immune response¹⁵. The major cell population that constitute to the adaptive immune system, the lymphocytes, can be further divided into B cells, that mediate a humoral immune response, and T cells that lead to a cellular immune response.

2.4 T cells and T cell activation

T lymphocytes make up a major part of the adaptive immunity and are characterized by the expression of the surface protein CD3. They are derived from the bone marrow but migrate into the thymus where they develop the T cell receptors (TCR) and are selected for their specificity to foreign antigens in the first step. These T cells are only able to recognize antigens that are presented on a major histocompatibility (MHC) complex as short peptide fragments^{18,19}.

There are two major T cell subsets:

- The T helper cells express the surface protein CD4 and have a high affinity for the MHC Class II receptor. They induce the activation of other cells like cytotoxic T cells and lead to antibody class switching in B cell via the release of cytokines.
- The cytotoxic T cells express the surface protein CD8 and are involved in the defence against viruses and tumours. They recognize virus infected or degenerated endogenous cells via their MHC Class I complex and induce their destruction.

Likewise, the MHC receptor subtypes are expressed differentially²⁰: The MHC class I receptor is normally found on almost all cell types and present peptides from fragments of non-self proteins from cytosolic proteins such as viruses but also tumor specific peptides²¹. The expression of the MHC class II receptor is restricted to antigen presenting cells like B cells, macrophages and dendritic cells. Therefore peptides are presented that are derived from phagocytosed extracellular proteins²². For both MHC types, the expression is tightly regulated via cytokine release like interferons from other immune cells.

The initiation of adaptive immune responses takes places in lymphoid organs²³. Here, during the naïve CD4 T cell activation, an immunological synapse (IS) is formed and the T helper cell receives two signals: first, the TCR/CD3 complex binds to the MHC II peptide complex²⁴. This process also requires for the engagement of the CD4 or CD8 coreceptor. Here, the molecules

are approaching in close spatial proximity. This again triggers the phosphorylation of intracellular kinases to activate an intracellular pathway. The second signal provides the verification for the activation process. Here, the costimulatory molecule CD28 on the T cell surface binds to B7 molecules on the antigen presenting cell^{25,26}.

Briefly, the engagement of the TCR to a pMHC complex leads to a phosphorylation of ITAMs (immunoreceptor tyrosine-based activation motif), that are associated to the CD3 receptor. The ITAMs are phosphorylated via two different enzymes that belong to the Src (sarcoma-associated kinase)-family: Fyn (fibroblast yes-related non-receptor kinase) and Lck (lymphocyte kinase), as they are recruited to the intracellular domain of the CD3 coreceptor during activation. The negatively charged phosphate groups at the ITAMs serve as binding partner for SH2 (src homology 2) domains for Zap-70 (ζ -associated protein of 70 kDa). After Zap-70 is recruited to the cell membrane, it becomes activated via Lck. There are several transmembrane adapter proteins that, once they are phosphorylated, recruit further cytosolic proteins like phospholipase C γ (PLC γ), protein kinase C θ (PKC θ) and Ras (rat sarcoma).

PKC θ hydrolyzes PIP₂ (phosphatidylinositol-4,5 biphosphate) into IP₃ (inositoltriphosphate) and DAG (diacylglycol), which causes an increase of intracellular free calcium ions. The ions interact with calcineurin and calmodulin. Calcineurin causes the dephosphorylation of the transcription factor NFAT (nuclear factor of activated T cells). This in turn causes NFAT to translocate into the nucleus. Furthermore, DAG binds the cytosolic serine/threonine kinase PKC θ that induces the translocation of the transcription factor NF- κ B (nuclear factor 'kappa-light-chain-enhancer' of activated B-cells) into the nucleus. The GTPase Ras induces the MAP (mitogen-activated protein) kinase pathway, that activates the transcription factor complex AP-1 (activator protein 1) to translocate into the nucleus and bind to the DNA.

As a consequence of the T cell activation, several cytokines are released that regulate the differentiation of a T cell into a further subtypes of effector cells and their proliferation. The T Helper cell activation pathway is depicted in Figure 2²⁷.

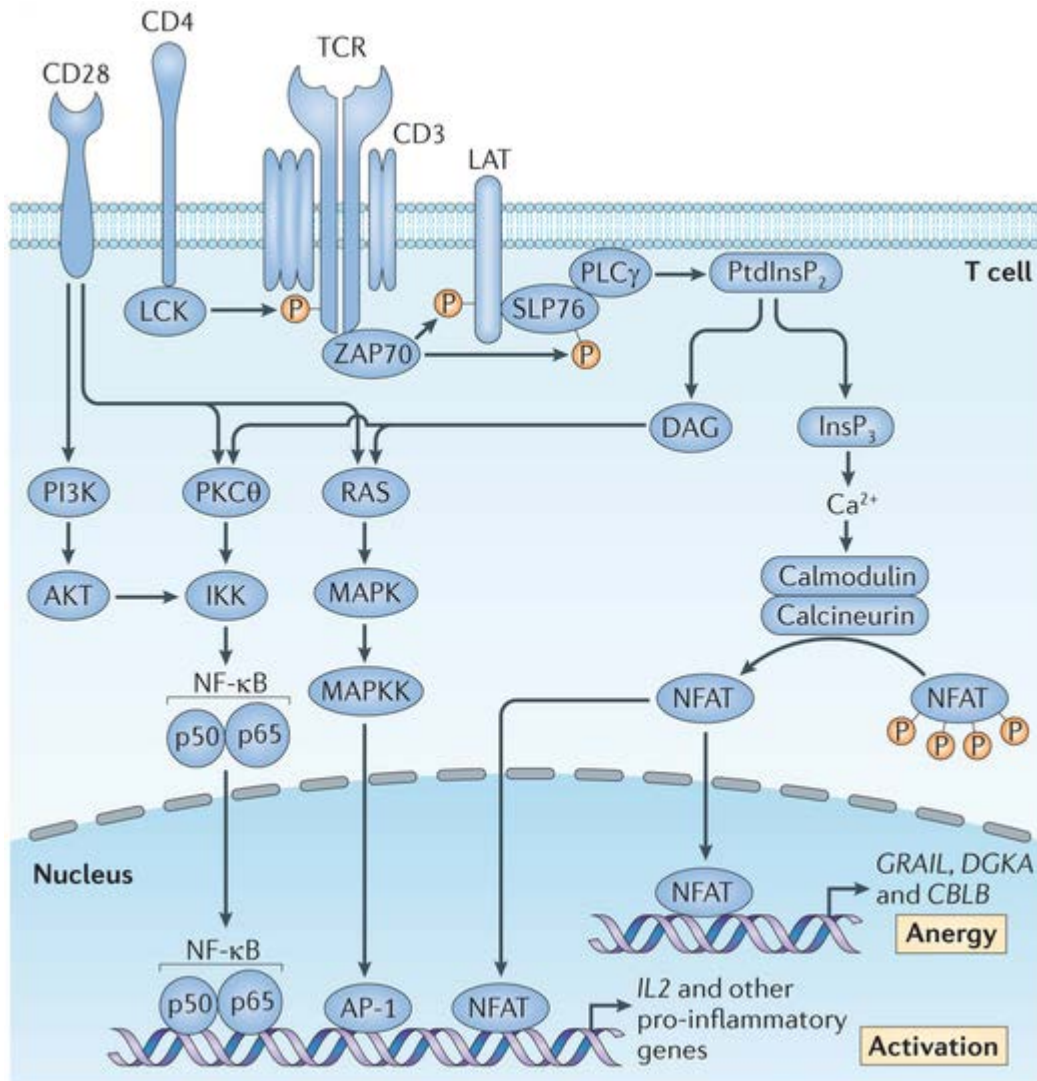


Figure 2: Activation of T helper cells. The engagement of the TCR and its coreceptor CD28 induces several intracellular pathways, mainly via PKC θ , Ras and PLC γ . Therefore, pro-inflammatory genes like IL-2 are transcribed and the T cell becomes activated. From: Pollizzi and Powell, 2014²⁷.

2.4.1 Structural rearrangements in the IS

During T cell activation, several structural rearrangements take place on the cell surface. After the T cell had successfully recognized a MHC-peptide complex, it is induced to stop migrating and forms a stable cell contact with the APC. For this, the TCR and its CD4 coreceptor both have to bind to the MHC-peptide to induce intracellular activation signaling²⁸. Here, the T cell builds up a pronounced polarization of to the antigen presenting cell as the microtubule organization center (MTOC) is reoriented to the immunological synapse (IS). This polarization process recruits all the cell surface receptors that are required for the immune response to the site of cell to cell contact²⁹.

Finally, the T cell builds a distinct structure at the interface to the antigen presenting cell in which the key molecules that play a major role in immune response regulation are organized in very distinct areas³⁰. This supra-molecular activation complex (SMAC) is subdivided into three different areas: in the central region of the SMAC (cSMAC) all the receptors that are required for a successful antigen recognition like the TCR and the CD3 coreceptor and their corresponding signaling kinases are gathered³¹. The receptors that are required for cell adhesion like LFA1 and ICAM1 are located in the peripheral SMAC surrounding the cSMAC. Also accessory receptors like the CD4 coreceptor are rapidly transferred to periphery³² after the initial contact to the APC has taken place. Molecules that are large and bulky and might have an inhibitory effect on synapse formation and T cell activation are located in the most distal region of the SMAC. Here molecules such as CD43, CD44 and CD45 can be found.

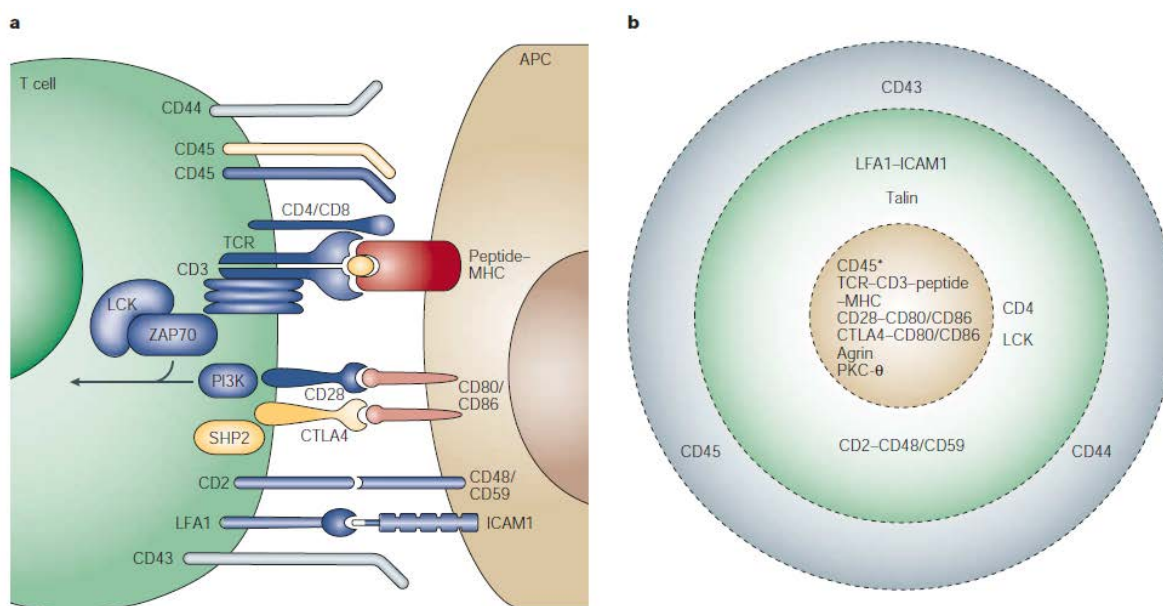


Figure 3: Structural rearrangements in the immunological synapse. Central: activation receptors, middle: adhesion molecules, periphery: large and inhibitory molecules. Inhibitory molecules are depicted in grey, whereas activating receptors are shown in blue. From: Huppa and Davis, 2003³⁰.

However, it was also shown that both the CD4 coreceptor and CD3 are internalized after strong activation signals via endocytosis. Whereas CD3 is recycled to the cell surface again, CD4 becomes degraded³³.

2.4.2 CD3 clustering immunodeficiencies

Some people fail to successfully create the immunological synapse and therefore are suffering from severe human primary immunodeficiencies, as the T cell cannot be activated and react properly to pathogen invasion into the body³⁴. Several of the immunodeficiencies that are described to impair the clustering of the CD3 coreceptor on T cells.

For example, patients that are deficient in the guanine nucleotide exchange factor dedicator of cytokinesis8 (DOCK8) are impaired in cytoskeletal rearrangements that are required for the formation of the IS. The DOCK8 deficiency is therefore characterized by a reduction of peripheral CD4 and CD8 T cells and impaired T cell proliferation and activation after CD3 receptor stimulation with anti-CD3³⁵. For that reason, patients are often affected by for example sinopulmonary and viral infections, hyper-IgE as well as cutaneous cancer and lymphoma^{36,37}.

Patients that are suffering from the Wiscott-Aldrich syndrome (WAS) have a gene mutation in *WAS* that causes a lack of functional Wiscott-Aldrich syndrome protein (WASP). However, WASP is essential for the activation of actin polymerization and therefore in those patients also the cytoskeletal rearrangements that are required to induce the formation of the IS after T cell activation is impaired³⁸. The syndrome is characterized by abnormal functions of most leukocytes. Patients often develop eczema and are in general very susceptible to infections as well as autoimmune disorders and lymphoma³⁹.

The MHC class II deficiency (bare lymphocyte syndrome) is a rare disease that is caused by mutations in the MHC class II, causing the respective molecule to be not expressed. For that reason, antigen presentation is impaired and the CD4 T cells cannot be activated specifically⁴⁰. Therefore, the patient's immune system is highly compromised. Those patients are extremely susceptible to all kinds of viral, bacterial and fungal infections⁴¹.

2.4.3 Lipid rafts

The lipid raft concept postulates that membrane trafficking and signaling can be regulated via nanoscale sphingolipid-cholesterol-protein assemblies within the cell membrane⁴². Those small structures are dynamically organized to merge to more stable larger raft structures to provide for specific molecular (lipid-lipid, lipid-protein and protein-protein) interactions after activation⁴³.

Lipid raft clusters in the TCR domains of activated T cells show a selective enrichment of cholesterol⁴⁴. Therefore the lipid rafts are recruited via radial movements that are regulated by actin filaments to the site of APC contact to form the cSMAC in the IS after TCR engagement. Here, inactive and dephosphorylated TCRs and their associated molecules (LAT, LCK and CD2) are replaced by active ones from the lipid rafts^{45,46} and the binding affinity and kinetics between the TCR and the pMHC is greatly enhanced⁴⁷.

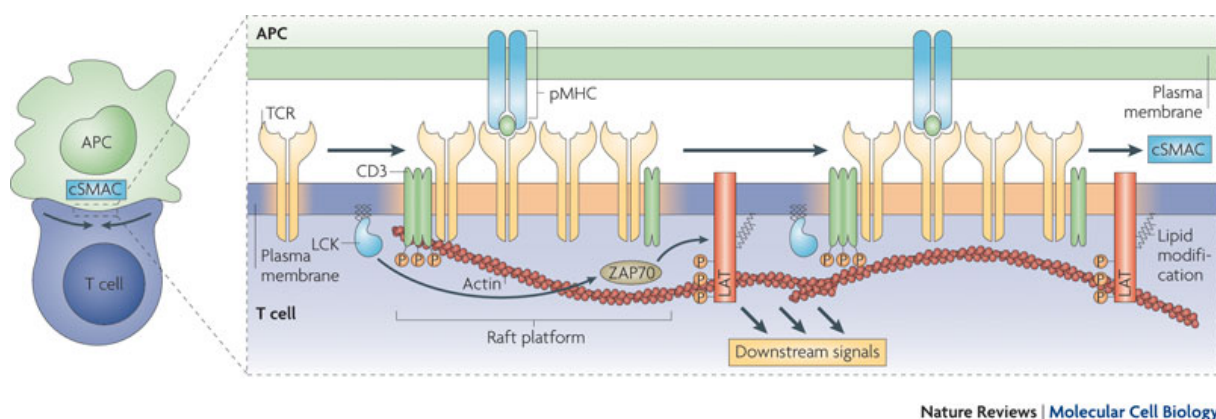


Figure 4: TCR and CD3 receptor organization on lipid rafts in the immunological synapse. The CD3 and TCR are organized in lipid rafts on the cell surface. After T cell activation, those rafts are relocated via actin filament rearrangements to the IS. From: Simons & Gerl, 2010⁴⁸.

There are several mechanisms that can be used to modify the integrity of the lipid rafts.

Hydroxypropyl Beta Cyclodextrin (hCD) is known to deplete the cholesterol molecules from lipid rafts due to its hydrophobic cavities as the chemical traps the molecules inside⁴⁹. It had been described in literature that hCD treatment of T lymphocytes reduces the efficient engagement of the TCR to pMHC⁵⁰.

hCD in a lower concentration can also be applied to resolve cholesterol in order to introduce additional cholesterol into the cell membrane as this leads to an enrichment of cholesterol in the lipid raft⁴⁹.

The antifungal agent nystatin can be used to disrupt lipid rafts as it sequesters the cholesterol molecules⁴⁹.

2.4.4 *Staphylococcal* enterotoxin B

Instead of specific antigens, also superantigens can be used to stimulate T cells unspecifically.

Staphylococcal enterotoxins belong to the family of superantigens, which are secreted by various strains of *Staphylococcus aureus*⁵¹. In humans, those toxins lead to the biological effects of food poisoning and can also have lethal effects in high doses, but furthermore those toxins do also cause strong immune responses which are magnitudes greater than immune responses caused by conventional antigens⁵². Similar to the conventional antigens, superantigens are presented to a TCR on the MHC class II receptor of the antigen presenting cell, but in contrary to the normal antigen activation, superantigens strongly crossing the TCR with the MHC receptor. This leads to an unspecific stimulation of the T cell. Although downstream signaling differs from normal antigen stimulation in some activation pathways⁵³, a non-MHC restricted T cell activation is triggered and leads to structural rearrangements on the cell surface as well as T cell proliferation and cytokine production. Additionally, the T cell activation via superantigens induces a strong internalization of the T cell receptor. As the *Staphylococcal enterotoxin* superantigen only interacts with the V β chain of the TCR, it can activate the large proportion of T cell subsets bearing the appropriate V β region regardless of the TCR chain specificities⁵⁴. In general, approximately 30% of the T cell population are activated by SEB⁵⁵.

2.5 Immune checkpoint inhibition

Some tumor cells developed certain mechanisms to escape from the immune response of the T cells and therefore impair the T cells' immune functionality⁵⁶. This effect is the so-called immune checkpoint inhibition, an effect that normally terminates the immune response after antigen activation. Here, the inhibitory receptor programmed cell death 1 (PD-1, also called CD279), a member of the CD28 superfamily⁵⁷, can be inducibly expressed on T lymphocytes, but also on B cells and myeloid cells⁵⁸. The receptor consists of a IgV-like domain with a transmembrane domain and a cytoplasmic tail that contains tyrosine-based signaling motifs⁵⁸ which negatively regulate T cell signaling⁵⁹. It inhibits the phosphorylation of Zap70 and protein kinase C θ at the CD3 coreceptor⁶⁰ as well as the induction of phosphatidylinositol-3 kinase activity and the downstream activation of Akt⁶¹ from the CD28

receptor. This leads to a reduced stability of synapse formation to the APC. During acute infections, the PD-1 is downregulated for the duration of the antigen exposure⁶².

The signaling of the PD-1 receptor can be induced via its engagement to the respective ligands PD-L1 (B7-H1) and PD-L2 (B7-DC). While the expression of PD-L2 is restricted to professional APCs⁶³, PD-L1 can be found on various tissues and immune cells.

The expression of PD-L1 is often upregulated on cancer cells and can be induced by proinflammatory cytokines such as type 1 and 2 interferons, TNF- α and IL-2, IL-7 and IL-15⁶⁴.

When T cells are constantly exposed to chronically infected cells, they will eventually become non-functional exhausted T cells⁶⁵. However, a PD-1 deficiency leads to autoimmune-related diseases with a later onset in life⁶⁶ as for example systemic lupus erythematosus. This indicates for PD-1 playing a major role in the regulation and the maintenance of self-tolerance of the immune response.

2.5.1 PD-1 and CD3 colocalization

Based on the suggestion that T cell activation is initiated via small TCR microclusters and its respective coreceptors and proximal signaling molecules⁶⁷, it was discovered that those clusters also play a role in the regulation of the immune response. PD-1 that is expressed on effector T cells is translocated to those TCR microclusters before it accumulates in the cSMAC after engagement to its ligands⁶⁸. In those microclusters the PD-1 receptor is located in close spatial proximity to the receptors to induce a SHP2-mediated suppression of Zap70 (see figure 5). Not only the clustering of PD-1, but also the colocalization with the TCR/CD3 complex seem to be required to successfully inhibit T cell activation via PD-1 signaling.

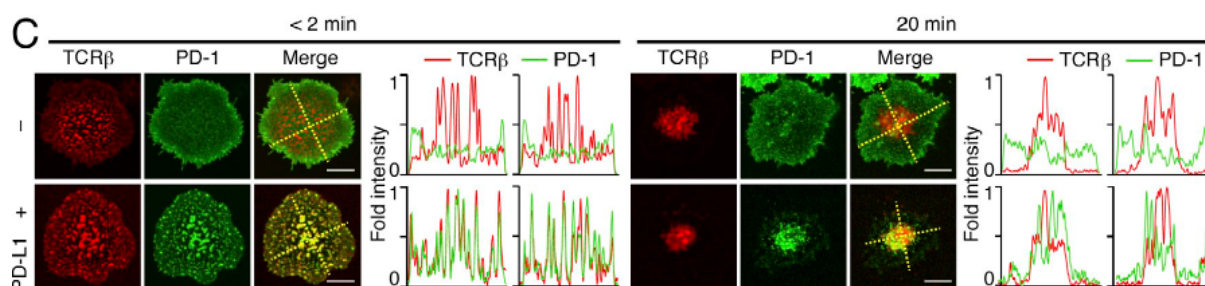


Figure 5: PD-1 colocalizes with the CD3 coreceptor in a ligand-dependent manner. Cells that were transfected with PD-1-EGFP (green) and stained with DyLight 649–labeled H57 Fab (red). Analysis was performed on a planar bilayer and realtime confocal microscopy at 2 minutes or 20 minutes after contact either in the presence or absence of PD-L1. The histograms show the fold fluorescence intensities of the TCR (red) and PD-1 (green). Bars = 5 μ m. From: Yokosuka et al., 2012⁶⁸.

Therefore the regulation of the T cell activation and immune response seems to be controlled via the spatiotemporal distribution of the TCR/CD3 complex together with the PD-1 receptor.

For that reason the regulation of the PD-1/TCR microclusters might represent a novel and promising target to block tumor checkpoint inhibition.

2.5.1 Pharmaceutical use immune checkpoint inhibition modulators

In order to restore the immune functionality of exhausted T cells, the PD-1/ PD-1 ligand interaction can be blocked for example by using monoclonal antibodies⁶⁹. This restores the functionality of the T cells *in vivo* and can be used for the treatment of certain cancer types⁷⁰.

In the last years, in the therapeutic area of immune checkpoint inhibition a monoclonal antibody (ipilimumab)⁷¹ directed against the immune checkpoint inhibitor receptor cytotoxic T-lymphocyte-associated Protein 4 (CTLA-4) had been tested for the treatment of metastatic melanoma. Although the therapeutic effect could be proven, patients suffered from severe and antigen unspecific side effects⁷².

In contrary, the mode of action of PD-1 checkpoint inhibition is in most cases restricted to the periphery during chronic infection, causing inflammation, or against cancer. For that reason, autoimmune-mediated side effects will be less dramatic⁷³. Mostly, but not exclusively, the expression level of PD-L1 on tumor tissue can be used as a prognostic factor and biomarker for an antibody immune therapy⁷⁴. Patients who are tested to be positive for this marker do mostly show a better therapeutic outcome to antibody treatment. However,

It is still debatable to use solely rely on the PD-L1 expression in patients material for different reasons: first, the development of adequate antibodies that will still bind successfully to its epitope in fixed and paraffin embedded tissue samples is highly difficult and therefore often unspecific. Furthermore, PD-L1 may not only be expressed on the tumor cells only, but also on the immune cells that infiltrate the tumor microenvironment⁷⁵⁻⁷⁷. For that reason, several patients who were tested to be PD-L1 negative nevertheless showed a good response to anti-PD1 directed immunotherapy⁷⁸.

Two of those PD-1 checkpoint inhibition modulators had already been tested in clinical trials and are also FDA-approved for several different cancer subtypes: nivolumab (trade name: Opdivo®) and pembrolizumab (Keytruda®) were proven to be efficient in restoring the antitumor immune response against several advanced cancer types, including lung cancer, colorectal cancer and renal cell cancer^{79,80}. Sill, also here several off-target effects such as autoimmune disorders like pneumonitis, vitiligo, colitis, hepatitis, hypophysitis and thyroiditis could be observed in patients⁸¹. Several more therapeutics targeting the PD-1/PD-L1 interaction are currently in the developmental pipeline of different pharmaceutical companies as there is still a high unmet need for the identification of new inhibitors and to clarify the detailed mechanism of work of pharmaceutically active compounds⁸².

2.6 Flow cytometry

In order to detect the presence of a certain target molecule on a cell, cells are commonly analyzed via flow cytometry⁸³.

Here, cells in a suspension are singularised and hydrodynamically focussed by a sheath fluid before beams of laser light are directed at the cell in an optical cuvette⁸⁴. Usually, multiple lasers of different wavelength excite the fluorochromes which are labelling certain target molecules on the cells. The fluorescent light that is then emitted by the fluorescent dyes falls through filters which block any light except for the aimed wavelengths and is directed via mirrors to the respective photomultiplier tubes (PMTs). Those PMTs amplify and digitalize the fluorescent signal, thereby providing multiparametric information on the deflection of light in the form of the forward scatter signal (FSC, corresponding to the cell size) and the side scatter signal (SSC, corresponding to the granularity of the cell) and the also on fluorescence intensities that had been detected from a single cell.

Data analysis is normally performed via gating based on the fluorescence intensity of a cell population⁸⁵. Here all events in a specific region in a diagram are selected for further analysis. Gates can be set in a hierarchic manner. This allows for a stepwise selection of specific subpopulations that are of special interest.

2.6.1 Fluorochromes

Fluorochromes absorb light of a certain wavelength, as the energy of the laser light puts the electrons of the fluorochrome from their ground state S_0 into an elevated energy state S_1 to S_2 . The time the fluorophore remains in the elevated level is referred to as the fluorescence lifetime. When an electron falls back into its basic energy state with the lowest vibrational energy level, photons are emitted again during the relaxation process. As a part of the energy is lost in the form of other de-excitation ways, the emitted light has a shorter wavelength compared to the excitation wavelength⁸⁶.

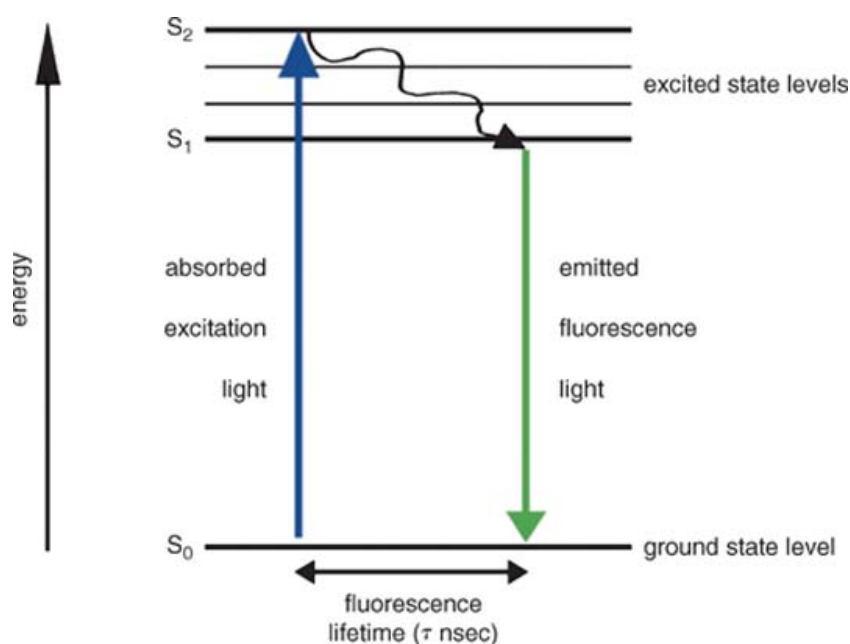


Figure 6: Energy states of an electron. The Jablonski diagram shows that in this example, the energy of the ultraviolet photon (blue) raises the energy level of a molecule from the ground state S_0 to an excited energy level S_1 to S_2 . When the photon drops from the excited state to the ground state level, energy is lost in the form of fluorescent light (green). The time between those states is referred to as fluorescence lifetime. From: Lleres et al., 2007⁸⁶.

The difference of wavelength between excitation maximum and emission maximum is referred to as stroke shift. However, fluorochromes do not only emit light of a certain

wavelength but a broad spectrum that is normally distributed around the emission maximum wavelength⁸⁷.

2.6.2 Express mode and post processing parser

Data acquisition and the evaluation of samples that are measured on the MACSQuant flow cytometer are controlled and provided within MACSQuantify Software. The measured data are stored in a digital format, that allows post measurement compensation and individual analysis by gating and cell counts. Analysis templates created within the software can be saved to facilitate future evaluations.

For an easy and fast analysis of complex cell analyses, as it might be required for multipanel analyses or for enrichment and enumeration kits, the MACSQuantify software offers several Express Modes. These Express Modes simplify the analysis via predefined experiment settings, including both acquisition templates for cell measurement and also the analysis templates for the evaluation. The analysis templates apply an automatic gating adapted to each individual sample to identify the cells of interest.

The sample grouping function allows the user to save more than one sample in one single data file. This might be necessary if volumes larger than 450 μ l have to be measured. It is also helpful when the same gates shall be applied to more than one sample. This has the advantage that control stainings can be included or that certain values can be offset against each other.

2.7 Objectives of the study

In the study presented here, an automated FRET-based program for the detection of protein-protein interactions was to be developed for a commercially available flow cytometer (MACSQuant). This program will identify each population of interest that will be required to determine the FRET efficiency by using defined gating algorithms. Based on relative changes in donor and acceptor fluorochromes intensity, the FRET efficiency can then be calculated by this program, therefore providing information on the increase or decrease of the proximity between two molecules of interest.

Using this method, a higher spatial resolution compared to conventional methods like confocal microscopy will be achieved. The analyses can be performed within a minimum of

time. This will allow for high-throughput screening, nevertheless without producing vast amounts of data or requiring expert knowledge for data analysis due to its automation.

The program shall be used to measure the clustering of surface receptors that is induced by T cell stimulation and also to unravel dynamic changes that take place both on the cell surface and on intracellular level, especially with regard to the spatial regulation of the CD3 and CD4 coreceptors.

Furthermore, we will use this assay to identify active checkpoint inhibition on T cells by measuring the clustering of PD-1 and CD3 via FRET after a prolonged T cell activation.

3. Material

3.1 Cells

Buffy coat	University Hospital of Dortmund
MDA-MB-231	ATCC
HuT-78	ATCC
Whole blood	Intern blood donation pool

3.2 Instruments

Centrifuge	Biofuge pico, Heraeus 4 KR, Heraeus
Confocal Laser Scanning Microscope	Zeiss LSM710
MACSQuant Analyzer 10	Miltenyi Biotec GmbH
MACSQuant VYB	Miltenyi Biotec GmbH
MACSQuant-X	Miltenyi Biotec GmbH
Sysmex KX-21 Hematology Analyzer	Sysmex GmbH
Photometer	Ultraspec 3300 pro, GE Healthcare
Vortex	Vortex genie 2, Scientific Industries
Incubator (HERA Cell 240i)	Thermo Fisher Scientific Inc.

3.3 Reagents

96-well imaging chamber	Zell-Kontakt
CliniMACS buffer	Miltenyi Biotec
Hematology Analyzer	Sysmex KX21N, Sysmex Corporation
Human Sera Type AB	BioWittaker
PenStrep	Lonza
MACS Bleach Solution	1% Active Cl ⁻

Material

MACSQuant Calibration Beads	Miltenyi Biotec
MACSQuant Running Buffer	Miltenyi Biotec
MACSQuant Storage Solution	Miltenyi Biotec
MACSQuant Washing Solution	Miltenyi Biotec
Pancoll	PAN Biotech
Paraformaldehyde 3.75%	Sigma Aldrich
PEB	1 x PBS, 2mM EDTA, 0,5% BSA
Phorbol 12-Myristate 13-Acetate	eBioscience
Red Blood Cell Lysis Solution	Miltenyi Biotec
RPMI 1640 cell culture medium	Miltenyi Biotec
<i>Staphylococcal</i> enterotoxin B	Sigma Aldrich
TransAct reagent	Miltenyi Biotec
DMEM cell culture medium	Miltenyi Biotec
Fetal Calf Serum	Biochrom AG
Trypsin-EDTA	Thermo Fisher Scientific Inc.
L-Glutamine	Lonza
Blood Dendritic Cell Isolation Kit II, human	Miltenyi Biotec
Pan T Cell Isolation Kit, human	Miltenyi Biotec
eFluor 514 Calcium Dye	eBioscience
MACS GMP TransAct CD3/CD28 kit	Miltenyi Biotec
Alexa Fluor 488 NHS Ester	Live Technologies
Alexa Fluor 555 NHS Ester	Live Technologies
Prionex	Pentapharm
MACSPlex Cytokine 12 Kit	Miltenyi Biotec
Trappasol	Cyclod. Techn. Dev. Inc
Cholesterol	Sigma
Nystatin	Sigma

3.4 Antibodies and antibody conjugates

CD3-FITC, human	Clone BW264/56, Miltenyi Biotec
CD3-VioBlue, human	Clone BW264/56, Miltenyi Biotec
CD3-VioBlue, human	Clone BW264/56, self-conjugated
CD3-APC, human	Clone BW264/56, Miltenyi Biotec
CD3-Alexa Fluor 488, human	Clone BW264/56, self- conjugated
CD3-Alexa Fluor 555, human	Clone BW264/56, self-conjugated
CD4-VioBlue, human	Clone VIT4, Miltenyi Biotec
CD4-APC, human	Clone VIT4, Miltenyi Biotec
PD-1-sFITC, human	Miltenyi Biotec
Anti CD3, human pure	Clone BW264/56, Miltenyi Biotec
Mouse anti-SEB antibody pure	Clone B87.10, ImmuQuest
Anti PD-L1 pure	Abcam
Anti PD-L2 pure	Abcam
APC anti-human CD274 (B7-H1, PD-L1)	BioLegend
Anti-PD-L2 FITC	Miltenyi Biotec
CD45-APC	Miltenyi Biotec
TCR	Miltenyi Biotec

3.5 Consumables, others

Cryo tubes	Thermo Fisher Scientific Inc.
Immersion oil, Immersol 518	Zeiss
PD 5, 10 columns	GE Healthcare
Pipette tips	Starlab
MACS Separator	Miltenyi Biotec
MACS separation columns	Miltenyi Biotec
Flat bottom cell culture plates	Falcon (BD Biosciences)
Round bottom cell culture plates	Falcon (BD Biosciences)
75cm ² cell culture flasks	Falcon (BD Biosciences)
Cell Strainer 70 µm	Miltenyi Biotec
Serological pipettes	Sarstedt
Microcentrifuge tubes	Starlab

3.6 Statistical Analysis

For the experiments in this thesis, biological replicates were performed for the same experiments but from blood samples drawn on separate days. Usually the number biological replicates was $n=3$, with the exception of the immunodeficient patients. Due to restricted availability, the number of replicates was only $n=2$. For the determination of significance between untreated and treated samples, the paired two-tailed Student's T test was used and for the comparison of multiple treatments, a one-way ANOVA test was followed by Holm-Sidak's multiple comparison test. Values with $p<0.05$ were considered to be significant. Error values for the biological replicates were determined as standard error of mean (s.e.m.).

3.7 Software

The statistical analyses were performed using GraphPad Prism version 6.02 and 7.00 for Windows. For all data and text editing, the software program Microsoft Word 365 Pro Plus (Microsoft) had been used. Python scripts were developed and edited using Spyder 3.5.2.5 (Spyder Development Team). MACSQuant data analysis was performed using either MACSQuantify Analysis software Versions 2.6 to 2.10 (Miltenyi Biotec GmbH) or a respective debug version for programming purposes. Confocal images were edited and analyzed using the ZEN2012 software (Zeiss). Graphical illustrations were designed using Adobe Illustrator CS3 13.0 (Adobe Systems). Furthermore, the EndNote X7 software (Thomson Reuters) was used for the citation of references within this thesis.

4. Methods

4.1 Cell isolation and cultivation

For the FRET experiments, primary cells from intern healthy blood donations from Miltenyi Biotec staff with given consent or from buffy coats from the University Hospital Dortmund had been isolated. For the measurements of immunodeficiencies, frozen PBMC samples from immunodeficient patients or the corresponding healthy control samples were obtained from the Center for Chronic Immunodeficiency Freiburg. The MDA-MB-231 cell line was obtained ATCC and stored intern cell stocks.

All cell culture work was carried out in tissue culture hoods using sterile and pyrogenfree reagents and consumables. Cells were always grown as monolayers in cell culture dishes or in cell culture flasks.

4.1.1 PBMC isolation

Peripheral blood mononuclear cells were isolated from buffy coat or whole blood on the day of blood draw. Three falcon tubes were filled with 15 ml Pancoll, and 25 ml of buffy coat that had been mixed with 10 ml CliniMACS buffer was carefully overcoated. For whole blood, 30 ml whole blood was diluted with 5 ml CliniMACS buffer before overcoating the Pancoll layer. The tubes were centrifuged for 35 minutes at 445 g with acceleration and break at the lowest level. Plasma was carefully removed and discarded. The lymphocytes on top the Pancoll layer were split into two fresh falcon tubes, filled up with CliniMACS buffer to 50 ml and centrifuged for 15 minutes at 300 g. Supernatant was removed, the cells were pooled into a fresh falcon tube and resuspended in 50 ml CliniMACS buffer. The PBMC were washed in RPMI supplemented with 2 mM L-glutamine and 0.05% (vol/vol) human AB-serum for 10 minutes at 200 g and resuspended in 10 ml RPMI with supplements buffer. The cell number was determined on the Sysmex hematology analyzer. For the CD3-CD4 and CD3 clustering FRET experiments, the cells were plated in a 24-well plate with 1×10^7 cells per well in 2 ml medium for 48-60 hours at 37°C and 5% CO₂. For PD-1 blocking experiments, the PBMCs were plated with 5×10^5 cells per well in a 24-well plate in RPMI with supplements for 3 days.

4.1.2 T cell isolation

Untouched T cells were isolated from PBMCs using the Pan T cell Isolation kit according to the user manual instructions. For comparison, T cells were also isolated using the Blood Dendritic Cell Isolation Kit II with the respective change that both kit reagents were added at once to the PBMCs in order to achieve a dendritic cell depletion and therefore a T cell isolation. All other steps were carried out according to the user manual.

For the PD-1 CD3 FRET experiments, either 1×10^6 T cells were plated in 1 ml RPMI supplemented with 2 mM L-glutamine and 0.05% (vol/vol) human AB-serum on a 24-well plate. For the downscale version for screening purposes 5×10^5 cells per well in 50 μ l RPMI with supplements a 384-well plate (downscale version) were cultured or co-cultured if indicated with MDA-MB-231 cells for 3 days at 37°C and 5% CO₂ in humidified atmosphere.

4.1.3 Freezing and thawing of cells

For the freezing of cells, the cells were resuspended in 1 ml of the respective cell medium supplemented with 20% FCS and 10% DMSO and frozen at -80°C before the cells were transferred into liquid nitrogen tanks.

Cells were thawed through incubation at 37°C in a water bath until the sample was almost thawed. Then the cells were quickly transferred into 12 ml of the respective cell medium in a 15 ml centrifuge tube and washed for 10 min at 300g. The supernatant was discarded and the cells were washed a second time with 12 ml medium. Afterwards the cells were transferred into cell culture plates or flasks and cultured under the required conditions.

4.1.4 MDA-MB-231 cultivation

The human breast cancer cell line MDA-MB-231 was cultured in 10 ml DMEM supplemented with 10% FCS (vol/vol) and 1% PenStrep (vol/vol, 10,000 U/ml) at 37°C with 5% CO₂ in a T-75 cell culture flask in a humidified atmosphere. Cells were passaged in a ratio of 3:10 twice a week. For this, the cells were rinsed with ClinIMACS buffer and incubated with 3 ml trypsin for approximately 5 minutes at 37°C. After the cells had detached from the flask, the cells were washed in 50 ml DMEM with supplements for 5 minutes at 300g, the supernatant was discarded and the cells were resuspended in 10 ml medium. 3 ml of cell solution was transferred into a fresh cell culture flask filled with 7 ml cell medium.

For the PD-1 CD3 FRET assay, 2.25×10^4 cells were plated in a 384-well plate or 5×10^5 cells were plated in a 24-well plate in DMEM with supplements and co-cultured with T cells as described in 4.1.2 T cell isolation.

4.2 T cell activation and SEB blocking

T cells were activated using either staphylococcal enterotoxin B (SEB) superantigen or the MACS GMP TransAct CD3/CD28 kit as described hereinafter.

4.2.1 Activation protocol for T cells with SEB

For the CD3-CD4 FRET experiments, 1×10^6 PBMCs were incubated with 2 μg SEB for 2 minutes at 37°C if not stated differently. Here, a the high SEB concentration was used to achieve a full saturation for the short incubation time. For SEB blocking experiments, 0.5 μg of the mouse anti-SEB antibody (clone B87.10)⁸⁸ was added to the cells. To achieve a molar antibody surplus of approximately 10x, here the SEB concentration was lowered to 0.2 μg accordingly. The blocking antibody was either pre-incubated with the SEB for 3h at 4°C or added to the cells in parallel with the SEB. For the PD-1 CD3 FRET experiments, the T cells were stimulated with 2 μg SEB for 3 days for the standard protocol. In the downscale version, the T cells were stimulated with 0.2 μg SEB for 3 days.

4.2.2 Activation protocol for PBMC with TransAct Kit

In order to activate T cells using the MACS GMP TransAct CD3/CD28 kit, 1×10^6 PBMCs were incubated with 500 ng of each the CD3-specific and the CD28-specific reagent for 2 minutes at 37°C.

4.2.3 Cytokine secretion assay

To validate the activation of the T cells, the cytokine secretion was determined after SEB stimulation. For this, 1×10^5 PBMCs were stimulated with 1 μg SEB in 200 μl RPMI medium with supplements over night at 37°C and 5% CO₂. In this experiment, the SEB concentration was reduced compared to the standard T cell stimulation protocol because of the increased incubation time. The secreted cytokines were stained and measured using the MACSPlex

Cytokine 12 Kit according to the user instructions and the results were evaluated via the respective MACSplex Cytokine 12 Express Mode program.

4.2.4 Calcium influx measurements

The intracellular, cytoplasmatic calcium influx into the activated cell was measured using the eFluor514 calcium indicator dye. This dye is suitable for calcium measurements on flow cytometers that are not equipped with an UV laser⁸⁹. 1×10^7 PBMCs were stained with 5 μ M eFluor514 in 1 ml RPMI with supplements for 30 min at 37°C. Afterwards, the cells were washed twice with the medium, resuspended in medium and kept at 37°C until stimulation.

4.3 Fluorochrome conjugation

The CD3 ϵ -chain specific antibody (clone BW264/56) was labeled with different fluorescent molecules for a later FRET analysis. For this purpose, the VioBlue dye was added in a ratio of 10 molecules per antibody molecules, Alexa Fluor 488 in a ratio of 7.5:1 and Alexa Fluor 555 in a ratio of 7.5:1. The anti-CD3 antibody was incubated on a shaker with the respective dye for 1.5 h in 0.1 M NaCO₃ at room temperature under light protective conditions. In the meantime, a Sephadex gel column was equilibrated three times with phosphate-EDTA-azide buffer. The unconjugated dye was removed from the antibody conjugates via the fractionation on the gel column. The antibody conjugates were eluted using phosphate-EDTA-azide buffer and were stored in a concentration of 100 μ g/ml with the addition of 0.1% Prionex as stabilizer. We determined the labeling ratios of fluorochrome to antibody ratios photometrically: The VioBlue conjugate had a labeling ratio of 4.18, the Alexa Fluor 488 conjugate a ratio of 2.95 and the Alexa Fluor 555 conjugate a ratio of 6.12. The antibody conjugates were titrated on PBMCs until they reached a saturation point. The CD3-VioBlue conjugate was furthermore cross-titrated with the CD3-FITC conjugate for the CD3 clustering FRET experiments in order to achieve a 50% reduction in fluorescence for the double labeled sample.

4.4 Staining protocols

For all the cell stainings in which Miltenyi Biotec antibody conjugates or BioLegend conjugates were used the cells were stained according to the instructions and concentrations indicated in user manual if not stated differently.

For the CD3 CD4 FRET assay, 1×10^6 PBMCs were stained with a FITC conjugated anti-CD4 antibody and a CD3-specific VioBlue antibody conjugate (Miltenyi sales LOT). For the CD3 homoclustering assay 1×10^6 PBMCs were stained either with 5 μ l of the self-conjugated anti-CD3 VioBlue conjugate and 10 μ l of the Miltenyi Biotec sales LOT anti CD4 FITC conjugate, or with 19 μ l anti-CD3 Alexa Fluor 555 conjugate and 2 μ l anti-CD3 Alexa Fluor 555 conjugate. The cells were stained at room temperature for 10 minutes in medium, then washed with medium for 5 minutes at 300g. The cells were resuspended in 200 μ l medium and kept at 37°C until T cell activation. In case the Alexa Fluor FRET pair had been used, the cells were first stained as described above, stimulated with SEB as described in 2.4.4 *Staphylococcal enterotoxin B* immediately fixed with 2.25% (vol/vol) paraformaldehyde at room temperature for 20 minutes.

If the lipid rafts were disrupted during the experiments, the cells were either stained with the FRET pair antibody conjugates as described above before SEB stimulation or following the SEB stimulation for the given time points.

For the CD3 PD-1 FRET experiments, 1×10^5 T cells were stained in 200 μ l medium for 3 days after SEB stimulation with 10 μ l of each the anti CD3-VioBlue (Miltenyi sales LOT) and anti-PD1 sFITC antibody conjugates, either in 200 μ l medium (normal approach) or in 50 μ l medium for the 384-well plate downscale approach. The cells were incubated with the antibody conjugates for 10 minutes at 4°C, then washed for 5 minutes at 300g with PEB buffer and resuspended in PEB buffer for cell measurements at the MACSQuant. Also for the downscale version, 10 μ l of each antibody conjugate was used as the whole well of cells was measured and stained and a complete saturation with the antibody fluorochrome conjugate was to be achieved.

4.5 Lipid raft integrity manipulation

To change the integrity of the lipid rafts, hydroxypropyl Beta Cyclodextrin (bCD), cholesterol and nystatin were incubated with the SEB stimulated PBMCs.

For the β CD, a 100 mM dilution was mixed by dissolving 2.74g β CD in 20 ml dH₂O. The cholesterol was dissolved to a 104 nM solution with 0.02g cholesterol in 20 ml dH₂O and the addition of 2.74g β CD, because otherwise cholesterol would not dissolve in water. Both dilutions were sterile filtered through a 0.2 strain and stored at 4°C.

The PBMCs were stimulated with 2 μ g SEB and incubated with each 20 μ l (corresponding to 10 mM) β CD or cholesterol or with 2 μ l nystatin solution for the given time points at 37°C.

4.6 Confocal laser scanning microscopy and sample preparation

For the observation under the confocal laser scanning microscope, PBMCs were stained with the indicated dyes as described in 4.4 and stimulated with SEB as described in 4.2 T cell activation and SEB blocking. The cells were fixed with 2.25% (vol/vol) paraformaldehyde for 20 minutes at room temperature, washed at 300g for 5 minutes and resuspended in 50 μ l PEB. The cells were analyzed on the Zeiss LSM 710 confocal microscope.

4.6.1 Colocalization analysis at the confocal microscope

The overlap coefficient was determined for the CD3 receptor and the CD4 coreceptor as described in **Fehler! Verweisquelle konnte nicht gefunden werden..** To compare the results obtained in the FRET experiments, the FRET values were normalized (FRET_n) via linear fitting according to the following equation:

$$FRET_n = FRET\ efficiency * 3.6 + 18.48$$

Further positive and negative controls were stained for the colocalization analysis. As positive controls, PBMCs were stained with CD3-FITC and CD45-APC as those receptors are known to colocalize as long as the T cell is not activated. Another positive control was the colocalization of CD3 and the TCR, as those receptors are described to form a complex. For a negative colocalization control, PBMCs were stained for CD3-FITC and CD45-APC after SEB stimulation for 1h at 37°C, because the stimulation causes the CD45 receptor to be segregated from the immunological synapse. All samples were fixed with 2.25% (vol/vol) paraformaldehyde.

4.7 Flow cytometry

For the flow cytometric analysis, all the samples that were stained with the Alexa Fluor dyes are analyzed on the MACSQuant VYB flow cytometer that is equipped with three lasers of 405 nm (violet), 488 nm (blue) and 561 nm (yellow) wavelength (see Table 1).

Laser	Channel	Filter (nm)	Dye or parameter
Violet 405 nm	V1	450/50	CFP, VioBlue
	V2	525/50	Pacific Orange™, VioGreen
Blue 488 nm	B1	525/50	GFP, FITC, YFP
	B2	614/50	PI, Lss-mKate, YFP
Yellow 561 nm	Y1	586/15	PE
	Y2	615/20	mCherry, dsRed, TexasRed®, PE-Vio615, ECD, PE-CF594, PE/Dazzle™ 594, PE-eFluor® 610
	Y3	661/20	PE-Cy™5, APC, mKate, PerCP-Vio700
	Y4	750 LP	PE-Cy7, APC-Cy7, PE-Vio770, APC-Vio770
Yellow 561 nm	FSC	561/10	Size
	SSC	561/10	Granularity

Table 1: Optical configuration of the MACSQuant VYB.

The optical configuration of the MACSQuant VYB can be found under: <http://www.miltenyibiotec.com/en/products-and-services/macs-flow-cytometry/flow-cytometers/macsquant-vyb/macsquant-vyb.aspx>.

Samples that were stained with the VioBlue and FITC FRET pair were measured either on the MACSQuant VYB or the MACSQuant Analyzer 10. This instrument is equipped with three excitation lasers for the wavelength 488 nm (blue), 640 nm (red) and 405 nm (violet) (see Table 2).

Laser	Channel	Filter (nm)	Dye or parameter
Violet 405 nm	V1	450/50	CFP, VioBlue
	V2	525/50	Pacific Orange™, VioGreen
Blue 488 nm	B1	525/50	GFP, FITC
	B2	585/40	PE
	B3	655-730	PI, PerCP, PE-Cy™5.5, PerCP-Vio700, PE-Vio615, ECD, PE-CF594, PE/Dazzle™ 594, PE-eFluor® 610
	B4	750 LP	PE-Cy7, PE-Vio770
Red 635 nm	R1	655-730	APC
	R2	750 LP	APC-Cy7, APC-Vio770
Blue 488 nm	FSC	488/10	Size
	SSC	488/10	Granularity

Table 2: Optical configuration of the MACSQuant Analyzer 10.

The optical configuration of the MACSQuant 10 can be found under: <http://www.miltenyibiotec.com/en/products-and-services/macs-flow-cytometry/flow-cytometers/macsquant-analyzer-10/macsquant-analyzer-10.aspx>

All calcium influx measurements were performed on a MACSQuant X instrument that is still under in-house development at Miltenyi Biotec GmbH. The optical configuration of this instrument corresponds to the configuration of the MACSQuant 10. The major difference concerning the calcium influx measurement is that the sample uptake is not finished before the data acquisition is started and therefore this instrument allows for a continuous sample uptake and measurement. Also the PD-1 FRET downscale experiments were measured at this instrument, because it allows for faster sample acquisition and is compatible with a 384-well plate.

In order to monitor the daily performance of the instruments, the machines were calibrated with MACSQuant calibration beads. No compensation was applied for all FRET measurements.

4.7.1 Gating strategy

In order to determine the median staining intensities in the donor, acceptor, and FRET channels the following gating strategy had been used:

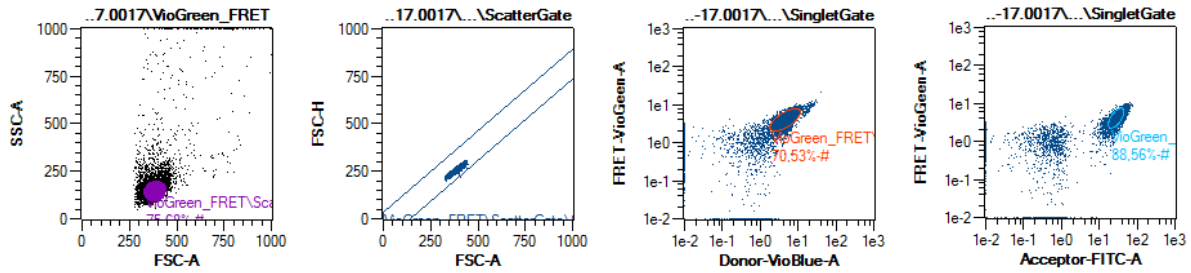


Figure 7: Gating strategy. Median staining intensities were read out by setting a first gate on the scatter parameters and a second gate on the singlet cells. Based on this target population, ellipse gates were set on the donor versus FRET channel and acceptor versus FRET channel double positive populations.

As the very first gate, the target population was defined in the FSC-A versus SSC-A plot based on their size and granularity. Using this population, a singlet gate was drawn in the FSC-A versus FSC-H plot in order to exclude all doublet cells that might display an increased area to height signal. This population was then used to find all donor-positive cells (only in the respective positive samples) in the donor channel (here: VioBlue) versus the FRET channel (here: VioGreen) and an ellipse gate was set on the double positive population. Next, the selected population was analyzed in the acceptor channel (here: FITC) versus the FRET channel in order to determine all cells that are positive for the acceptor dye, again only if the cells were positively stained.

4.8. The FRET Express Mode workflow

To simplify the FRET analysis, an “Express Mode” for the automated measurement and analysis via predefined settings and algorithms of the determination of the FRET efficiency was written. This program is embedded into the MACSQuantify software and was written in python programming language. The complete script can be found in the appendix.

Briefly, the process of the automatic FRET calculation program is the following:

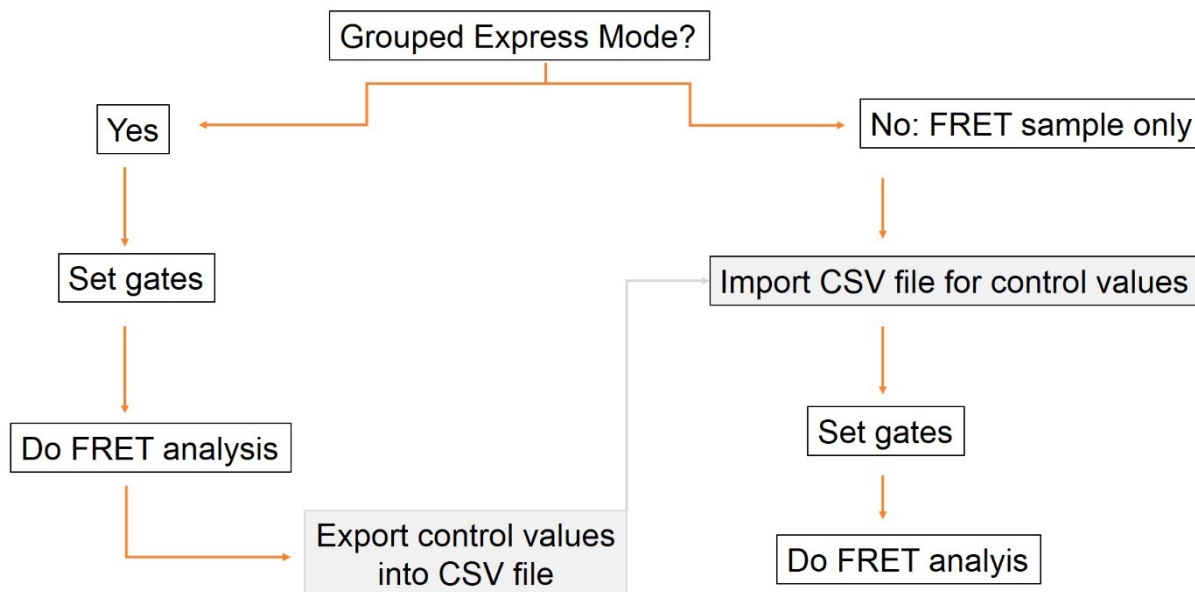


Figure 8: Work flow of the automatic FRET calculation program. In the first step, the express mode tests whether the sample is grouped or not. In case the sample is grouped, the standard FRET express mode algorithm is started, including gating and the FRET analysis. The results are then exported into a CSV file. If the sample is not grouped, the express mode algorithm is starting the analysis for one single FRET sample. Here, the CSV file is imported to provide the control values for the FRET calculation. Accordingly, the FRET sample is gated for the positive populations and the FRET analysis is done.

In the very first step, the FRET program tests whether the sample that is to be analyzed is a grouped sample or not. If the sample is grouped, then it is tested if all required controls are included in the samples that are to be measured in this experiment. On all groups, gates are set on the target populations according to the gating strategy in 4.7.1 Gating strategy in order to determine the required median intensities for the donor, acceptor and FRET channels. Next, all control parameters required for the FRET efficiency determination are calculated. The results are shown on different analysis pages and the control parameters are stored in a comma separated value (CSV) file.

In the case one samples is not grouped, it is assumed that the sample is a FRET sample that is to be analyzed with the program. Therefore, only the gating procedure is applied that is used for the FRET positive sample and the control values are imported from the CSV file. Based on those values, the FRET efficiency can be calculated and the results are depicted on one analysis page.

The algorithms behind the different functions are explained in detail in the next sections.

4.8.1 Import function

All the main functions of the MACSQuantify software are written in C++. Therefore, several scripts that serve as a basis for the express mode have to be imported in the beginning of the script. For example, the *os-module* (miscellaneous system operating interfaces) is required to use the program independent from the operating system. Further basis Express Mode functions, like *basisScript*, *utilities*, *copy*, *processSample*, *time*, *mq* and *expressModes* contain important basic algorithms that are required in the Express Modes functions. Some of these functions again contain further subfunctions that can be imported separately, like for example the function *basisGating*.

4.8.2 Default settings

The experimental settings are predefined in the FRET analysis Express Mode. Four different samples are required for the FRET calculation: 1) A blank sample is left unstained. It is used to determine the background fluorescence of the samples. 2) A donor only sample, in which only the donor protein is stained and likewise, 3) An acceptor only sample. Based on 2 and 3, the crosstalk between donor and acceptor and also the bleed through into the FRET channel can be calculated. 4) A FRET sample, in which both donor and acceptor proteins are stained. This sample is the one that is used to calculate the FRET efficiency on.

The default uptake volume for one sample is set to 100 μ l, and the sample volume is set to 250 μ l. Samples will not be mixed before measurement. The flow rate for the measurement is set to medium speed with no auto flow rate. No event limit is applied in the default settings. All channel annotations can be done manually by the user. The default groups for the VioBlue-FITC FRET pair are predefined for the experiment as:

- 1: 'Blank',
- 2: 'VioBlue_Donor',
- 3: 'FITC_Acceptor',
- 4: 'VioGreen_FRET'

For the Alexa Fluor 488 and Alexa 555 FRET pair, those parameters were changed accordingly.

4.8.3 Automatic gating

The gating on the target population is defined by several algorithms. Those algorithms can be found in the class *analyzeFRET* where the gating coordinates for all four samples are calculated. First all potential preexisting subpopulations are removed and a progress viewer for the gating procedure is started. In the express mode, the different samples are called as *Fractions*. Those *Fractions* are identified via the function *retrieveFractions*. This function automatically returns the different samples, the blank, donor only, acceptor only and FRET sample.

The coordinates for the gates are calculated on the basis of one dimensional histograms. Accordingly, for each channel in one dotplot, a separate fluorescence intensity histogram is created for the detection of the desired populations. Those histograms consist of 512 channels. During several smoothing steps and a so-called binning function the median and median values of adjacent channels are taken as one new data point. As a consequence, the whole histogram is smoothed and therefore reduced in its size and corrected for measurement outliers.

In histograms with defined borders on the X-axis all events that would be out of this range are displayed in the first channel on the left side (0), and in the last channels on the right (256), respectively. These events therefore pile up in the direction of the Y-axis. As a consequence, all those events would give false results in these channels as described in the following. Therefore, in the *zeroBounds* function all events in these channels are removed. Using those two-dimensional histograms, the coordinates for the gates are calculated. For this purpose, the function *FWHM* (full width, half maximum) determines the maximum of the histogram, using the peak with the highest number of event counts if more than one peak was determined in the histogram. Then the function returns two values, one for the left half maximum and one for the right one of a peak. In order to define the left border of the peak and therefore a split if a bimodal distribution can be found, the median of the two half maxima is determined and subtracted by 3.5 times its standard deviation.

Using this approach to determine the coordinates of the events for a given parameter, several gating functions were developed and implemented in the program *standardGating*. Therefore, several gating functions for the creation of a for example a singlet gate or ellipse gate are called up from this program and are used to find the target populations in the FRET express mode. The color of the gated region is set in HTML code individually for each gate.

4.8.4 FRET calculation

FRET efficiency is calculated automatically in this program according to the steps described in 2.2. At the beginning of workflow of the FRET program, the user is permitted to type in the alpha factor manually into the sample description. The value is extracted by using regular expression search algorithms in the function *getAlphaFromDescription*. Alternatively, a default alpha value is set to 0.3533 (as determined for the CD3 homocustering VioBlue FITC FRET pair).

As normally the FRET efficiency would be calculated within the script once the program analysis was started, no change in FRET efficiency can be updated if the user would change the gate positions after the FRET calculation was finished. For that reason, the FRET calculation was placed into a *textblock* module. *Textblocks* are part of the analysis pages and therefore update themselves as soon as the region in a plot is changed. Thus, a new *textblock* script was created which contains all the FRET calculations. It can be assigned in the analysis pages. Based on the different *fractions* (with a small first letter), the median intensity values are determined by the program and updated if the gates are changed.

The median fluorescence intensities are loaded in for the donor, acceptor and FRET channel. The FRET efficiency calculation is performed according to the FRET calculation described in 2.2 FRET Efficiency calculation.

4.8.5 Acquisition page

During sample measurement, the cell populations and the gates which are set on the target populations will be visible. Therefore, the class *FRETAquisitionPage* is created in the beginning. There is a general page template containing all page setups which are based on the function *basisEasyPage*, which can be filled with plots and tables. In this class, first the scatter and fluorescence channels are defined from the *utilites*. The sample which is displayed on the page is always the current *live* sample. Four plots are shown on this page: the first one is a dotplot, showing the measured cell population in a FSC-SSC plot. Furthermore, the three histograms for donor, acceptor and FRET intensity are depicted here.

4.8.6 Analysis pages

Several different analysis pages give the user detailed information about the samples and their FRET efficiency. The analysis pages are based on the same structure as the acquisition page, only this time the fluorescence intensity determination and FRET calculation results are included in those pages for all four samples.

Class *FRETAnalysePage1* shows the target population on the FSC-SSC dotplot, and the single histograms for the donor, acceptor and FRET channel based on the target gate. Also the gates on the positive populations in the histogram are displayed. Furthermore, the self-updating tables created in the *textblock* are retrieved, thus the median intensity values for donor, acceptor and FRET channel are displayed. This page is created for each the blank, donor only, acceptor only and FRET sample individually.

All calculations that are required to determine the FRET efficiency are shown in *class FRETAnalysePage2*. Here, the tables for an overview on all single median intensities, the background subtraction, the crosstalk values, the alpha factor input and the FRET efficiency result are displayed. These tables are also constructed in the FRET *textblock* to enable calculation updates in case the gates are changed.

The sixth page, *class FRETAnalysePage3*, gives the user an overview on all the most important results at once. This page includes plots of the FRET sample, showing the target gate in the FSC-SSC dotplot and the positive cells in histograms for donor, acceptor and FRET channel. Furthermore, tables based on the *textblock* are included. These tables show the median intensities of all the FRET samples, the alpha factor and the overall FRET efficiency.

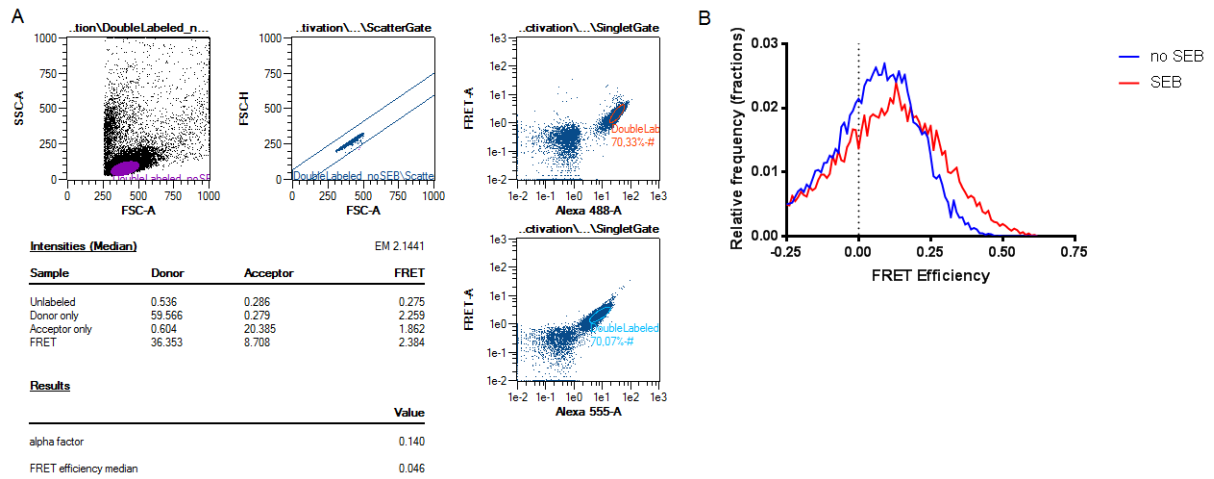


Figure 9: The FRET Express Mode Program. The program provides an output analysis page with information on: (A) the automatic gating procedure and the results of FRET efficiency calculation, and (B) shows the FRET efficiency distribution for both no activation and T cell activation with 2 μ g SEB, including the negative FRET values. From: von Kolontaj et al., 2016

4.8.7 The FRET efficiency histogram

In order to enable the plotting of a histogram of the FRET efficiency on a cell-by-cell basis, a histogram for the FRET efficiency is created based on the calculated values.

For that, a new FRET efficiency channel has to be integrated into the sample file. However, an *.mqd* file that had once been created cannot be overwritten retrospectively but the acquisition of a sample is already finished before the FRET analysis. Therefore, a new *.mqd* file is generated containing a “FRET Efficiency” channel and all other channels that are required for a complete FRET analysis. The channels are imported from the *.mqd* file that is to be analyzed, while all the background intensity values and the crosstalk values were previously stored in an *extension* and can be assigned in this class of the script. Next, for each single cell the median intensity values for donor, acceptor and FRET channel are determined and subtracted by the background intensities.

The FRET efficiency is then calculated for each single cell as previously described in 4.8.4 FRET calculation and the new FRET file containing the new FRET channel is created and automatically opened in the MACSQuantify Software.

4.8.8 FRET Post Processing Parser

For screening approaches in which multiple FRET values are to be analyzed in a large scale, a FRET Post Processing Parser was written to export the FRET efficiency results into one excel

sheet per measured multiwell plate. For this, the Post Processing Parser calls up the FRET express mode for each FRET sample that is measured on the plate. The FRET efficiency is determined as described previously for each sample and the corresponding result is written into one Excel sheet that contains information on the sample name, the Sample ID and description as well as the start time, analysis status and the date that the FRET calibration was performed.

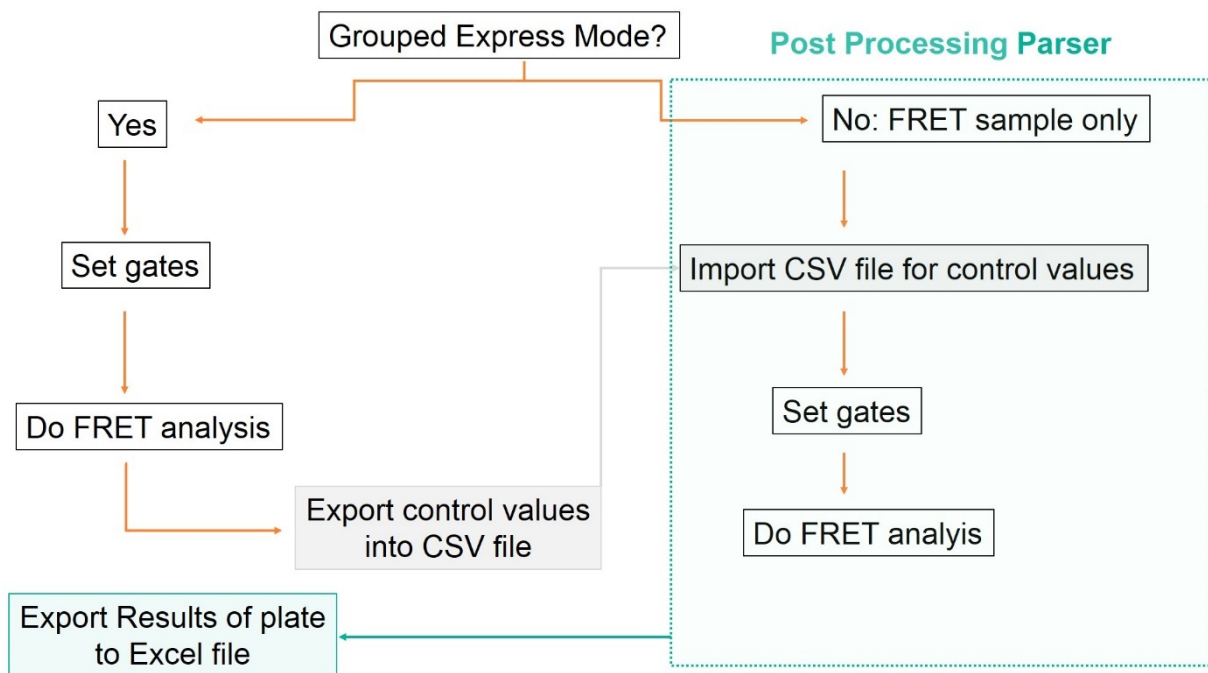


Figure 10: Workflow of the FRET Post Processing Parser. In green the functional area of the Post Processing Parser is depicted. The Post Processing Parser extends the FRET express mode regarding an additional export function. This function is only started if the sample that is to be analyzed was not grouped. As a result, the most relevant values of each FRET sample is exported automatically into one excel sheet per analysis run.

4.9 Validation of the FRET Express Mode

In order to validate the results that are obtained using the FRET Express Mode we developed antibody-based FRET calibration beads. For that purpose, we took protein A/G-coated polymethyl methacrylate beads and labeled them with the CD3-specific antibody conjugates conjugated to Alexa Fluor 488 as the FRET donor fluorophore and to Alexa Fluor 555 as an acceptor. Here we varied the donor to acceptor ratios, as it is known that an increased acceptor to donor ratio increases the FRET efficiency⁹⁰. The results achieved using the FRET

Express Mode were then compared to the respective results obtained by previously published FRET analysis program⁹¹.

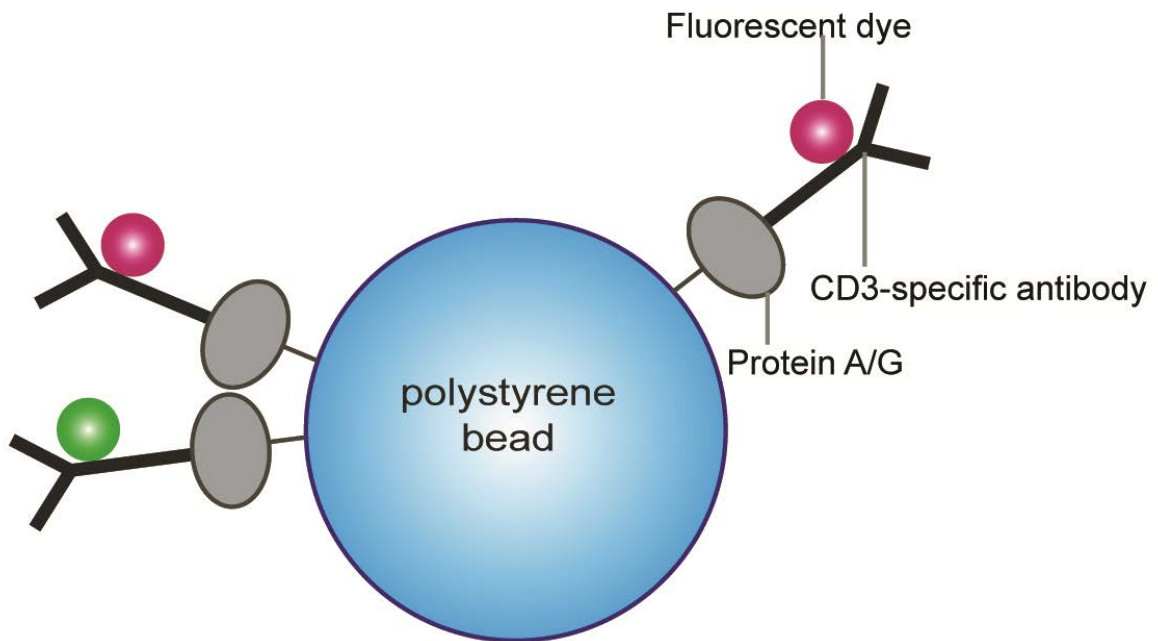


Figure 11: Validation of the FRET Express Mode program. FRET calibration beads are protein A/G coated polystyrene beads that are loaded with different donor to acceptor ratios of Alexa Fluor 488 and Alexa Fluor 555 conjugated CD3-specific antibodies. From: von Kolontaj et al., 2016¹¹.

5. Results

5.1 Validation of the FRET program with FRET calibration beads

Data files of FRET calibrations were analyzed in the FRET program and the results were compared to the calibration results determined by a previously published program (compare 4.9 Validation of the FRET Express Mode).

The FRET efficiency increased among the increase of the acceptor to donor fluorophore ratio. We could measure values from 0.5% FRET efficiency for the donor only control up to 67.7% FRET efficiency for the ratio of 5.7 acceptor antibody conjugates per donor.

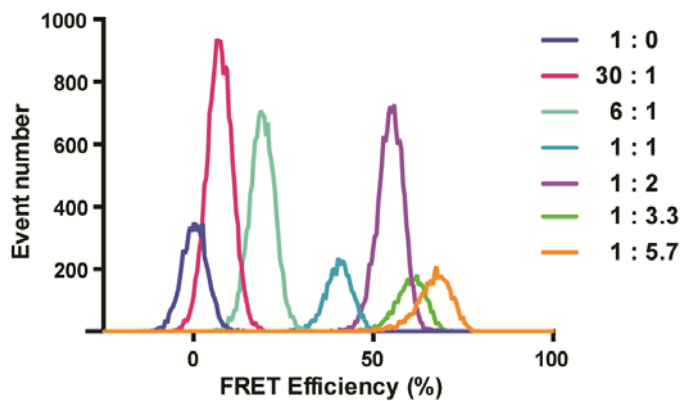


Figure 12: Increasing amount of acceptor to donor fluorescent molecule ratios lead to an increase in FRET efficiency. Here, FRET calibration beads with different acceptor to donor antibody conjugate ratios were analyzed for their FRET efficiency. From: von Kolontaj et al., 2016¹¹.

The correlation between the program and the FRET calibration was 0.9993 as determined via Person correlation with the two-tailed $p < 0.0001$.

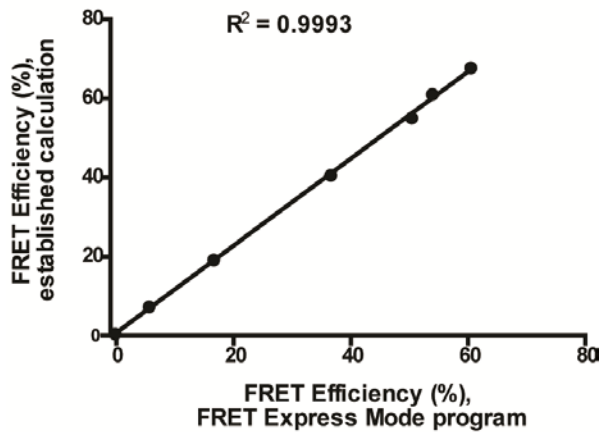


Figure 13: Validation of the FRET Express Mode using the Pearson correlation for FRET calibration beads compared to published calculations. The results were analyzed using the ReFlex program developed and published by Szentesi *et al.* From: von Kolontaj *et al.*, 2016¹¹.

5.2. CD3-CD4 interaction

The interaction of the CD3 and CD4 coreceptors was measured by the determination of the FRET efficiency after T cell activation and was confirmed by colocalization analysis on the confocal microscope.

5.2.1 CD3-CD4 FRET

We could detect the interaction of CD3 and CD4 on T cells after the activation of PBMCs with SEB. Here, a CD3-specific VioBlue antibody conjugate and a CD4-specific FITC antibody conjugate were used. Due to the crosslinking of the SEB of the TCR with the MHCII on the antigen presenting cells, the T cells were stimulated unspecifically. This causes a strong activation of the T cell that is marked by structural rearrangements of the receptors on the cell surface.

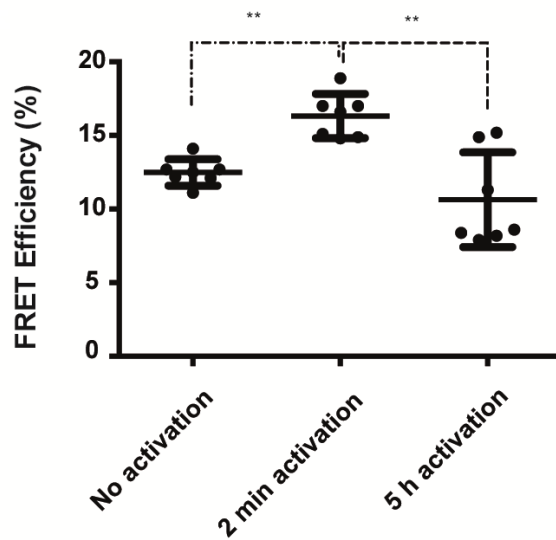


Figure 14: FRET Efficiency for CD3 and CD4 coreceptor clustering after no stimulation or 2 µg SEB superantigen stimulation for two minutes or five hours, ** $P < 0.01$. From: von Kolontaj et al., 2016¹¹.

The FRET efficiency increased significantly after the short 2 minute activation from $12.5 \pm 0.3\%$ to $16.3 \pm 0.6\%$ (ANOVA, $P = 0.0016$). After 5 hours of SEB stimulation, the FRET efficiency decreased again significantly to $10.6 \pm 1.2\%$.

5.2.2 CD3-CD4 CLSM colocalization and correlation

In order to prove that the results of the CD3-CD4 FRET system are not only an artifact, but can be further confirmed via another method, the colocalization of CD3 and CD4 was analyzed via confocal laser scanning microscopy (CLSM). Here PBMC, which were stained, activated with SEB and fixed with paraformaldehyde were imaged under the CLSM and analyzed for colocalization. As positive colocalization control, both CD3 and the TCR as a complex and CD3 and CD45 without SEB treatment were included in the experiments. As a negative control, the colocalization of CD3 and CD4 after SEB treatment was analyzed.

For colocalization analysis, the cells were analyzed with the colocalization tool of the Zeiss ZEN2010 software (see 2.8). For comparison with the FRET program results in a graph, the axes had to be adapted. Therefore the results of the FRET program were first plotted against the results of the colocalization tool. The formula of a regression line between those results ($y = 3.604x + 18.482$) was used to normalize the FRET program results according to the colocalization tool results. Then both results could be compared in one curve. It can be seen

that the scope of both the CLSM colocalization and the FRET analysis program results are very similar.

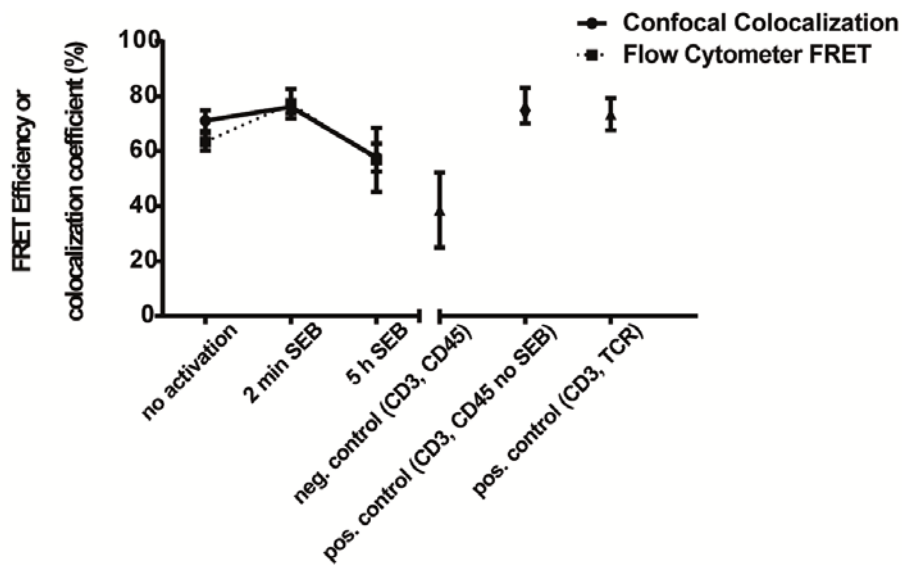


Figure 15: Comparison between the colocalization coefficient (overlap coefficient after Manders) for CD3-FITC and CD4-APC and the normalized FRET efficiency. As colocalization controls, the colocalization of CD3 and the TCR or CD3 and CD45 (no activation) had been used as a positive control, whereas the colocalization of CD3 and CD45 after 2 μ g SEB activation for 1 hour had been used as a negative control. From: von Kolontaj et al., 2016¹¹.

On the images it can be seen that the not activated T cells show an equal and regular distribution of CD3 and CD4 on the cell surface. After the short activation with SEB, microclusters of CD3 and CD4 begin to form. Here, a large proportion of the cell surface is colored in yellow, indicating that FITC and APC are measured in the same pixel. After five hours of SEB incubation, CD3 forms large clusters on the T cell surface. Furthermore, much CD3-FITC signal can be found inside the cells while CD4-APC fluorescence is strongly decreased.

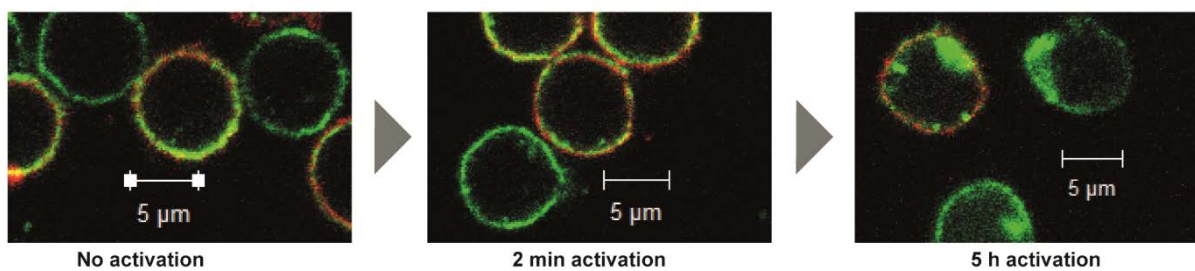
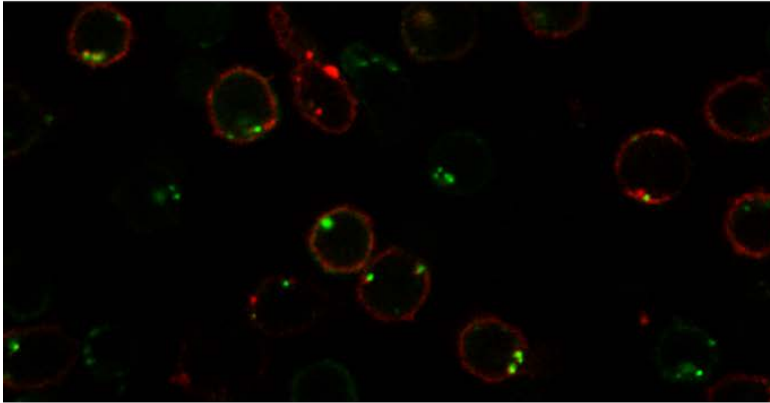


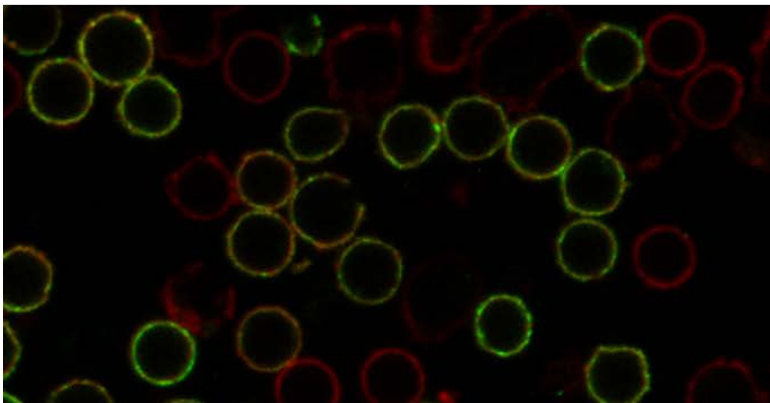
Figure 16: Confocal images of CD3-FITC (green) and CD4-APC (red) stained receptors on the cell surface for no activation or two minute/five hour 2 μ g SEB activation. From: von Kolontaj et al., 2016¹¹.

The segregation of CD45 from the immunological synapse and from the CD3 coreceptor could be seen on the fluorescent images (colocalization negative control). In the positive controls, the CD3 receptor signal is colocalizing with both the CD45 receptor and the TCR.

A CD3 and CD45, 2 μ g SEB



B CD3 and CD45, no SEB



C CD3 and TCR $\alpha\beta$

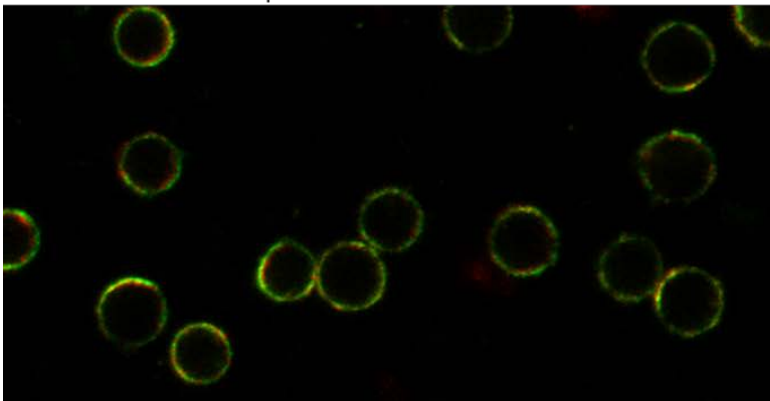


Figure 17: Colocalization controls. The confocal images show the colocalization of CD3 and CD45, either (A) after 2 μ g SEB activation (negative control) or (B) without SEB activation (positive control). Another positive control was (C) the colocalization of the CD3 ϵ -chain and the TCR $\alpha\beta$ receptor. Anti-CD3-FITC is shown in green, anti-CD45-APC in red and anti-TCR $\alpha\beta$ -APC also in red. From: von Kolontaj et al., 2016¹¹.

5.3. CD3 homoclustering

It was described that immediately after T cell activation, the CD3 coreceptor is clustering in lipid rafts to form the immunological synapse. This was proven by measuring the increase in FRET efficiency for CD3 homoclustering after T cell activation or the respective inhibited increase in immunocompromised patients. The T cell activation and the structural rearrangements were furthermore confirmed by cytokine secretion assays, compared to intracellular calcium influx and disturbed with substances that change the lipid raft integrity.

5.3.1 CD3 homoclustering FRET

The clustering of the CD3 coreceptor after SEB stimulation was analyzed via antibody conjugates that were directed against the CD3 coreceptor for both the donor and the acceptor dye. Two different FRET pairs were used: either VioBlue with FITC or Alexa Fluor 488 with Alexa Fluor 555. The FRET efficiency increased significantly increase (ANOVA, $P = 0.0011$ for the VioBlue and $P = 0.0332$ for the Alexa FRET pair) after a 2 minute SEB activation from $4.9 \pm 0.2\%$ to $10.4 \pm 0.8\%$ (VioBlue FRET pair) or from $4.8 \pm 0.1\%$ to $8.0 \pm 0.4\%$ % (Alexa FRET pair) during cluster formation.

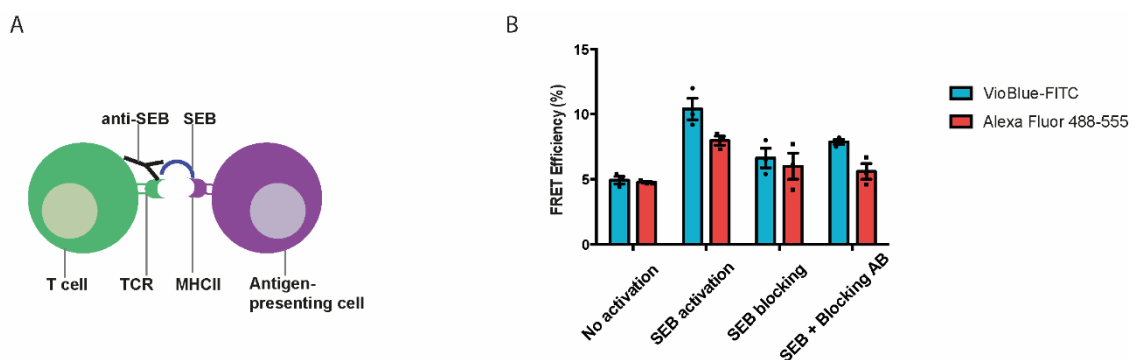


Figure 18: T cell inhibition by SEB superantigen blocking antibody. (A) Schematic view of the SEB-specific antibody inhibition. (B) CD3 coreceptor homoclustering and activation validation using the FRET pair VioBlue and FITC or Alexa Fluor 488 and Alexa Fluor 555, showing the FRET efficiencies for no activation, two minute 0.2 μg SEB activation or 0.2 μg SEB blocked with the 0.5 μg SEB-specific antibody either after a three-hours pre-incubation or added with the SEB in parallel to the cells. From: von Kolontaj et al., 2016¹¹.

We could inhibit the increase in FRET efficiency by adding a SEB-specific blocking antibody that is binding to the SEB domain that would normally crosslink to the TCR (Figure 18 A). For

these experiments, the antibody was either preincubated with the SEB (SEB blocking), leading to a reduction in FRET efficiency to $E = 6.6 \pm 0.8\%$ (VioBlue FRET pair) and $E = 6.0 \pm 1.0\%$ (Alexa FRET pair) or added to the PBMCs in parallel with the SEB (SEB + Blocking AB), reducing the FRET efficiency to $7.9 \pm 0.2\%$ FRET efficiency (VioBlue FRET pair) and in $E = 5.6 \pm 0.3\%$ (Alexa FRET pair)(see Figure 18 B).

5.3.2 Cytokine secretion

The cytokine secretion of PBMCs that were stimulated with SEB over night was analyzed to confirm the activation of the T cells.

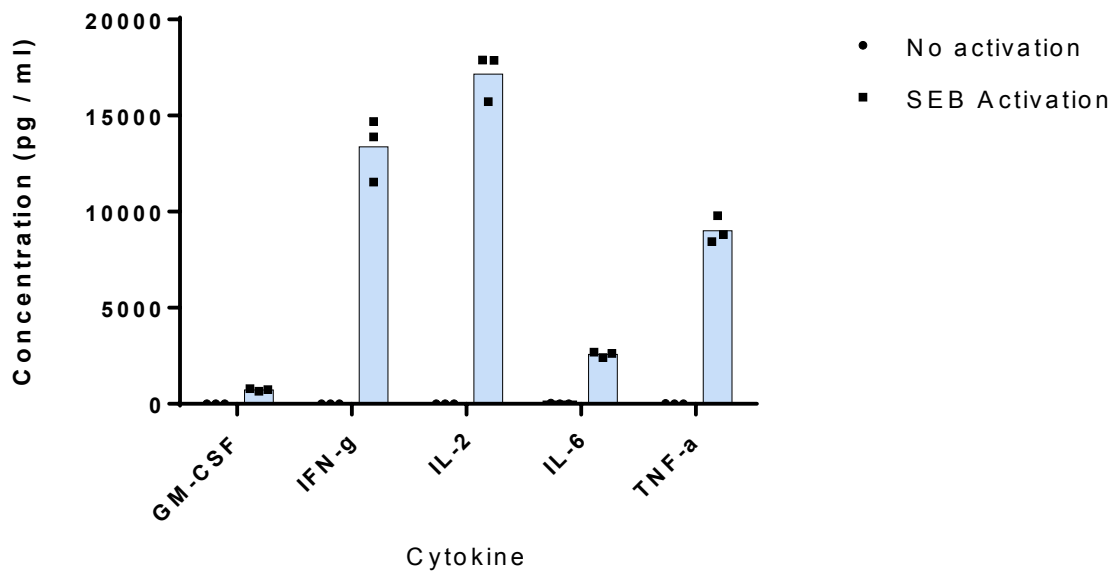


Figure 19: Cytokine secretion of activated T cells. Human PBMCs were activated with 1 μg SEB and cultured over night. The cytokine expression was determined using the MACSPlex cytokine secretion kit. Results of most relevant cytokines, $n = 3$, technical replicates. From: Kolontaj et al., 2016¹¹.

The most relevant cytokines that indicate for T cell activation, namely GM-CSF, IFN- γ , IL-2, IL-6 and TNF- α were analyzed for their concentration in the supernatant. While almost no cytokines could be detected if the PBMCs were not activated, the concentration was strongly increased after T cell activation. GM-CSF showed a median concentration of $732.67 \text{ pg/ml} \pm 36.29$, IFN- γ a concentration of $13377.13 \text{ pg/ml} \pm 943.53$, IL-2 $17160 \text{ pg/ml} \pm 720.31$, IL-6 2576.87 ± 81.88 and TNF- α a concentration of $9014.4 \text{ pg/ml} \pm 404.89$.

5.3.3 Calcium Influx versus FRET efficiency as activation marker

The increase in intracellular calcium after T cell activation was determined via the eFluor514 intensity increase and compared to the results obtained via measuring FRET. Here, the PBMCs were stimulated either with SEB or by using the TransAct activation kit 30 seconds after the acquisition of the measurement was started.

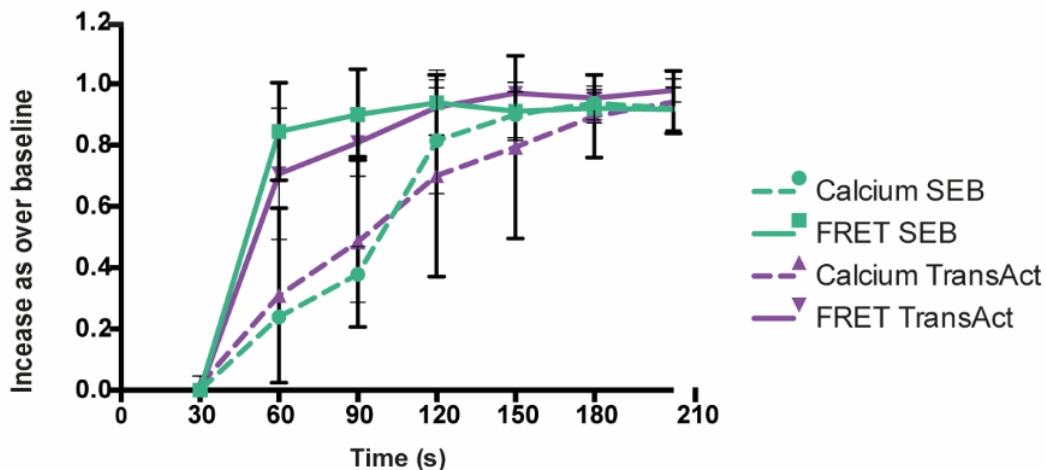


Figure 20: Time course measurement of FRET efficiency for the clustering of the CD3 coreceptor, compared to calcium influx measured by eFluor514 intensity after 2 μ g SEB or 0.5 μ g TransAct CD3/CD28 Kit activation. From: von Kolontaj et al., 2016¹¹.

The maximum FRET efficiency after both SEB and TransAct kit stimulation was reached almost immediately after T cell activation at the time point 60 seconds. Here, the maximum FRET increase over baseline was 0.84 ± 0.09 for SEB stimulation and 0.70 ± 0.12 for TransAct activation. The intracellular calcium influx reached its maximum intensity at a later time point. At the time point 120 seconds the plateau for the maximum calcium dye intensity was reached almost equally for SEB stimulation (0.82 ± 0.1 increase) and TransAct bead activation (0.7 ± 0.19 increase).

5.3.4 CD3 clustering as diagnostic tool for immunodeficiencies

The homoclustering of the CD3 coreceptor on immunodeficient patients compared to healthy individuals using FRET assay with the Alexa Fluor FRET pair. All patients were suffering from defects affecting the dynamic structural rearrangement of the CD3 receptor

on the cell surface. For the PBMCs of healthy individuals, the FRET efficiency increased from 5.9 ± 0.5 to 9.4 ± 0.4 after SEB stimulation of the T cells.

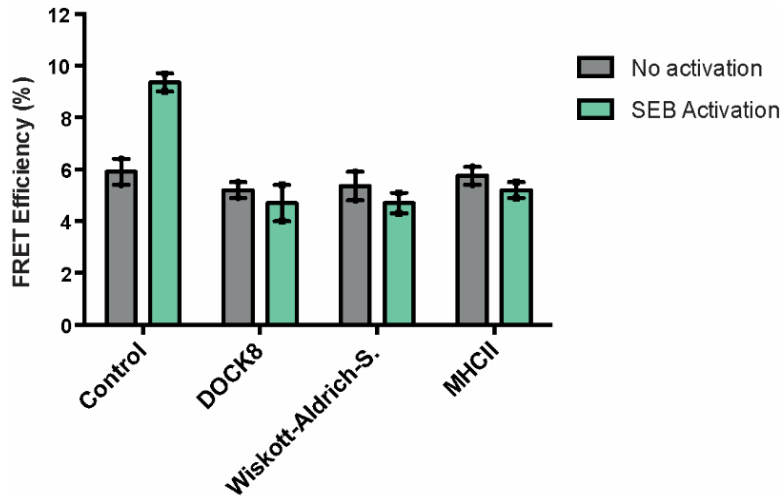


Figure 21: Detection of different immunodeficiencies in patients using FRET Express Mode and analyzing the clustering of the CD3 coreceptors after treatment with $2 \mu\text{g}$ SEB. Patients were suffering from a DOCK8-deficiency, the Wiskott-Aldrich-Syndrome or a MHCII-deficiency. From: von Kolontaj et al., 2016¹¹.

For the immunocompromised patients, no increase in FRET efficiency could be detected after SEB activation. The patients suffering from a DOCK8 syndrome showed a change in FRET efficiency from 5.2 ± 0.3 to 4.0 ± 0.7 after the PBMCs were treated with SEB. The FRET efficiency of patients affected by the Wiskott-Aldrich-Syndrome changed from 5.4 ± 0.6 to 4.7 ± 0.4 , and patients suffering from a MHC class II deficiency had a change in FRET efficiency from 5.8 ± 0.4 to 5.2 ± 0.3 .

5.3.5 Lipid raft disruption

The integrity of lipid rafts of T cells was tested via the CD3 homoclustering FRET assay after different chemical treatments. Here, T cells were either not activated, stimulated with SEB for 1h and treated with bCD or cholesterol.

When measuring the median intensities of the donor (VioBlue), acceptor (FITC) and FRET channel (VioGreen), it could be observed that the intensity mostly did not change regardless of the T cell treatment (compare Figure 22). The mean VioBlue fluorescence intensity was 6.1 ± 0.23 when the T cell was not activated, 5.77 ± 0.53 after SEB activation, 6.01 ± 0.34

after SEB and bCD treatment. In a similar way, also the values for FITC hardly changed (14.09 ± 0.00 , no activation; 12.41 ± 0.01 , SEB activation; 13.02 ± 1.23 , SEB and bCD) and VioGreen (4.09 ± 0.12 , no activation; 3.94 ± 0.23 , SEB activation; 3.77 ± 0.28 , SEB and bCD). Only the cells that were treated with cholesterol showed higher fluorescence intensities in all the fluorescent channels (VioBlue: 8.06 ± 0.04 , FITC: 15.54 ± 0.93 , VioGreen: 4.99 ± 0.07).

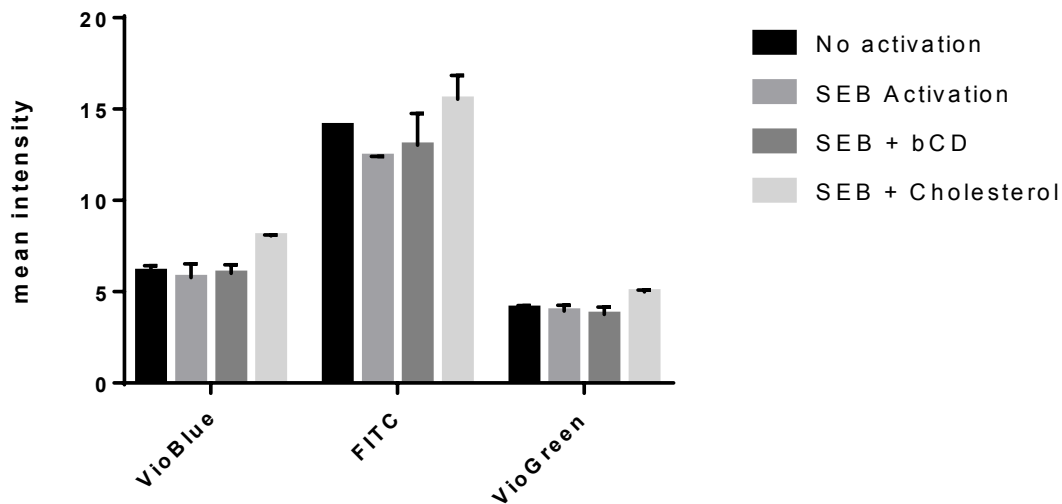


Figure 22: Mean fluorescence intensity of VioBlue, FITC and VioGreen after different T cell treatments affecting the lipid raft integrity. n=2 biological replicates.

However, when comparing and calculating the FRET efficiencies after the different treatments, it could be measured that after SEB activation, the FRET efficiency increased from $4.03\% \pm 0.51$ to 5.73 ± 0.34 . After treatment with bCD, the FRET efficiency was strongly decreased to -1.5 ± 3 . When the PBMC were treated with cholesterol, the FRET efficiency was 2.5 ± 1.43 and therefore comparable to the FRET efficiency measured if the T cell was not activated.

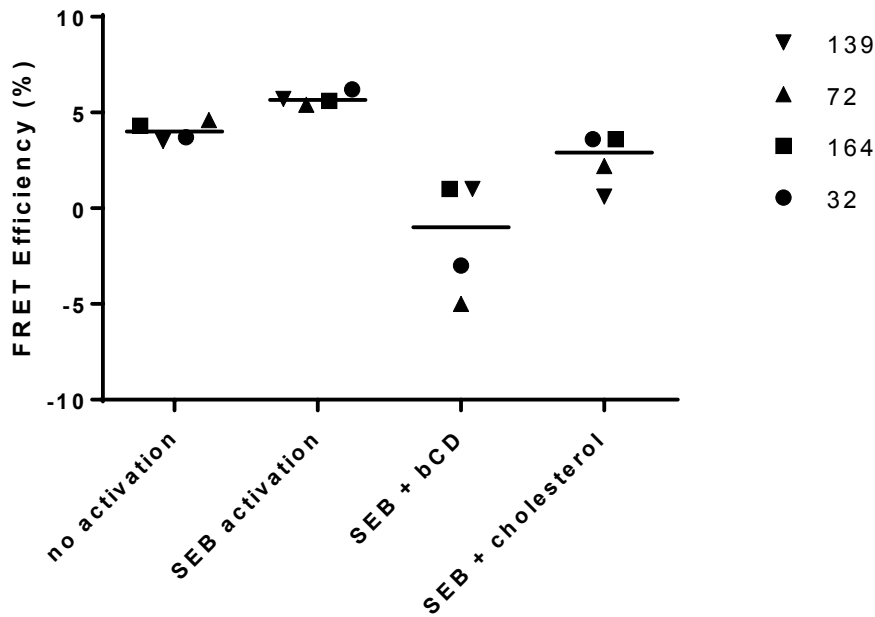


Figure 23: FRET efficiency after T cell stimulation via SEB and bCD or cholesterol treatment for n=4 blood donors. The diagram shows the correlation between lipid raft integrity and the corresponding FRET efficiency for CD3 homocustering.

In the next experiment, the FRET efficiency was determined over a time course of three hours. Here, also a T cell sample that was treated with nystatin was included.

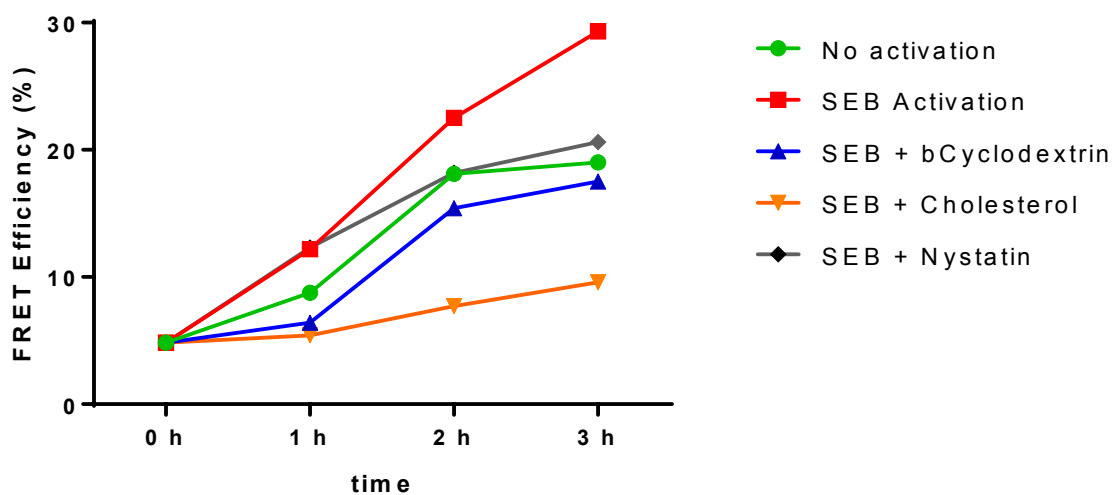


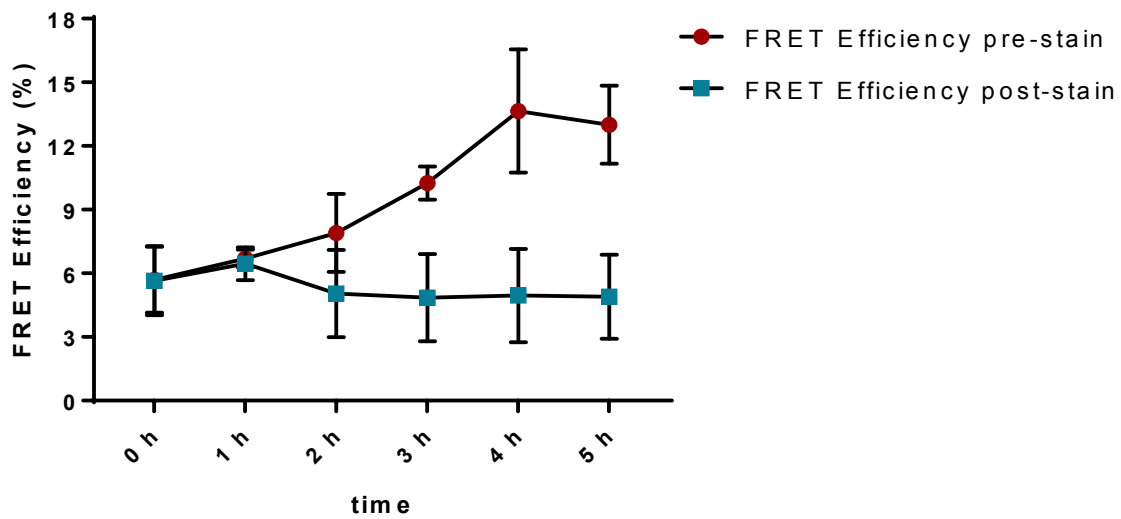
Figure 24: FRET efficiency after 0-3h treatment of T cells with SEB or other substances that are known to have an impact on lipid raft integrity. FRET efficiency was determined for CD3 homocustering after the given time intervals.

The increase in FRET efficiency was highest for the PBMCs that were stimulated with SEB and not treated any further (from 4.84% to 29.3%). T cells that were stimulated with SEB and treated with nystatin or bCD showed a similar increase in FRET efficiency as the T cells that were not activated at all (to 19.0 for no activation, 17.5% for SEB and bCD and 20.6% for SEB and nystatin). Only T cells that were activated with SEB and treated with cholesterol almost showed no increase at all in FRET efficiency when comparing the time points 0 h (4.84% FRET efficiency) to 3 h stimulation (9.6% FRET efficiency).

5.3.6 Long term dynamic rearrangement of the CD3 coreceptor

In order to analyze the long-term changes in FRET efficiency, PBMCs were stimulated with SEB for the given time points and either stained with the VioBlue and FITC FRET conjugates before or after the stimulation.

a)



b)

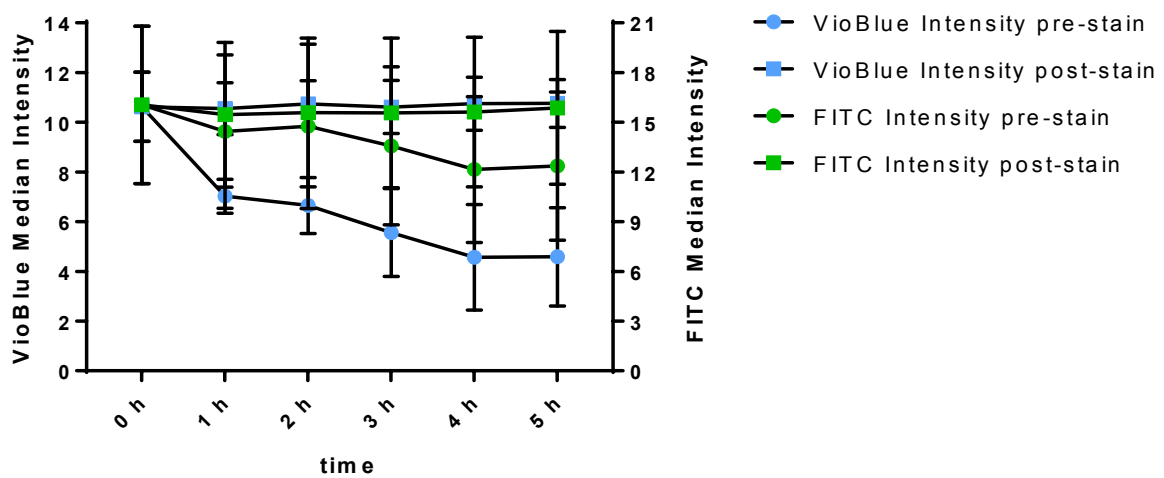


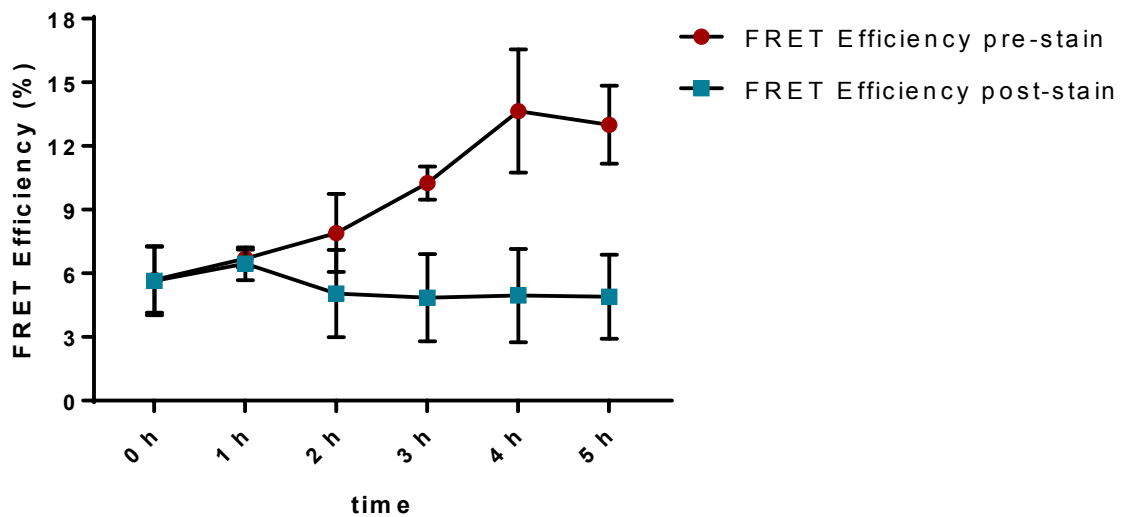
Figure 25: Long-term changes in FRET efficiency, compared to the median fluorescence intensity of VioBlue and FITC after T cell stimulation with SEB. The cells were either stained for CD3 with the FRET antibody conjugates before or after SEB stimulation for the given time points.

We could observe a constant increase in FRET efficiency over time in case the T cells were stained with the antibody conjugates before SEB stimulation. Here, the FRET efficiency

Results

constantly increased from $5.7\% \pm 1.1$ up to $13.0\% \pm 1.3$. However, if the T cells were stained after the T cell stimulation for the indicated time points and were analyzed for FRET, the FRET efficiency after 5 hours of stimulation ($4.9\% \pm 1.4$) was comparable to the FRET efficiency that was determined if the cells were not activated ($4.9\% \pm 1.4$). Only for a very short period of time (1h) after T cell activation, an increase in FRET efficiency could be measured, where the FRET efficiency increased to $6.45\% \pm 0.55$.

This effects could be supported by determining the median fluorescence intensity of the VioBlue and FITC conjugates (



b)

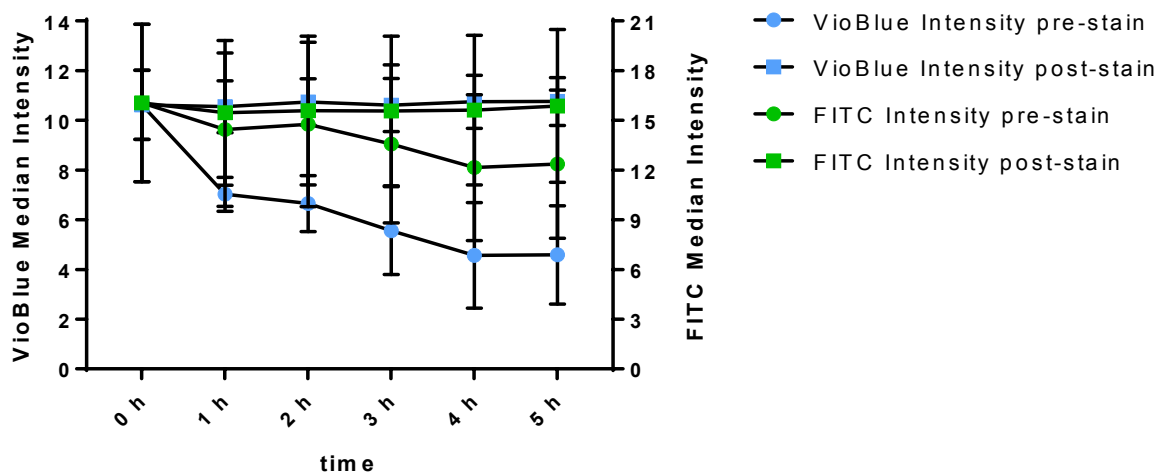


Figure 25 B). When the T cell was stained before stimulation, the FITC median intensity constantly decreased over time (from 16.05 ± 3.36 to 12.36 ± 3.17 after 5 h). This effect was even more pronounced for the VioBlue conjugate. Here the decrease in intensity was even stronger, with the median VioBlue intensity decreasing from 10.62 ± 0.98 at time point 0 to 4.59 ± 1.4 after 5 h of stimulation. When the T cells were stained after stimulation, no decrease in fluorescent intensity for both the VioBlue and FITC conjugate could be observed. The median fluorescent intensity was 10.63 ± 0.99 (VioBlue) and 16.05 ± 3.36 (FITC) at time point 0, and 10.76 ± 0.68 (VioBlue) and 15.87 ± 3.26 (FITC) after 5 hours of SEB stimulation.

5.4 Immune checkpoint inhibition

For immune checkpoint inhibition, the clustering of CD3 with PD-1 was determined via FRET using the FITC and VioBlue FRET pair.

5.4.1 PD-1 expression on T cells

PD-1 expression after T cell stimulation was determined for PBMCs of two blood donors and evaluated for the percentage of PD-1-positive cells and PD-1 median intensity.

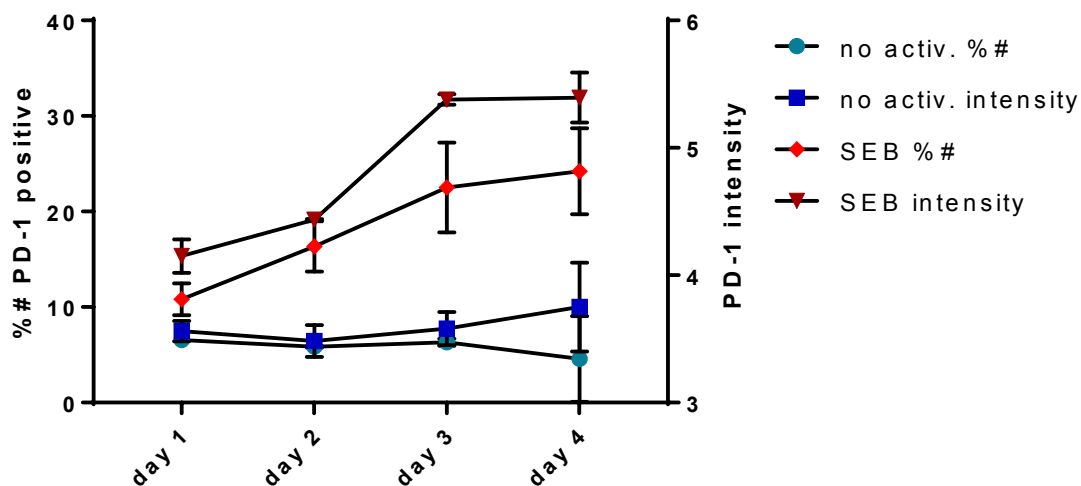


Figure 26: PD-1 expression on T cells after SEB stimulation as assessed via staining with an anti-PD-1 fluorescent antibody conjugate. The proportion of positively stained cells is compared to the median fluorescence intensity.

Both blood donors responded slightly heterogeneously to SEB stimulation regarding their expression of PD-1. However, we could observe an increase in the amount of PD-1 positive cells for both donors the longer the PBMCs were stimulated with SEB from $10.82\% \pm 1.18$ positive cells at day 1 to $24.21\% \pm 4.5$ PD-1 positive cells at day 4. If the cells were not stimulated with SEB, the amount of PD-1 positive cells remained constant with $6.56\% \pm 0.66$ PD-1 positive cells at day 1 and $4.58\% \pm 4.48$ positive cells at day 4. Also the PD-1 intensity increased from 4.15 ± 0.13 at day 1 to 5.4 ± 0.2 at day 4. If the T cells were not activated, the PD-1 intensity remained relatively constant from day 1 (3.56 ± 0.08) to day 4 (3.75 ± 0.35)

5.4.2 PD-L1 and PD-L2 expression on antigen presenting tumor cell lines

In order to find the best antigen presenting cell line to induce PD-1 expression and its clustering with the CD3 coreceptor on T cells, several cell lines were screened for PD-L1 and PD-L2 expression.

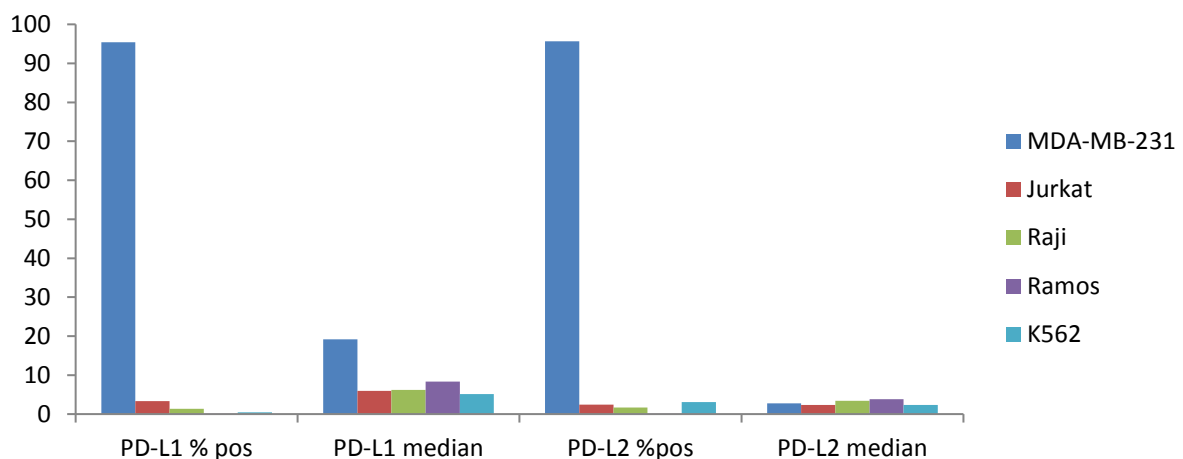


Figure 27: PD-L1 and PD-L2 expression on different tumor cell lines. Different tumor cell lines were stained with anti PD-L1 and PD-L2 fluorescence antibody conjugates and the proportion of positive cells as well as the median fluorescence intensity is shown.

We found the cell line MDA-MB-231 the highest PD-1 ligand expressing cell line for both PD-L1 and PD-L2. Here, almost all cells were tested to be positive for PD-L1 (95.42%) and PD-L2 (95.62%), compared to all other cell lines, that did not exceed 10% positive cells for both PD-L1 and PD-L2. Also the median fluorescence intensity was highest for the MDA-MB-231 cell line with a median intensity of 19.22, compared to a median intensity ranging from 5.13 to

8.3 for all other tested cell lines. The marker PD-L2 was found to be not that highly expressed on all cell lines. Here, the median fluorescent intensity ranged from 2.33 to 3.85 for all cell lines.

5.4.3 T cell isolation and its effect on FRET efficiency

To validate that the increase in FRET efficiency after stimulation with SEB is derived from structural rearrangements of the receptors on the T cell and not any other cell type that can be found in PBMCs, different separation methods and treatments of T cells were tested here. For this, the T cells were separated using two different approaches: the Pan T cell isolation kit and the DC isolation kit that was modified into a depletion kit. The cells were either cultivated as PBMCs, as pure isolated T cells or in co-cultivation with the tumor cell line MDA-MB-231 and either stimulated with SEB or left untreated.

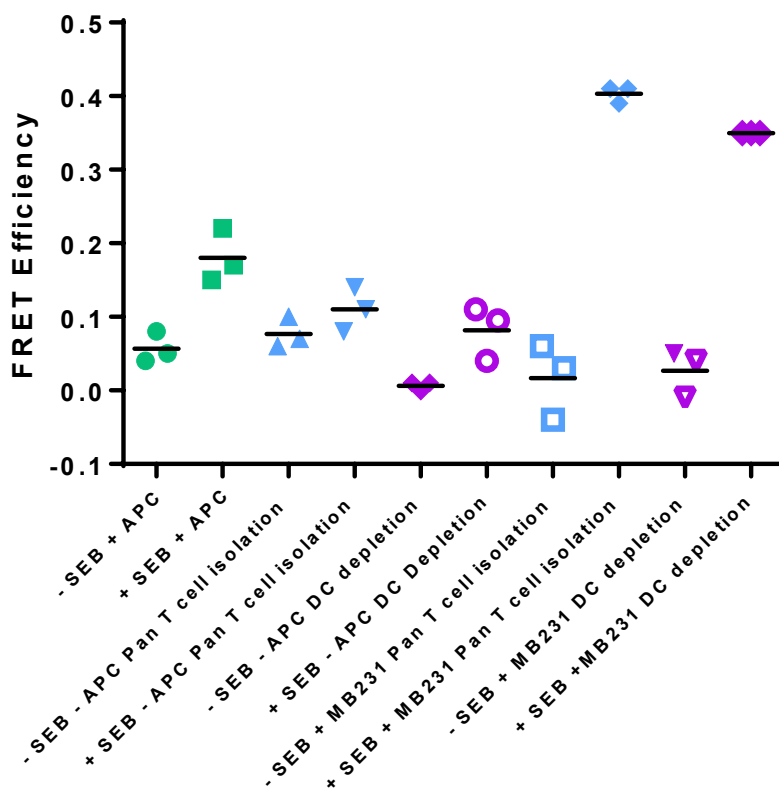


Figure 28: FRET efficiency for CD3 and PD-1 clustering after different T cell isolation protocols and under different culture conditions for n = 3 biological replicates. The T cells were either plated as complete PBMC or isolated according to the isolation kits described above and co-cultured with the MDA-MB-231 tumor cell line +/- SEB as indicated.

We could measure that for pure T cells the treatment of SEB could increase the FRET efficiency only marginally (from $3.8\% \pm 0.07$ to $6.52\% \pm 1.28$ for Pan T cell isolation and from $5.2\% \pm 0.08$ to $5.6\% \pm 0.18$ for the DC depletion protocol). The increase is less pronounced than the increase in FRET efficiency that can be observed for the treatment of PBMCs with SEB (from $0.99\% \pm 0.04\%$ to $5.97\% \pm 0.1$). Co-cultivation of the T cells with the tumor cell line MDA-MB-231 even further decreased the FRET efficiency if the T cells were not activated. Here the FRET efficiency was $4.57\% \pm 0.64$ for Pan T cell isolation and $3.44\% \pm 0.1$ for the DC depletion protocol. However, as soon as the T cells were both co-cultivated with MDA-MB-231 cells and stimulated with SEB, the FRET efficiency increased strongly to $9.64\% \pm 0.36$ for the Pan T cell isolation kit and to 10.24 ± 0.01 for the DC depletion protocol.

5.4.4 PD-1 CD3 FRET and PD-L blocking

In the next test, the PD-1 ligands PD-L1 and PD-L2 were blocked using specific blocking antibodies and the impact on the fluorescence intensity of PD-1 and the FRET efficiency for CD3-PD-1 clustering on PBMCs was determined.

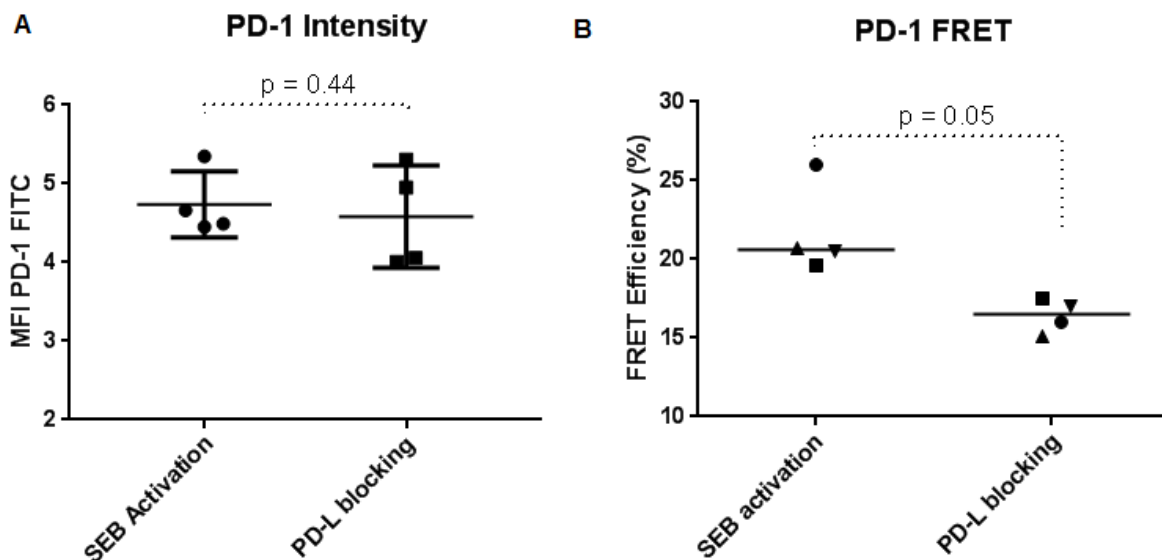


Figure 29: Blocking of PD-L1 and PD-L2 and the impact on PD-1 median fluorescence intensity (A) and PD-1 CD3 FRET (B). n = 4 biological replicates. PBMCs were stimulated with SEB and either treated with the anti PD-L1 and PD-L1 blocking antibodies or left untreated.

The median fluorescence intensity for PD-1 was comparable for both conditions. T cells that were stimulated with SEB showed a fluorescence intensity of $4.74\% \pm 0.21$, and T cells that were both stimulated with SEB but treated with PD-L1 and PD-L2 blocking antibodies had a median fluorescence intensity for PD-1 of $4.58\% \pm 0.33$. However, when the same cells were analyzed for their FRET efficiency for PD-1 and CD3 clustering, the FRET efficiency for SEB activation only was higher ($E = 21.7\% \pm 1.45$, $p = 0.05$) than for the cells that were furthermore treated with the PD-1 ligand blocking antibodies ($E = 16.4\% \pm 0.53$).

5.4.5 Impaired signaling on T cell lines

Cell lines do normally not show such a high donor variation as primary cells do and furthermore they have the advantage that they are easier to obtain and to culture in large scales. For that reason, the clustering of CD3 and PD-1 was determined by measuring FRET on two different T cell lines, namely Jurkat cells and HuT-78 cells.

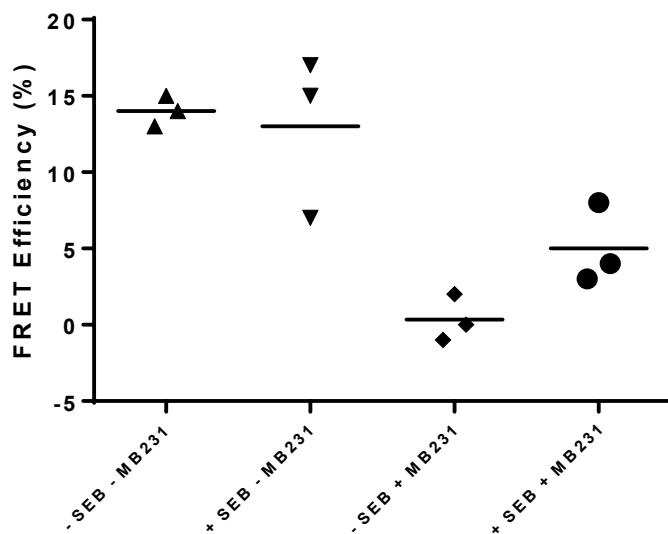


Figure 30: FRET efficiency for the CD3-PD-1 interaction on Jurkat cells after SEB stimulation for $n = 3$ technical replicates. Jurkat T cells were co-cultured with MDA-MB-231 cells and treated with SEB as indicated.

On Jurkat cells, the FRET efficiency did not increase when the pure Jurkat cells were stimulated with SEB ($E = 14\% \pm 0.58$ for no activation and $E = 13\% \pm 3.06$ FRET when treated with SEB). The FRET efficiency further decreased when the Jurkat cells were co-cultivated with MBA-MB-231 cells to $0.33\% \pm 0.82$ FRET efficiency. After co-cultivation with the tumor

cell line and SEB stimulation, the FRET efficiency was still decreased compared to untreated Jurkat cells ($E = 5\% \pm 1.53$).

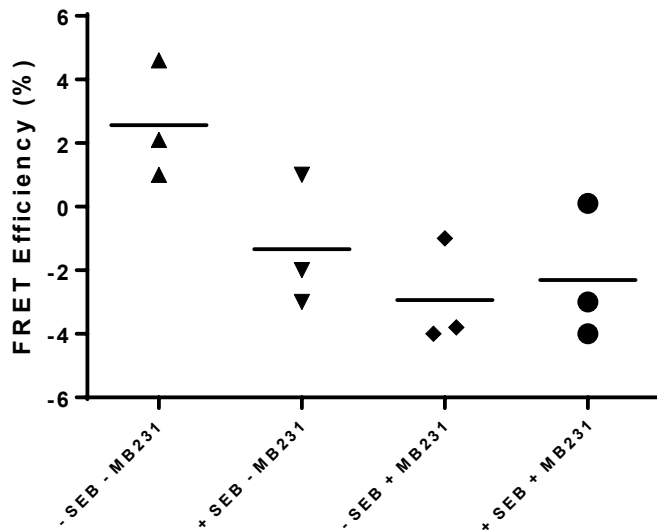


Figure 31: FRET efficiency for CD3-PD-1 interaction on HuT-78 cells after SEB stimulation for $n = 3$ technical replicates. Here, HuT-78 T cells were co-cultured with MDA-MB-231 cells and treated with SEB as indicated.

A similar effect could be observed for the HuT-78 T cell line. Also here the FRET efficiency decreased from $2.57\% \pm 1.07$ to $-1.33\% \pm 1.2$ when the pure HuT-78 cells were treated with SEB. After co-cultivation with MDA-MB-231 cells the FRET efficiency further decreased to $E = -2.93\% \pm 0.97$. When the HuT-78 cells were co-cultured with the tumor cell line and treated with SEB, FRET efficiency was still decreased with $2.3\% \pm 1.23$ FRET efficiency compared to untreated pure HuT-78 cells.

5.4.6 Downscale of the PD-1 CD3 FRET assay for a screening approach

As the PD-1 FRET assay should allow for a compound screening on substances that inhibit the clustering of CD3 with the PD-1 receptor on T cells and therefore rescue the immune response, the assay was transferred to buffy coats instead of whole blood and downscaled to a 384-well plate format. T cells were isolated from the buffy coats using the Pan T cell isolation kit.

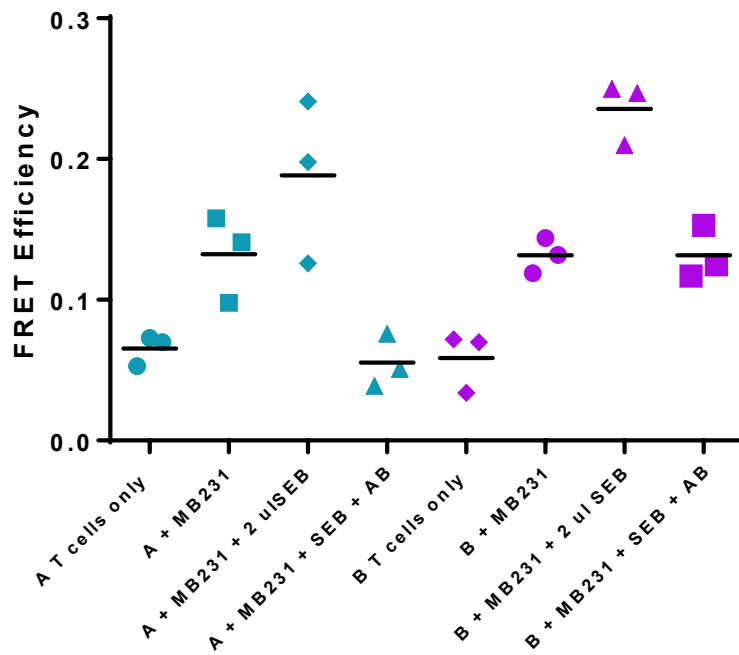


Figure 32: FRET efficiency for CD3 and PD-1 clustering in the downscaled screening approach. For two different blood donors (buffy coats), each $n = 3$ technical replicates. The isolated T cells were co-cultured with MDA-MB-231 cells and treated with SEB as indicated. PD-L1 and PD-L2 were blocked via specific antibodies in case of (+AB).

Here the FRET efficiency increased for both blood donors when the T cells were co-cultured with the MDA-MB-231 cell line from 0.07 ± 0.01 to 0.13 ± 0.02 (donor A) and from 0.06 ± 0.01 to 0.13 ± 0.01 for donor B, respectively. When the T cells were co-cultivated with the tumor cell line and activated with SEB, the FRET efficiency further increased to 0.19 ± 0.03 (donor A) and 0.24 ± 0.01 (donor B). This increase in FRET efficiency could be inhibited when the cells were treated with blocking antibodies directed against PD-L1 and PD-L2. Here, the FRET efficiency was decreased again to 0.06 ± 0.01 for donor A and 0.13 ± 0.01 for donor B.

Confocal images confirmed a slightly increased PD-1 expression when the T cells were co-cultured with MDA-MB-231 tumor cells (see Figure 33). However, hardly any areas that are double positive for both markers (orange) can be found here. After an additional SEB stimulation the PD-1 expression further increased and the proportion of colocalization seemed higher compared to non-activated T cells. When the T cells were treated with the blocking antibodies directed against the ligands of PD-1, PD-1 expression was still high. However, the distribution of this receptor seemed more diffuse and did not correlate with the CD3 receptor location.

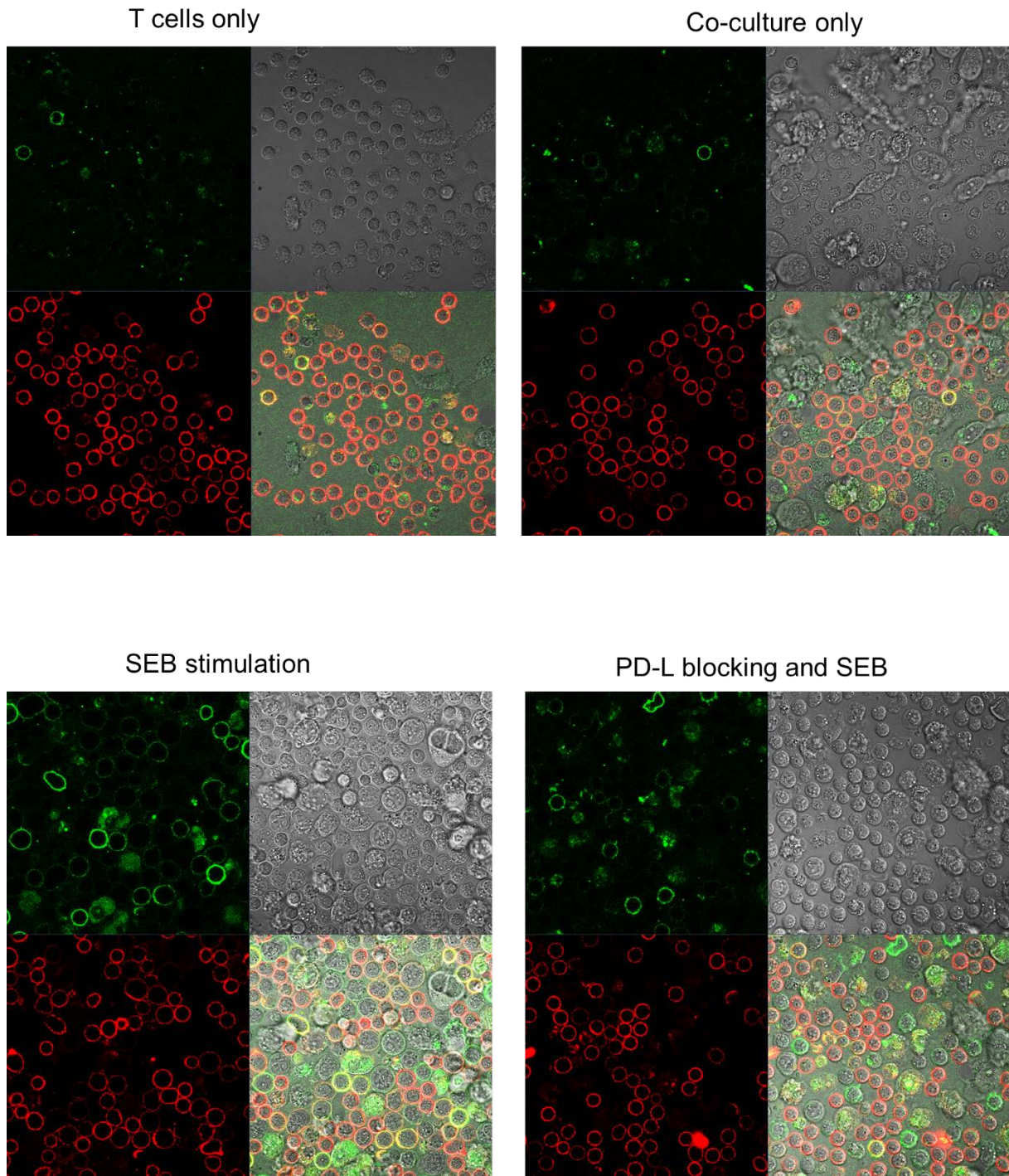


Figure 33: Confocal analysis of CD3 and PD-1 colocalization after different treatments. PD-1 was stained with a FITC-conjugated antibody (green) and CD3 with an APC-conjugated antibody (red).

6. Discussion

6.1 FRET analysis program validation

To validate the results that were generated using the FRET express mode, we produced FRET calibration beads that had different molecular ratios of donor to acceptor antibody conjugates. As it could be expected according to Fábíán et al.⁹⁰, the FRET efficiency increased with the increase of acceptor to donor ratio, as there is a higher likelihood for the energy to be transferred from a donor molecule to an acceptor molecule.

The results of the FRET analysis program for the calibration beads were also highly comparable to the results obtained via conventional FRET analysis as here the ReFlex FRET analysis program had been used⁴. Due to the high correlation of 0.9993, we could show that the results that are obtained using the FRET analysis program are precise and therefore the program can be used for the evaluation of biologic questions on molecular interactions⁹².

6.2 CD3 and CD4 interaction

The FRET program was used to determine the interaction between the T cell receptor/CD3 complex and the CD4 coreceptor after SEB activation of human T lymphocytes. We could prove that the FRET efficiency for the FITC and VioBlue FRET pair increased after stimulation, as the SEB unspecifically crosslinks the MHCII receptor of the APC and the TCR/CD3 complex on the T cell, causing structural rearrangements on the cell surface.

Yet, in all the analyses, doublet cells were excluded. The reason for this is that because during measurement on the flow cytometer, the interacting cells are pulled apart by the sheath fluid and are therefore present as single cells during sample acquisition.

In general, differences in the FRET efficiency results between the individual blood donors were measured. This can be explained by individual expression level of the V β 3 chain⁹³ on the leukocytes of each blood donor. As SEB is binding to this specific TCR chain, the more V β 3 chains are expressed by one donor, the stronger is the T cell activation by *Staphylococcal* enterotoxin B and therefore the FRET efficiency increased. Furthermore, as SEB only activates approximately 30% of the total T cell population⁹⁴, the FRET efficiency median results here only represent the average of the overall increase in FRET efficiency for the total T cell population of one blood donor and not specifically for the T cells that were

activated via SEB. This further explains the reason why the increase in FRET efficiency is not highly pronounced in this model.

6.2.1 Colocalization on the confocal laser scanning microscope

The colocalization of the CD3 coreceptor and CD4 receptor on T cells that were activated with SEB was also analyzed via confocal laser scanning microscopy. Here, the CD3 coreceptor was stained with a FITC conjugate and CD4 receptor with an APC conjugate. In general, the scope of the curve for both the FRET efficiency and the colocalization coefficient for the colocalization of CD3 and CD4 before and after SEB stimulation were highly comparable, indicating that the FRET assay is an adequate assay to determine molecular interaction. This is further supported when the colocalization controls are taken into account. Here, the colocalization coefficient results for the 2 minute SEB stimulation for the CD3 and CD4 interactions are approaching the value of the positive controls (CD3 and CD45 or CD3 and TCR $\alpha\beta$ without SEB stimulation) and after 5 hours of SEB stimulation, the colocalization coefficient is comparable to the negative colocalization control values (CD3 and CD45 after SEB stimulation for no colocalization). However, here the great advantage of this method is that the determination of molecular interactions using the FRET assay is much more accurate than determining colocalization on the confocal microscope, as the resolution of the FRET assay is much higher with approx. 10 nm compared to approx. 200 nm on the confocal microscope⁹⁵.

Additionally, the confocal images revealed phenotypic changes of the receptor distribution after SEB stimulation. When the T cell was not activated, the CD3 and CD4 receptors were regularly distributed on the cell membrane. After the short activation with SEB for two minutes, small activation clusters of CD3 and CD4, so called microclusters, begin to form. However, as the resolution of the confocal microscope is not high enough to determine such small distances, the changes are hardly visible by eye. Yet, this difference can precisely determined via FRET, as here the FRET efficiency increased significantly. After five hours of incubation, large clusters of the CD3 coreceptor have formed. They build up the immunological synapses to the antigen presenting cells. The CD4 receptor staining is very dim in this picture, indicating that most of the CD4 coreceptor was internalized and degraded inside the cell. This further supports the strong decrease in FRET efficiency after 5 hours of SEB stimulation.

Altogether, this comparison between the FRET assay and colocalization analysis on the confocal microscope shows that there are no artifacts produced by FRET analysis for protein-protein interactions, but instead that the FRET analysis is a much more specific assay than the colocalization measurement on the confocal laser scanning microscope.

6.3 CD3 homoclustering FRET

The homoclustering of the CD3 receptor after T cell activation via SEB was determined using two different FRET pairs, VioBlue with FITC as well as Alexa Fluor 488 with Alexa Fluor 555. The data shows that for both FRET pairs, we can measure an increase in FRET efficiency after T cell stimulation that is caused by the reduced spatial distance between the CD3 receptors during the formation of the CD3 nanoclusters. Furthermore, the increase in FRET efficiency can be blocked when a blocking antibody that is specifically directed against the T cell binding domain of the SEB molecule⁸⁸. This effect is not only pronounced when the SEB is pre-incubated with the blocking antibody before it is added to the T cells, but also to a lesser extent inhibits the T cell activation when the blocking antibody is added in parallel with the SEB to the cells. This indicates for a successful inhibition of T cell activation due to the blocking antibody that can also be determined using the FRET assay. Therefore, we could show that determining T cell activation using CD3 homoclustering FRET is a sensitive and also precise tool.

Differences between the two different FRET pairs regarding the absolute FRET efficiency results are likely to be due to biological differences, as both FRET pairs are normalized in the FRET calculation for relative energy transfer and the flow cytometer instrument is calibrated on a daily routine.

6.3.1 CD3 homoclustering versus T cell activation measurements

When we compared the FRET assay to other common methods that are used to determine T cell activation, we could show that the increase in FRET efficiency is indeed induced by the structural rearrangements as the T cell is activated here that are required to trigger intracellular T cell activation signaling.

We determined the cytokine secretion by using the MACSPlex cytokine secretion kit. Here we could measure an increase in secreted cytokine concentration after 24 stimulation with

SEB. The measured cytokines GM-CSF, IFN- γ , IL-2, IL-6 and TNF- α are positively correlated with T cell activation. Therefore, the increase in cytokine concentration that the T cell was successfully activated via SEB and that the T cell activation determined here also correlated with the activation status of the T cell that was determined via FRET.

Likewise, we determined the calcium influx into the cytoplasm as this method is commonly used as one of the very early cell activation markers. Here, eFluor 514 calcium indicator dye was used to measure the relative calcium influx into the cytoplasm of the T cell. For that reason, different activation methods were compared. First, the cells were stimulated with SEB as described previously. Furthermore, the T cells were activated with the TransAct beads, which have the CD3 and CD28 antibodies coupled onto two separate nanobeads. It was expected that their special features facilitate the clustering of CD3 and CD28 on the cell membrane and lead to strong T cell activation⁹⁶. We could observe that for those two T cell activation methods both the FRET efficiency and the calcium intensity increased. However, the increase in FRET efficiency was even faster than the calcium influx. This can be explained by looking at the order of structural rearrangements taking place after T cell activation. Indeed, the formation of the CD3 microclusters that we could measure via FRET is required to trigger the calcium influx into the cell⁹⁷. For that reason, we concluded that the CD3 homoclustering FRET assay is not only an adequate tool to measure T cell activation, but that it is working in an even faster fashion than intracellular calcium influx measurements.

6.3.2 CD3 clustering as a diagnostic marker

After we could validate that we can use the FRET assay measuring the homoclustering of the CD3 coreceptor to successfully determine T cell activation, we tested if we could also detect defects in the structural rearrangements in immunocompromised patients using this FRET assay. In healthy control samples, the increase in FRET efficiency after SEB activation was strongly pronounced as it was in the last experiments. But indeed, we could not measure the increase in FRET efficiency after T cell stimulation with SEB for patients suffering from diseases that impair cytoskeletal rearrangements (DOCK8-deficiency and Wiskott-Aldrich-Syndrome) or even more upstream are impaired in a proper activation of the T cell (MHCII-deficiency patients).

Therefore, the CD3 homoclustering FRET assay can be used to detect defects in structural rearrangements also in clinical settings.

Common laboratory tests for those diseases include for example immune globulin level determination, functional tests of the immune cells and genetic sequencing⁹⁸.

However, those tests are usually time laborious and have a high workload on the personnel. An automated FRET assay that detects impairments in the structural rearrangements might offer a fast alternative and simple alternative for the diagnosis of those diseases.

6.3.3 Lipid raft manipulation

The CD3 coreceptor is described to be organized in lipid rafts. Lipid rafts are built up mainly from cholesterol and play a major role in the organization of cell surface proteins and receptors. We manipulated those lipid rafts via different substances that are described to have an impact on the concentration or fluidity of cholesterol in order to determine the impact of the lipid raft integrity on CD3 homoclustering as measured via FRET. First, we compared the mean intensity values for the CD3 coreceptor staining for the FITC and VioBlue conjugate and also in the VioGreen channel. Here it was obvious that for all treatments (no activation, SEB activation and bCD) the intensities were comparable, so the general expression level of the receptor did not change. Only when the cells were treated with additional cholesterol, all intensities were slightly increased, but only to a small extend. This might be caused by the high concentration of cholesterol that may slightly inhibiting the recycling process of the CD3 receptor⁹⁹.

However, when we dissolved the lipid rafts using bCD⁴⁹, the we could observe that the FRET efficiency was strongly decreased, even compared to non-activated T cells. The bCD might therefore have increased the distance between the CD3 molecules on the cell surface, so that they cannot successfully transfer the energy between the single FRET dyes anymore. For that reason, it can be concluded from this experiment that already before T cell activation, the CD3 molecules are pre-arranged in smaller clusters in lipid rafts, that will form larger clusters as soon as the T cell is activated¹⁰⁰. On the other side, when the cells were treated with cholesterol, the FRET efficiency after SEB stimulation was comparable to the one measured when the T cell was not activated at all. It is described that high concentrations of cholesterol may decrease the fluidity of lipid rafts¹⁰¹. As a consequence, this might impair the CD3 molecules within the lipid rafts in being arranged into close spatial distance after T cell stimulation and therefore to no increase in FRET efficiency.

In the next experiment we analyzed the long-term effect of lipid raft manipulation over 3 hours. Here, we also included nystatin to change the lipid raft behavior. Nystatin chelates the cholesterol molecules within the lipid raft and therefore deregulates its structure. Here, all the different treatments (bCD, cholesterol, nystatin) that disrupt the lipid raft integrity, reduced the FRET efficiency after SEB stimulation compared to no lipid raft treatment. This effect was even more pronounced after a longer period of time of 2 to 3 hours.

Therefore, the FRET data do not only supports that the CD3 receptor is located and organized within lipid rafts. The CD3 homoclustering FRET assay can also be used to reveal those minor structural changes that are derived from varying lipid raft integrities on the cell surface.

6.3.4 CD3 homoclustering and long-term dynamic rearrangements

When we analyzed the change in FRET efficiency for CD3 homoclustering after long term stimulation of T lymphocytes with SEB, we could observe that the FRET efficiency constantly increased among with an increased stimulation of the cells while the median fluorescence intensity of the FRET dyes decreased over time. However, we could only measure this effect when we stained the T cells before stimulation. In contrast, when we stained the T cells after stimulation immediately before the flow cytometry measurements, the median fluorescence intensity of the dyes staining the CD3 receptors remained constant, and so did the FRET efficiency over time. Comparing the data from those two different setups, we could conclude that the CD3 coreceptor is constantly degraded, but a remaining portion can be found in homoclusters on cell surface or even in intracellular vesicles. Comparing those data with the lipid raft dissolved experiment, the FRET flow cytometry assay does not only provide spatial information, but we could also detect the spatial dynamic changes of CD3 molecule arrangement on cell over time in their lipid rafts. At the same time, the CD3 receptors are also newly transcribed and expressed on the cell surface. We could conclude this from the post-activation staining data, as here the overall fluorescence intensity for CD3 remained constant.

Taking together this data and previously described results (compare Finetti et al., 2009¹⁰²), we developed the following model for the dynamic rearrangement of the CD3 receptor during T cell activation:

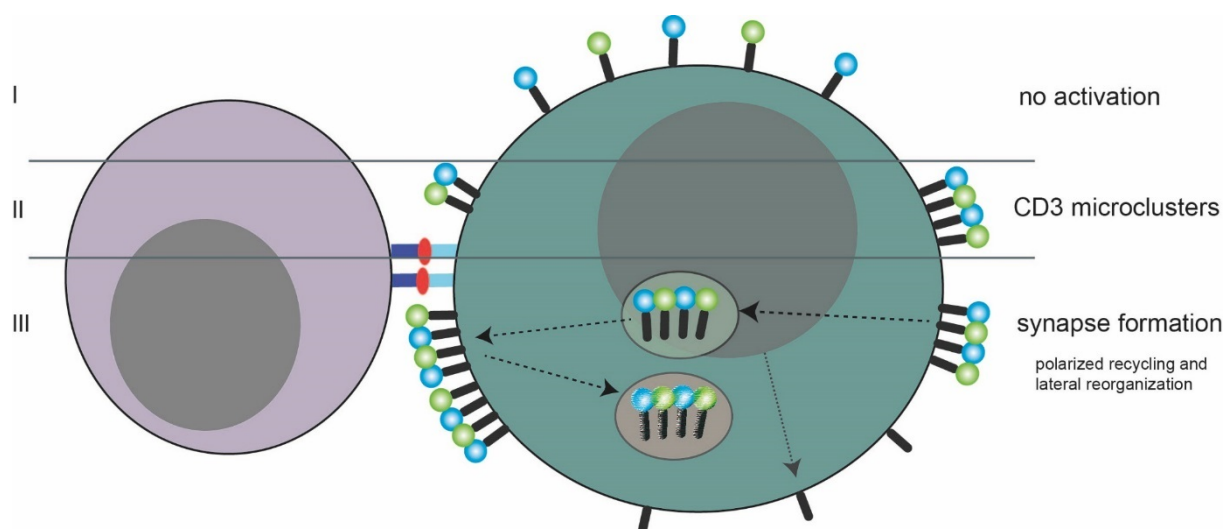


Figure 34: Model for dynamic rearrangement of the CD3 coreceptor on lipid rafts during T cell activation. The CD3 microclusters are recycled to the immunological synapse and partly degraded during this process. In the meantime, new CD3 receptors are transcribed and transported to the cell surface.

Before T cell activation, the CD3 receptors are equally distributed over the cell surface in their lipid rafts (step I, Figure 34: Model for dynamic rearrangement of the CD3 coreceptor on lipid rafts during T cell activation.). Immediately after the T cell becomes activated by the APC, CD3 microclusters are formed via lipid rafts, bringing the receptors into close proximal distance (step II). As the immunological synapse is further established and also during synapse maintenance, the CD3 receptor clusters are constantly recycled in a polarized manner to the site of the IS, either on the cell membrane via lateral reorganization and also via intracellular endosomal vesicles (step III). Some of those CD3 molecules are also degraded in endosomal compartments during this process. However, at the same time, new CD3 receptor molecules are transcribed and transported to the cell surface.

Further follow up experiments could support our model of the CD3 receptor recycling via intracellular vesicles. For example, the endosomal uptake could be inhibited by blocking substances such as dynasore¹⁰³. Measuring the FRET efficiency over a longer period of time should lead to more constant values and also unchanged fluorescence intensities. Moreover, comparing the FRET efficiency results to confocal images or image stream instrument data might prove the spatial reorganization that we can measure in the FRET assay. In addition, comparing the FRET efficiency for the dynamic changes of lipid raft proteins versus non-lipid raft protein after T cell stimulation might reveal the dependency of the cell's structural organization on lipid rafts.

6.4 Immune checkpoint inhibition

We did not only use the FRET assay to detect the activation of T lymphocytes. We also wanted to study the structural rearrangements that are required to suppress the immune response. It had previously been described that the ligation of the PD-1 receptor to its ligands PD-L1 and PD-L2 on the antigen presenting cell is successfully terminating the immune response of the T cell¹⁰⁴. It had also been discovered that during this process structural rearrangements are taking place on the cell surface, bringing the PD-1 receptor into close spatial distance to the CD3 coreceptor⁶⁸. This structural rearrangement is required to terminate the immune response. However, usually PD-1 is expressed at a very low level. For that reason, we stimulated the PBMCs from whole blood with SEB for a long period of time (up to 4 days), as here the PD-1 ligand can be expressed in the APCs that are present in the PBMC. We measured the increase in median fluorescence intensity of PD-1. Only after T cell stimulation, but not for non-activated T cells both the fluorescence intensity and the number of PD-1 positive T cells increased. Therefore, we decided that SEB is also suitable for our experiments to trigger PD-1 expression for later FRET assays.

Furthermore, we screened several tumor cell lines for the expression of PD-L1 and PD-L2 via flow cytometry. We found out that the breast cancer cell line MBA-MD-231 is the cell line with the highest proportion and expression level of both PD-L1 and PD-L2. For that reason, we used that cell line for the substitution of the autologous APCs if required in the FRET experiments.

6.4.1 PD-1 CD3 FRET and isolated T cells

In order to measure the clustering of PD-1 with the CD3 coreceptor, we used anti-PD-1 sFITC and anti CD3-VioBlue as antibodies for our FRET experiments.

We could show that when we stimulated T cells with their autologous APCs in the form of isolated PBMCs from whole blood, we successfully measured an increase in FRET efficiency compared to no activation. When we isolated the T cells from the PBMCs using two different isolation protocols, no strong increase in FRET efficiency could be measured after T cell activation. Therefore, the antigen presenting cell and also its expressed PD-1 ligands are assumed to be essential to induce the structural rearrangements of PD-1 on the cell surface. When we co-cultured the T cells with the MDA-MB-231 cell line we could also increase the FRET efficiency to a great extend. However, this was only true if SEB was added as a

stimulating agent to the cells. Therefore, also here the T cell stimulation seemed to be required to enable a successful clustering of PD-1 with the CD3 receptor. The tumor cell line was even more adequate for the CD3 and PD-1 clustering experiment, as here the FRET efficiency was much higher compared to the use of autologous APCs. This might be due to the very high expression of both PD-L1 and PD-L2 that the MDA-MB-231 was described and tested to be positive for^{105,106}.

This FRET assay can most probably also be applied on other checkpoint inhibitors like CTLA-4. For that reason, also for those receptors the clustering potency of this checkpoint inhibitor can be measured and from those results it can be derived whether the checkpoint inhibition is active or not. Furthermore different cell treatment protocols can be compared here.

It could also be of great interest to test a CRISPR/Cas9 library on the tumor cell line that is used as APC via the CD3 and PD-1 clustering FRET assay. This might help to identify genes that are both important for the PD-L expression and to induce the PD-1 and CD3 clustering that is initiating the termination of the immune response. In that way, different knock-out variants could be identified that might rescue the anti-tumor immune response and could serve as a basis for the identification of new anti-tumor drugs.

Finally, in order to test the clinical relevance of the CD3 and PD-1 clustering mechanism that is measured here, another interesting follow up experiment might be to repeat this test on tumor patient material. Here it one could test if the structural rearrangements do also have a clinical impact. For example, there could be a correlation between an impaired clustering of the CD3 and PD-1 receptors and a higher tumor prevalence due to that reason. It might also be worth testing if patients with a difference in CD3 and PD-1 as determined via FRET do show a difference in the response to checkpoint inhibitor anti-tumor therapy. If a difference could be found, this FRET assay could be used as a prognostic marker if or even as a test for which tumor therapy against which checkpoint inhibitor can be applied for one single patient.

6.4.2 PD-1 CD3 FRET and PD-L blocking

Next, we tested if we could inhibit the clustering of the CD3 and PD-1 receptors when we used antibodies that are specifically directed against PD-L1 and PD-L2. Here, we stimulated

PDBMCs with SEB and measured the impact of the blocking antibody on PD-1 ligand expression and on the FRET efficiency for CD3 PD-1 clustering. The blocking antibody had no impact on PD-1 expression as the median intensity of the anti-PD-1 sFITC conjugate was comparable for antibody treatment and untreated cells as determined via flow cytometry. However, we could identify a strong difference in FRET efficiency. Therefore, we could conclude that the blocking antibody successfully inhibits the clustering of the CD3 and PD-1 receptor on the T cell's surface that is required to terminate the immune response. This does imply that the anti-tumor response of the T cell could be restored by the application of the blocking antibody.

Also for this assay, there are be different follow up experiments that might support the efficiency of the FRET experiment that is used here and would be worth testing for. If the lipid rafts of the T cells were disturbed by using either bCD, cholesterol or nystatin, it could be expected that also here an impact on the FRET efficiency could be observed. The reason for that is that the fluorescent dyes labeling the CD3 and PD-1 receptors on the cell surface will not be clustered in such a close spatial distance as compared to completely functional lipid rafts considering the molecular impacts of the lipid raft modifying substances as it is described in 6.3.3.

Furthermore, if the endosomal uptake was blocked in this experimental setup, for example by using chemicals like Dynasore, the FRET efficiency is supposed to remain at a high or even increased level over an increase of time. Here, the blockade of the endosomal uptake will inhibit the degradation especially of the CD3 coreceptor, but also the downregulation of the PD-1 receptor on the T cell's surface. As a result, CD3 and PD-1 will either remain in close special distance, or the density of the two receptors might even increase as new receptors are transcribed and transported to the cell surface. This will increase the likelihood of energy being transferred between the fluorescent dyes and therefore lead to the increase in FRET efficiency.

As mentioned in 2.5.1 Pharmaceutical use immune checkpoint inhibition modulators the PD-1 directed antibody immunotherapy show a good efficiency in many different kind of tumors and there are constantly new tumor subtypes that are tested to respond to this therapy in ongoing clinical trials¹⁰⁷⁻¹¹⁰.

However, because of the sometime very severe side effects that can be observed under the PD-1 directed immunotherapy¹¹¹, there is still a great unmet need for new substances that

are safer in their application for the patient. There is only one therapeutic antibody, atezolizumab (trade name: Tecentriq) that is directed against PD-L1 and has recently been approved by the FDA for the treatment of urothelial carcinoma¹¹².

This FRET assay might offer a fast and simple platform to screen for those substances⁷ that restore the T cell's immune function. Here we can clearly differentiate if a substance inhibits the T cell's immune response by measuring the structural rearrangements on the cell surface that are required for the inhibition of the immune response. Probably this assay might help to find substances that influence the checkpoint inhibition via a different mode of action, so that not only antibodies but also small molecules could be used as therapeutic agents.

6.4.3 Downscale of the PD-1 CD3 FRET for screening purposes

We transferred the FRET assay for measuring the interaction between CD3 and PD-1 on the cell surface of T lymphocytes as described previously into a smaller scale, using 0.5% of the cell volume that were used in the previously described PD-1 and CD3 clustering assay in a 384-well plate format. Here, the T cells were isolated from buffy coats instead of whole blood in order to achieve a higher yield in total cell number per blood donor.

We could observe that the FRET efficiency only increased if the tumor cell line was present compared to pure isolated T cells. As expected, the FRET efficiency was highest for SEB stimulation of the T cells that were co-cultured cells with the MDA-MB-231 tumor cell line, because here the PD-1 checkpoint inhibition is supposed to occur due to the long T cell activation. When we blocked the checkpoint inhibition by applying antibodies that were directed against PD-L1 and PD-L1, the FRET efficiency was strongly decreased again for both blood donors.

Those flow cytometry FRET results could be confirmed by confocal images in which PD-1 and CD3 were fluorescently labeled. PD-1 expression was very dim for pure T cells, but increased after the T cells were co-cultured with MDA-MB-231 tumor cells. However, PD-1 and CD3 only colocalized when those co-cultured cells were stimulated with SEB. This corresponds to the increase in FRET efficiency that we could also measure under this conditions. Also here, when the tumor cell line was treated with the blocking antibodies that are directed against the PD-1 ligand, the colocalization of PD-1 and CD3 strongly decreased although the expression level of PD-1 did not change.

The data that is discussed here is very consistent with the results that were obtained in the experiments that were performed without the downscale approach. Therefore, we could conclude that the downscaling of this experimental approach and also the T cell isolation from buffy coats instead of whole blood was successful and can be used for screening purposes.

Even so, if one would detect a potential hit for a substance where the FRET efficiency was significantly reduced due to the clustering of PD-1 and CD3 on a T cell, the results will have to be handled with great care. The reason for this is that the substances that are to be screened might have wide-ranging impact on general cellular behavior and performance, as those substances might not only target the rearrangement of the PD-1 receptor directly, but may also impact any upstream processes in the cell that could be essential for cell survival. Therefore, further methods should be applied for a hit substance in order to validate that the checkpoint inhibition pathway is targeted specifically.

Beyond that, to prove the functionality of this FRET screening approach for clinical drug discovery, an antibody that is already used in the clinical setting for the treatment of patients could be tested as a positive control. Until now, there is only one PD-1 checkpoint inhibitor antibody approved that is targeting PD-1 ligands: the anti PD-L1 antibody atezolizumab was approved by the FDA for the treatment of urothelial carcinoma and also non-small cell lung cancer in 2016^{112,113}. This antibody might serve as a good reference to validate the results of a PD-1 clustering FRET screening.

6.5 Conclusions

In the study presented here an automated FRET assay had been developed that allows for the detection of protein-protein interactions and also their dynamic changes via FRET efficiency calculation on a commercially available flow cytometer.

In this study, it could be shown that this FRET program is working for different applications, using fluorophores coupled to different monoclonal antibodies as FRET dyes. T cell activation could be measured via both CD3 and CD4 receptor clustering, as well as CD3 coreceptor homoclustering FRET.

Furthermore, it could be demonstrated that the increase in FRET efficiency correlated with the T cell activation status when the receptors began to cluster after a very short amount of time. Using this method, the T cell activation could be measured even faster than with the conventional calcium influx assay. Based on the change in FRET efficiency over a time period of several hours, also conclusions could be drawn on the dynamics of CD3 recycling and degradation processes on an activated T cell. In addition, even receptor clustering impairments on T cells using blood samples from patients suffering from severe immune deficiencies could be validated using this automated FRET assay.

However, we were not only able to detect T cell activation, but could also measure immune checkpoint inhibition occurring on T cells using the automated FRET assay. Here, the clustering of the PD-1 receptor with the CD3 increased when the T cell was stimulated unspecifically via SEB, leading to an increase in FRET efficiency. This effect was further pronounced when a tumor cell line was used to induce checkpoint inhibition instead of an autologous APC. The increase in FRET efficiency could be blocked for the immune checkpoint inhibition as determined by an inhibited FRET efficiency increase by using specific antibodies that are directed against the ligands of PD1. Therefore, the automated FRET assay can further be applied for compound screenings on pharmacologically active substances that inhibit tumor immune escape mechanisms.

Apart from that, the automated FRET assay can be used to detect a wide range of molecular interactions on cells and is not only limited to proteins that are expressed on the cell surface. For that reason, this program can be applied to reveal a wide range of dynamic processes that regulate cell behavior and fate.

7. Acknowledgements

Es gibt viele Personen, ohne die mir diese Arbeit nicht möglich gewesen wäre. Der Dank dafür geht an euch!

Eicke Latz möchte ich für seine großartigen Ideen und Diskussionen und vor allem auch für die Annahme der Betreuung meiner Arbeit danken. Danke auch an Joachim Schultze für die Zweitbetreuung der Arbeit. Gabor Horváth aus der AG Latz verdanke ich unendlich viel Wissen über FRET und auch über dessen Anwendungen in der Biologie.

Vielen Menschen bei Miltenyi Biotec gebührt ein herzliches Dankeschön.

Ohne Martin Büscher wäre diese Arbeit nie geschrieben worden. Danke, dass du mir so viele Möglichkeiten und Chancen für wissenschaftlichen Austausch und Kooperationen und so viele Freiheiten gegeben hast. Es hat mir sehr viel Spaß gemacht, in deinem Team zu arbeiten! Ich verdanke dir wirklich sehr viel.

Brigitte Raab und Thomas Novotny: Danke euch, dass ihr mir so oft geholfen habt, wenn ich bei der Programmierung des Express Modes nicht weiter kam und dass ihr sogar die MASQuantify Software angepasst habt, um meine Ideen und Wünsche zu ermöglichen.

Meinem Büro in jeder Besetzung danke ich für eure moralische Unterstützung und auch euer fachliches Wissen. Es hat mir viel Spaß mit euch gemacht! Danke auch an meine Kolleginnen aus der Biologie: egal, ob es um Sport (Body Attack!), feiern oder einfach nur um den Austausch in jeder Lebenslage ging: es hat mir immer wahnnig viel Spaß gemacht mit euch.

Ein großer Dank gebührt auch meinen großartigen Freunden, besonders Anna und Alina, für all eure Unterstützung und die tolle Zeit, die wir hatten, auch wenn die Versuche mal wieder nicht funktionierten. Auf euch kann ich immer zählen.

Ich danke vor allem meiner Familie, meinen Eltern und Lara, für ihre Unterstützung in jeder Lebenslage. Auch wenn ihr meistens garnicht wusstet, woran ich gerade arbeite: danke für euer bedingungsloses Vertrauen. Es gibt mir viel Kraft zu wissen, dass ihr immer für mich da seid. Und zu guter Letzt gilt mein größter Dank Felix. Manchmal hast du mir durch die richtigen Fragen viel weiter geholfen, als du es selber vermutet hättest. Ich kann mich immer auf dich verlassen, und dafür bin ich dir unendlich dankbar!

8. References

- 1 Foerster, T. Zwischenmolekulare Energieumwandlung und Fluoreszenz. *Annalen der Physik* **437**, 55-75, doi:10.1002/andp.1948370105 (1948).
- 2 Banning, C. *et al.* A flow cytometry-based FRET assay to identify and analyse protein-protein interactions in living cells. *PLoS One* **5**, e9344, doi:10.1371/journal.pone.0009344 (2010).
- 3 Stryer, L. Fluorescence Energy Transfer as a Spectroscopic Ruler. *Annual Review of Biochemistry* **47**, 819-846 (1978).
- 4 Horvath, G. *et al.* Selecting the right fluorophores and flow cytometer for fluorescence resonance energy transfer measurements. *Cytometry A* **65**, 148-157, doi:10.1002/cyto.a.20142 (2005).
- 5 Vereb, G., Nagy, P. & Szollosi, J. Flow cytometric FRET analysis of protein interaction. *Methods Mol Biol* **699**, 371-392, doi:10.1007/978-1-61737-950-5_18 (2011).
- 6 Selvin, P. R. The renaissance of fluorescence resonance energy transfer. *Nat Struct Biol* **7**, 730-734, doi:10.1038/78948 (2000).
- 7 Roszik, J., Toth, G., Szollosi, J. & Vereb, G. Validating pharmacological disruption of protein-protein interactions by acceptor photobleaching FRET imaging. *Methods Mol Biol* **986**, 165-178, doi:10.1007/978-1-62703-311-4_11 (2013).
- 8 Batard, P. *et al.* Use of phycoerythrin and allophycocyanin for fluorescence resonance energy transfer analyzed by flow cytometry: advantages and limitations. *Cytometry* **48**, 97-105, doi:10.1002/cyto.10106 (2002).
- 9 Szentesi, G. *et al.* Computer program for determining fluorescence resonance energy transfer efficiency from flow cytometric data on a cell-by-cell basis. *Comput Methods Programs Biomed* **75**, 201-211, doi:10.1016/j.cmpb.2004.02.004 (2004).
- 10 Trón, L. *et al.* Flow cytometric measurement of fluorescence resonance energy transfer on cell surfaces. Quantitative evaluation of the transfer efficiency on a cell-by-cell basis. *Biophysical Journal* **45**, 939-946 (1984).
- 11 von Kolontaj, K., Horvath, G. L., Latz, E. & Buscher, M. Automated nanoscale flow cytometry for assessing protein-protein interactions. *Cytometry A* **89**, 835-843, doi:10.1002/cyto.a.22937 (2016).
- 12 Leavesley, S. J., Britain, A. L., Cichon, L. K., Nikolaev, V. O. & Rich, T. C. Assessing FRET using spectral techniques. *Cytometry A* **83**, 898-912, doi:10.1002/cyto.a.22340 (2013).

- 13 Gayed, P. M. Toward a modern synthesis of immunity: Charles A. Janeway Jr. and the immunologist's dirty little secret. *Yale J Biol Med* **84**, 131-138 (2011).
- 14 Medzhitov, R. Recognition of microorganisms and activation of the immune response. *Nature* **449**, 819-826, doi:10.1038/nature06246 (2007).
- 15 Iwasaki, A. & Medzhitov, R. Control of adaptive immunity by the innate immune system. *Nat Immunol* **16**, 343-353, doi:10.1038/ni.3123 (2015).
- 16 Flajnik, M. F. & Kasahara, M. Origin and evolution of the adaptive immune system: genetic events and selective pressures. *Nat Rev Genet* **11**, 47-59, doi:10.1038/nrg2703 (2010).
- 17 Kurtz, J. Memory in the innate and adaptive immune systems. *Microbes Infect* **6**, 1410-1417, doi:10.1016/j.micinf.2004.10.002 (2004).
- 18 Garcia, K. C. & Adams, E. J. How the T cell receptor sees antigen--a structural view. *Cell* **122**, 333-336, doi:10.1016/j.cell.2005.07.015 (2005).
- 19 Bouvier, M. & Wiley, D. C. Importance of peptide amino and carboxyl termini to the stability of MHC class I molecules. *Science* **265**, 398-402 (1994).
- 20 Steimle, V., Siegrist, C. A., Mottet, A., Lisowska-Grospierre, B. & Mach, B. Regulation of MHC class II expression by interferon-gamma mediated by the transactivator gene CIITA. *Science* **265**, 106-109 (1994).
- 21 Hewitt, E. W. The MHC class I antigen presentation pathway: strategies for viral immune evasion. *Immunology* **110**, 163-169 (2003).
- 22 Kim, A. *et al.* Studying MHC class II peptide loading and editing in vitro. *Methods Mol Biol* **960**, 447-459, doi:10.1007/978-1-62703-218-6_33 (2013).
- 23 Itano, A. A. & Jenkins, M. K. Antigen presentation to naive CD4 T cells in the lymph node. *Nat Immunol* **4**, 733-739, doi:10.1038/ni957 (2003).
- 24 Friedl, P. & Brocker, E. B. TCR triggering on the move: diversity of T-cell interactions with antigen-presenting cells. *Immunol Rev* **186**, 83-89 (2002).
- 25 Gonzalo, J. A. *et al.* Cutting edge: the related molecules CD28 and inducible costimulator deliver both unique and complementary signals required for optimal T cell activation. *J Immunol* **166**, 1-5 (2001).
- 26 Acuto, O. & Michel, F. CD28-mediated co-stimulation: a quantitative support for TCR signalling. *Nat Rev Immunol* **3**, 939-951, doi:10.1038/nri1248 (2003).
- 27 Pollizzi, K. N. & Powell, J. D. Integrating canonical and metabolic signalling programmes in the regulation of T cell responses. *Nat Rev Immunol* **14**, 435-446, doi:10.1038/nri3701 (2014).

References

- 28 Irvine, D. J., Hue, K. A., Mayes, A. M. & Griffith, L. G. Simulations of cell-surface integrin binding to nanoscale-clustered adhesion ligands. *Biophys J* **82**, 120-132, doi:10.1016/S0006-3495(02)75379-4 (2002).
- 29 Davis, M. M. *et al.* Dynamics of cell surface molecules during T cell recognition. *Annu Rev Biochem* **72**, 717-742, doi:10.1146/annurev.biochem.72.121801.161625 (2003).
- 30 Huppa, J. B. & Davis, M. M. T-cell antigen recognition and the immunological synapse. *Nature Reviews Immunology* **3**, 973-983, doi:10.1038/nri1245 (2003).
- 31 Monks, C. R., Freiberg, B. A., Kupfer, H., Sciaky, N. & Kupfer, A. Three-dimensional segregation of supramolecular activation clusters in T cells. *Nature* **395**, 82-86, doi:10.1038/25764 (1998).
- 32 Zal, T., Zal, M. A. & Gascoigne, N. R. Inhibition of T cell receptor-coreceptor interactions by antagonist ligands visualized by live FRET imaging of the T-hybridoma immunological synapse. *Immunity* **16**, 521-534 (2002).
- 33 Liu, H., Rhodes, M., Wiest, D. L. & D.A.A., V. On the Dynamics of TCR:CD3 Complex Cell Surface Expression and Downmodulation. *Immunity* **13**, 665-675 (2000).
- 34 Al-Herz, W. *et al.* Primary immunodeficiency diseases: an update on the classification from the international union of immunological societies expert committee for primary immunodeficiency. *Front Immunol* **5**, 162, doi:10.3389/fimmu.2014.00162 (2014).
- 35 Lambe, T. *et al.* DOCK8 is essential for T-cell survival and the maintenance of CD8+ T-cell memory. *Eur J Immunol* **41**, 3423-3435, doi:10.1002/eji.201141759 (2011).
- 36 Zhang, Q. *et al.* Combined immunodeficiency associated with DOCK8 mutations. *N Engl J Med* **361**, 2046-2055, doi:10.1056/NEJMoa0905506 (2009).
- 37 Engelhardt, K. R. *et al.* Large deletions and point mutations involving the dedicator of cytokinesis 8 (DOCK8) in the autosomal-recessive form of hyper-IgE syndrome. *J Allergy Clin Immunol* **124**, 1289-1302 e1284, doi:10.1016/j.jaci.2009.10.038 (2009).
- 38 Blundell, M. P., Worth, A., Bouma, G. & Thrasher, A. J. The Wiskott-Aldrich syndrome: The actin cytoskeleton and immune cell function. *Dis Markers* **29**, 157-175, doi:10.3233/DMA-2010-0735 (2010).
- 39 Thrasher, A. J. New insights into the biology of Wiskott-Aldrich syndrome (WAS). *Hematology Am Soc Hematol Educ Program*, 132-138, doi:10.1182/asheducation-2009.1.132 (2009).
- 40 Reith, W. & Mach, B. The bare lymphocyte syndrome and the regulation of MHC expression. *Annu Rev Immunol* **19**, 331-373, doi:10.1146/annurev.immunol.19.1.331 (2001).

- 41 Elhasid, R. & Etzioni, A. Major histocompatibility complex class II deficiency: a clinical review. *Blood Rev* **10**, 242-248 (1996).
- 42 Simons, K. & Ikonen, E. Functional rafts in cell membranes. *Nature* **387**, 569-572, doi:10.1038/42408 (1997).
- 43 Lingwood, D. & Simons, K. Lipid rafts as a membrane-organizing principle. *Science* **327**, 46-50, doi:10.1126/science.1174621 (2010).
- 44 Zech, T. *et al.* Accumulation of raft lipids in T-cell plasma membrane domains engaged in TCR signalling. *EMBO J* **28**, 466-476, doi:10.1038/emboj.2009.6 (2009).
- 45 Campi, G., Varma, R. & Dustin, M. L. Actin and agonist MHC-peptide complex-dependent T cell receptor microclusters as scaffolds for signaling. *J Exp Med* **202**, 1031-1036, doi:10.1084/jem.20051182 (2005).
- 46 Kaizuka, Y., Douglass, A. D., Vardhana, S., Dustin, M. L. & Vale, R. D. The coreceptor CD2 uses plasma membrane microdomains to transduce signals in T cells. *J Cell Biol* **185**, 521-534, doi:10.1083/jcb.200809136 (2009).
- 47 Huang, J. *et al.* The kinetics of two-dimensional TCR and pMHC interactions determine T-cell responsiveness. *Nature* **464**, 932-936, doi:10.1038/nature08944 (2010).
- 48 Simons, K. & Gerl, M. J. Revitalizing membrane rafts: new tools and insights. *Nat Rev Mol Cell Biol* **11**, 688-699, doi:10.1038/nrm2977 (2010).
- 49 Zidoventzki, R. & Levitan, I. Use of cyclodextrins to manipulate plasma membrane cholesterol content: evidence, misconceptions and control strategies. *Biochim Biophys Acta* **1768**, 1311-1324 (2007).
- 50 Huppa, J. B. *et al.* TCR-peptide-MHC interactions *in situ* show accelerated kinetics and increased affinity. *Nature* **463**, 963-967, doi:10.1038/nature08746 (2010).
- 51 Stiles, B. G. & Krakauer, T. Staphylococcal Enterotoxins: a Purging Experience in Review, Part I. *Clinical Microbiology Newsletter* **27**, 179-186, doi:10.1016/j.clinmicnews.2005.11.001 (2005).
- 52 Stiles, B. G. & Krakauer, T. Staphylococcal Enterotoxins: a Purging Experience in Review, Part II. *Clinical Microbiology Newsletter* **27**, 187-193, doi:10.1016/j.clinmicnews.2005.12.001 (2005).
- 53 Watson, A. R. & Lee, W. T. Defective T cell receptor-mediated signal transduction in memory CD4 T lymphocytes exposed to superantigen or anti-T cell receptor antibodies. *Cell Immunol* **242**, 80-90, doi:10.1016/j.cellimm.2006.09.008 (2006).
- 54 Swaminathan, S., Furey, W., Pletcher, J. & Sax, M. Crystal structure of staphylococcal enterotoxin B, a superantigen. *Nature* **359**, 801-806, doi:10.1038/359801a0 (1992).

- 55 Krakauer, T. Update on Staphylococcal Superantigen-Induced Signaling Pathways and Therapeutic Interventions. *Toxins* **5**, 1629-1654, doi:10.3390/toxins5091629 (2013).
- 56 Andorsky, D. J. *et al.* Programmed death ligand 1 is expressed by non-hodgkin lymphomas and inhibits the activity of tumor-associated T cells. *Clin Cancer Res* **17**, 4232-4244, doi:10.1158/1078-0432.CCR-10-2660 (2011).
- 57 Keir, M. E., Butte, M. J., Freeman, G. J. & Sharpe, A. H. PD-1 and its ligands in tolerance and immunity. *Annu Rev Immunol* **26**, 677-704, doi:10.1146/annurev.immunol.26.021607.090331 (2008).
- 58 Riley, J. L. PD-1 signaling in primary T cells. *Immunol Rev* **229**, 114-125, doi:10.1111/j.1600-065X.2009.00767.x (2009).
- 59 Francisco, L. M., Sage, P. T. & Sharpe, A. H. The PD-1 pathway in tolerance and autoimmunity. *Immunol Rev* **236**, 219-242, doi:10.1111/j.1600-065X.2010.00923.x (2010).
- 60 Sheppard, K. A. *et al.* PD-1 inhibits T-cell receptor induced phosphorylation of the ZAP70/CD3zeta signalosome and downstream signaling to PKCtheta. *FEBS Lett* **574**, 37-41, doi:10.1016/j.febslet.2004.07.083 (2004).
- 61 Parry, R. V. *et al.* CTLA-4 and PD-1 receptors inhibit T-cell activation by distinct mechanisms. *Mol Cell Biol* **25**, 9543-9553, doi:10.1128/MCB.25.21.9543-9553.2005 (2005).
- 62 Bally, A. P., Austin, J. W. & Boss, J. M. Genetic and Epigenetic Regulation of PD-1 Expression. *J Immunol* **196**, 2431-2437, doi:10.4049/jimmunol.1502643 (2016).
- 63 Latchmann, Y. *et al.* PD-L2 is a second ligand for PD-1 and inhibits T cell activation. *Nature Immunology* **2**, 261-268 (2001).
- 64 Sharpe, A. H., Wherry, E. J., Ahmed, R. & Freeman, G. J. The function of programmed cell death 1 and its ligands in regulating autoimmunity and infection. *Nat Immunol* **8**, 239-245, doi:10.1038/ni1443 (2007).
- 65 Wherry, E. J. *et al.* Molecular signature of CD8+ T cell exhaustion during chronic viral infection. *Immunity* **27**, 670-684, doi:10.1016/j.immuni.2007.09.006 (2007).
- 66 Okazaki, T. & Honjo, T. The PD-1-PD-L pathway in immunological tolerance. *Trends Immunol* **27**, 195-201, doi:10.1016/j.it.2006.02.001 (2006).
- 67 Saito, T., Yokosuka, T. & Hashimoto-Tane, A. Dynamic regulation of T cell activation and co-stimulation through TCR-microclusters. *FEBS Lett* **584**, 4865-4871, doi:10.1016/j.febslet.2010.11.036 (2010).

- 68 Yokosuka, T. *et al.* Programmed cell death 1 forms negative costimulatory microclusters that directly inhibit T cell receptor signaling by recruiting phosphatase SHP2. *J Exp Med* **209**, 1201-1217, doi:10.1084/jem.20112741 (2012).
- 69 Pen, J. J. *et al.* Interference with PD-L1/PD-1 co-stimulation during antigen presentation enhances the multifunctionality of antigen-specific T cells. *Gene Ther* **21**, 262-271, doi:10.1038/gt.2013.80 (2014).
- 70 Topalian, S. L., Drake, C. G. & Pardoll, D. M. Targeting the PD-1/B7-H1(PD-L1) pathway to activate anti-tumor immunity. *Curr Opin Immunol* **24**, 207-212, doi:10.1016/j.coi.2011.12.009 (2012).
- 71 Buchbinder, E. I. & Desai, A. CTLA-4 and PD-1 Pathways: Similarities, Differences, and Implications of Their Inhibition. *Am J Clin Oncol* **39**, 98-106, doi:10.1097/COC.0000000000000239 (2016).
- 72 Walker, L. S. Treg and CTLA-4: two intertwining pathways to immune tolerance. *J Autoimmun* **45**, 49-57, doi:10.1016/j.jaut.2013.06.006 (2013).
- 73 Zitvogel, L. & Kroemer, G. Targeting PD-1/PD-L1 interactions for cancer immunotherapy. *Oncoimmunology* **1**, 1223-1225, doi:10.4161/onci.21335 (2012).
- 74 Festino, L. *et al.* Cancer Treatment with Anti-PD-1/PD-L1 Agents: Is PD-L1 Expression a Biomarker for Patient Selection? *Drugs* **76**, 925-945, doi:10.1007/s40265-016-0588-x (2016).
- 75 Kim, H. R. *et al.* PD-L1 expression on immune cells, but not on tumor cells, is a favorable prognostic factor for head and neck cancer patients. *Sci Rep* **6**, 36956, doi:10.1038/srep36956 (2016).
- 76 Ameratunga, M. *et al.* PD-L1 and Tumor Infiltrating Lymphocytes as Prognostic Markers in Resected NSCLC. *PLoS One* **11**, e0153954, doi:10.1371/journal.pone.0153954 (2016).
- 77 Li, Y. *et al.* Prognostic impact of programmed cell death-1 (PD-1) and PD-ligand 1 (PD-L1) expression in cancer cells and tumor infiltrating lymphocytes in colorectal cancer. *Mol Cancer* **15**, 55, doi:10.1186/s12943-016-0539-x (2016).
- 78 Grigg, C. & Rizvi, N. A. PD-L1 biomarker testing for non-small cell lung cancer: truth or fiction? *J Immunother Cancer* **4**, 48, doi:10.1186/s40425-016-0153-x (2016).
- 79 Hamid, O. *et al.* Safety and tumor responses with lambrolizumab (anti-PD-1) in melanoma. *N Engl J Med* **369**, 134-144, doi:10.1056/NEJMoa1305133 (2013).
- 80 Topalian, S. L. *et al.* Survival, durable tumor remission, and long-term safety in patients with advanced melanoma receiving nivolumab. *J Clin Oncol* **32**, 1020-1030, doi:10.1200/JCO.2013.53.0105 (2014).

- 81 Topalian, S. L. *et al.* Safety, activity, and immune correlates of anti-PD-1 antibody in cancer. *N Engl J Med* **366**, 2443-2454, doi:10.1056/NEJMoa1200690 (2012).
- 82 Philips, G. K. & Atkins, M. Therapeutic uses of anti-PD-1 and anti-PD-L1 antibodies. *Int Immunol* **27**, 39-46, doi:10.1093/intimm/dxu095 (2015).
- 83 Shapiro, H. M. Trends and developments in flow cytometry instrumentation. *Ann N Y Acad Sci* **677**, 155-166 (1993).
- 84 Shapiro, H. M. in *Practical Flow Cytometry* 101-223 (John Wiley & Sons, Inc., 2005).
- 85 Shapiro, H. M. in *Practical Flow Cytometry* 225-256 (John Wiley & Sons, Inc., 2005).
- 86 Lleres, D., Swift, S. & Lamond, A. I. Detecting protein-protein interactions in vivo with FRET using multiphoton fluorescence lifetime imaging microscopy (FLIM). *Curr Protoc Cytom* **Chapter 12**, Unit12 10, doi:10.1002/0471142956.cy1210s42 (2007).
- 87 Zacharias, D. A. & Tsien, R. Y. Molecular biology and mutation of green fluorescent protein. *Methods Biochem Anal* **47**, 83-120 (2006).
- 88 Hamad, A. R. A., Herman, A., Marrack, P. & J.W., K. Monoclonal Antibodies Defining Functional Sites on the Toxin Superantigen Staphylococcal Enterotoxin B. *J Exp Med* **180**, 615-621 (1994).
- 89 Paredes, R. M., Etzler, J. C., Watts, L. T., Zheng, W. & Lechleiter, J. D. Chemical calcium indicators. *Methods* **46**, 143-151, doi:10.1016/j.ymeth.2008.09.025 (2008).
- 90 Fabian, A. I., Rente, T., Szollosi, J., Matyus, L. & Jenei, A. Strength in numbers: effects of acceptor abundance on FRET efficiency. *Chemphyschem* **11**, 3713-3721, doi:10.1002/cphc.201000568 (2010).
- 91 Roszik, J., Lisboa, D., Szollosi, J. & Vereb, G. Evaluation of intensity-based ratiometric FRET in image cytometry--approaches and a software solution. *Cytometry A* **75**, 761-767, doi:10.1002/cyto.a.20747 (2009).
- 92 Szollosi, J., Vereb, G. & Nagy, P. The flow of events: How the sequence of molecular interactions is seen by the latest, user-friendly high throughput flow cytometric FRET. *Cytometry A* **89**, 881-885, doi:10.1002/cyto.a.22994 (2016).
- 93 Niedergang, F. *et al.* The Staphylococcus aureus enterotoxin B superantigen induces specific T cell receptor down-regulation by increasing its internalization. *J Biol Chem* **270**, 12839-12845 (1995).
- 94 Krakauer, T. Chemotherapeutics targeting immune activation by staphylococcal superantigens. *Med Sci Monit* **11**, RA290-295 (2005).
- 95 Wilson, T. Resolution and optical sectioning in the confocal microscope. *J Microsc* **244**, 113-121, doi:10.1111/j.1365-2818.2011.03549.x (2011).

- 96 Yokosuka, T. *et al.* Spatiotemporal regulation of T cell costimulation by TCR-CD28 microclusters and protein kinase C theta translocation. *Immunity* **29**, 589-601, doi:10.1016/j.immuni.2008.08.011 (2008).
- 97 Joseph, N., Reicher, B. & Barda-Saad, M. The calcium feedback loop and T cell activation: how cytoskeleton networks control intracellular calcium flux. *Biochim Biophys Acta* **1838**, 557-568, doi:10.1016/j.bbamem.2013.07.009 (2014).
- 98 Buchbinder, D., Nugent, D. J. & Phillipovich, A. H. Wiskott-Aldrich syndrome: diagnosis, current management, and emerging treatments. *Appl Clin Genet* **7**, 55-66, doi:10.2147/TACG.S58444 (2014).
- 99 Rouquette-Jazdanian, A. K., Pelassy, C., Breitmayer, J. P. & Aussel, C. Full CD3/TCR activation through cholesterol-depleted lipid rafts. *Cell Signal* **19**, 1404-1418, doi:10.1016/j.cellsig.2007.01.015 (2007).
- 100 Petruk, A. A. *et al.* The structure of the CD3 zeta/zeta transmembrane dimer in POPC and raft-like lipid bilayer: a molecular dynamics study. *Biochim Biophys Acta* **1828**, 2637-2645, doi:10.1016/j.bbamem.2013.07.019 (2013).
- 101 Jury, E. C., Flores-Borja, F. & Kabouridis, P. S. Lipid rafts in T cell signalling and disease. *Seminars in cell & developmental biology* **18**, 608-615, doi:10.1016/j.semcd.2007.08.002 (2007).
- 102 Finetti, F. *et al.* Intraflagellar transport is required for polarized recycling of the TCR/CD3 complex to the immune synapse. *Nat Cell Biol* **11**, 1332-1339, doi:10.1038/ncb1977 (2009).
- 103 Gillespie, E. J. *et al.* Selective inhibitor of endosomal trafficking pathways exploited by multiple toxins and viruses. *Proceedings of the National Academy of Sciences of the United States of America* **110**, E4904-4912, doi:10.1073/pnas.1302334110 (2013).
- 104 Fife, B. T. *et al.* Interactions between PD-1 and PD-L1 promote tolerance by blocking the TCR-induced stop signal. *Nat Immunol* **10**, 1185-1192, doi:10.1038/ni.1790 (2009).
- 105 Koirala, P. *et al.* Immune infiltration and PD-L1 expression in the tumor microenvironment are prognostic in osteosarcoma. *Sci Rep* **6**, 30093, doi:10.1038/srep30093 (2016).
- 106 Mazel, M. *et al.* Frequent expression of PD-L1 on circulating breast cancer cells. *Mol Oncol* **9**, 1773-1782, doi:10.1016/j.molonc.2015.05.009 (2015).
- 107 Killock, D. Haematological cancer: Anti-PD-1 therapy with nivolumab after allo-HSCT for Hodgkin lymphoma. *Nat Rev Clin Oncol*, doi:10.1038/nrclinonc.2017.50 (2017).

- 108 Mazza, C., Escudier, B. & Albiges, L. Nivolumab in renal cell carcinoma: latest evidence and clinical potential. *Ther Adv Med Oncol* **9**, 171-181, doi:10.1177/1758834016679942 (2017).
- 109 Rexer, H., Steiner, T. & Grunwald, V. [First-line therapy in advanced renal cell carcinoma : A randomized phase II study to examine early switch of tyrosine kinase inhibitors to nivolumab compared to continued tyrosine kinase inhibitor therapy in patients with advanced or metastatic renal cell carcinoma and stable disease after three months of treatment (NIVOSWITCH)-AN 38/15 of the AUO]. *Urologe A* **56**, 509-511, doi:10.1007/s00120-017-0343-2 (2017).
- 110 Sun, L. M. *et al.* Nivolumab effectively inhibit platinum-resistant ovarian cancer cells via induction of cell apoptosis and inhibition of ADAM17 expression. *Eur Rev Med Pharmacol Sci* **21**, 1198-1205 (2017).
- 111 Nishijima, T. F., Shachar, S. S., Nyrop, K. A. & Muss, H. B. Safety and Tolerability of PD-1/PD-L1 Inhibitors Compared with Chemotherapy in Patients with Advanced Cancer: A Meta-Analysis. *Oncologist*, doi:10.1634/theoncologist.2016-0419 (2017).
- 112 Russo, I. *et al.* Immunotherapy-related skin toxicity: bullous pemphigoid in a lung adenocarcinoma patient treated with the anti-PDL1 antibody atezolizumab. *Eur J Dermatol*, doi:10.1684/ejd.2016.2959 (2017).
- 113 Sgambato, A., Casaluca, F. & Gridelli, C. The role of checkpoint inhibitors immunotherapy in advanced non-small cell lung cancer in the elderly. *Expert Opin Biol Ther*, 1-7, doi:10.1080/14712598.2017.1294157 (2017).

9. Appendix

9.1 The FRET Express Mode Script

```

from expressModes import basisEasyPageManager
from expressModes import basisEasyPage
from expressModes import basisGating
from expressModes import basisEasyPageTemplate
from expressModes import em_utilities
from expressModes import standardGating
from expressModes import basisExpressMode

import mq
import re
import os
import time
import expressModes

from mq import mDebug

from __main__ import App
from __main__ import Script
from __main__ import Config

em_version = expressModes.__version__
em_version = '.'.join([str(elm) for elm in em_version])
em_name = 'FRETexportData'

DOTPLOT = basisEasyPageTemplate.BasisEasyPlotTemplate.DOTPLOT
DENSITYPLOT = basisEasyPageTemplate.BasisEasyPlotTemplate.DENSITYPLOT
HISTOGRAM = basisEasyPageTemplate.BasisEasyPlotTemplate.HISTOGRAM
SCRIPTTEXT = basisEasyPageTemplate.BasisEasyPlotTemplate.SCRIPTTEXT
EDITVIEWOFF = basisEasyPageTemplate.BasisEasyPlotTemplate.EDITVIEWOFF
HIDENONE = basisEasyPageTemplate.BasisEasyPlotTemplate.HIDENONE
HIDEOOTHER = basisEasyPageTemplate.BasisEasyPlotTemplate.HIDEOOTHER
HIDEALL = basisEasyPageTemplate.BasisEasyPlotTemplate.HIDEALL

#default settings for processing FRET application

Annotations = {
    'VioBlue' : 'Donor-VioBlue',
    'VioGreen' : 'FRET-VioGeen',
    'FITC' : 'Acceptor-FITC',
    'PE' : 'PE',
    'PI' : 'PI',
    'APC' : 'APC'
}

```



```

#colors
black = "#000000"
purple = "#8904B1"
darkblue = "#084B8A"
lightblue = "#00BFFF"
red = "#FF4000"
green = "#04B404"
grey = "#6E6E6E"

def defaultSettings( ):
    return {
        'PerformSampleMixing' : "Off", #changed from False to off between EM versions
        'UptakeVolume'      : 100,
        'SampleVolume'     : 250,
        'Mode'              : 'Standard',
        'EventLimited'     : False,
        'EventLimit'       : 10000,
        'FlowRate'         : 'Medium',
        'AutoFlowRate'     : False,
        'Reagents'         : (),
        'Annotations'      : em_utilities.getAnnotations( Annotations )
    }

#-----
# Global Variables for this modules
#-----
channel_list = ( 'FSC', 'SSC', 'VioBlue', 'VioGreen', 'FITC' )

#-----
# default Groups
#-----
def defaultGroups( ):
    return {
        1 : 'Blank',
        2 : 'VioBlue_Donor',
        3 : 'FITC_Acceptor',
        4 : 'VioGreen_FRET',
        #5 : 'APC_Donor',
        #6 : 'Cy5_Acceptor',
        #7 : 'APC-Cy5_FRET',
        #8 : 'FITC_Donor',
        #9 : 'mCherry_Acceptor',
        #10: 'PI_FRET'
    }

#-----
# Acquisition Page
#-----

```

```

class FRETAcquisitionPage( basisEasyPage.BaseEasyPage ):

    def __init__( self, MainFrame ):

        basisEasyPage.BaseEasyPage.__init__( self, MainFrame, "FRETAcquisitionPage" )
        self._setInfo( "FRET acquisition" )
        SampleName = "live"

        Sample = App.sample( SampleName )
        Sample.removeSubPopulations()

        channels_A = em_utilities.get_channelNames( "A", channel_list, Sample )
        channels_H = em_utilities.get_channelNames( "H", channel_list, Sample )

        Plot1 = [ DOTPLOT, SampleName, channels_A['FSC'], channels_A['SSC'], { 'edit' :
False, 'populations' : (SampleName,) }, HIDDENONE ]
        Plot2 = [ DOTPLOT, SampleName, channels_A['FSC'], channels_H['FSC'], { 'edit' :
False, 'populations' : (SampleName,) }, HIDEOTHER ]
        Plot3 = [ DOTPLOT, SampleName, channels_A['VioGreen'], channels_A['VioBlue'],
{ 'edit' : False, 'populations' : (SampleName,) }, HIDEOTHER ]
        Plot4 = [ DOTPLOT, SampleName, channels_A['VioGreen'], channels_A['FITC'], { 'edit' :
False, 'populations' : (SampleName,) }, HIDEOTHER ]
        PageDesc = [ Plot1, Plot2, Plot3, Plot4 ]

        Plots = basisEasyPageTemplate.BasisEasyPlotTemplate( self )
        Plots._drawPlots( PageDesc, "view4" )

        for plot in self.plots():
            plot.setTableRegionFuncs( ["Path", "%-#"] )

        self._mainFrame( ).setSave( Config.SB_Analysis )

#-----
# Analyse Pages
# 1: Group-Member specific Page
# 2: Script-Text only
# 3: Final Result
# 4: Page for data from mqd-Writer => calculated FRETEfficiency for all events
#-----
class FRETAnalysePage2( basisEasyPage.BaseEasyPage ):

    def __init__( self, MainFrame, SampleName, alpha, fractions, fractionName ):
        basisEasyPage.BaseEasyPage.__init__( self, MainFrame, "FRETAnalysePage2" )
        self.fractions = fractions
        self.fractionName = fractionName
        self.alpha = alpha
        sample = App.sample( SampleName )
        self.channels_A = em_utilities.get_channelNames( "A", channel_list, sample )

```

```

# self.channels_H = em_utilities.get_channelNames( "H", channel_list, sample )
self.__drawPlots( SampleName )

def __drawPlots( self, SampleName ):

    # legend = "$setvar( 'FRET', textblocks.FretCalculation.Fret(sample,
's', %f ) )$" %( em_version, self.alpha )
    # legend += " $$var['FRET'].getIntensities()$$ <p></p>"
    # legend += " $$var['FRET'].getBackGround()$$ <p></p>"
    # legend += " $$var['FRET'].getCrosstalk()$$ <p></p>"
    # legend += " $$var['FRET'].getResults()$$"

    legend = createIntensitiesTable( SampleName, self.fractions, self.channels_A )
    legend += "<p></p>"
    legend += createBackGroundTable( SampleName, self.fractions, self.channels_A )
    legend += "<p></p><p></p><BR><BR>"
    legend += createCrosstalkTable( SampleName, self.fractions, self.channels_A )
    legend += "<p></p>"
    legend += createResultsTable( SampleName, self.fractions, self.alpha, self.channels_A )

    PageDesc = [ [ SCRIPTTEXT, SampleName, legend, (), EDITVIEWOFF ] ]

    Plots = basisEasyPageTemplate.BasisEasyPlotTemplate( self )
    Plots._drawPlots( PageDesc, "view1" )

    for plot in self.plots():
        plot.setTableRegionFuncs( ["Path", "%-#"] )

    self._mainFrame( ).setSave( Config.SB_Analysis )

class FRETAnalysePage3( basisEasyPage.BaseEasyPage ):

    def __init__( self, MainFrame, SampleName, alpha, fractions, fractionName ):
        basisEasyPage.BaseEasyPage.__init__( self, MainFrame, "FRETAnalysePage3" )
        # self.mySample = App.sample(SampleName)
        self.fractions = fractions
        self.fractionName = fractionName
        self.alpha = alpha
        sample = App.sample( SampleName )
        self.channels_A = em_utilities.get_channelNames( "A", channel_list, sample )
        self.channels_H = em_utilities.get_channelNames( "H", channel_list, sample )

        self.__drawPlots( SampleName )

    def __drawPlots(self, SampleName ):

        fraction = self.fractions["VioGreen_FRET"]
        GO_FR = fraction['GroupGateName'].name() #Ohne Gate

```

```

G2_FR = fraction['ScatterGate'].name() #Target Population
G3_FR = fraction['SingletGate'].name() #Singlet Gate
G4_FR = fraction['Donor'].name()
G5_FR = fraction['Acceptor'].name()

# legend = "$setvar( 'FRET', textblocks.FretCalculation.Fret(sample,
's', %f ) )$" %( em_version, self.alpha )
# legend += "$var['FRET'].getIntensities()$" <p></p>"
# legend += "$var['FRET'].getResults()$"

legend = createIntensitiesTable( SampleName, self.fractions, self.channels_A )
legend += "<p></p>"
legend += createResultsTable( SampleName, self.fractions, self.alpha, self.channels_A )

Plot1 = [ DOTPLOT, G0_FR, self.channels_A['FSC'], self.channels_A['SSC'], { 'edit' :
False, 'populations' : (G0_FR,G2_FR) }, HIDDENONE ]
Plot2 = [ DOTPLOT, G2_FR, self.channels_A['FSC'], self.channels_H['FSC'], { 'edit' :
False, 'populations' : (G2_FR,G3_FR) }, HIDDENONE ]
Plot3 = [ DOTPLOT, G3_FR, self.channels_A['VioBlue'], self.channels_A['VioGreen'],
{ 'edit' : False, 'populations' : (G3_FR,) }, HIDDENONE ]
Plot4 = [ DOTPLOT, G3_FR, self.channels_A['FITC'], self.channels_A['VioGreen'],
{ 'edit' : False, 'populations' : (G3_FR,) }, HIDDENONE ]

Table = [ SCRIPTTEXT, SampleName, legend, (), EDITVIEWOFF ]

PageDesc = [ Plot1, Plot2, Plot3, Table, Plot4 ]

Plots = basisEasyPageTemplate.BasisEasyPlotTemplate( self )
Plots._drawPlots( PageDesc, "view6b" )

for plot in self.plots():
    plot.setTableRegionFuncs( ["Path", "%-#"] )

self._mainFrame( ).setSave( Config.SB_Analysis )

class FRETAnalysePage1( basisEasyPage.BaseEasyPage ):

def __init__( self, MainFrame, SampleName, alpha, fractions, fractionName ):
    basisEasyPage.BaseEasyPage.__init__( self, MainFrame, "FRETAnalysePage1" )
    Sample = App.sample(SampleName)
    self.fractions = fractions
    self.fractionName = fractionName
    self.alpha = alpha
    self.channels_A = em_utilities.get_channelNames( "A", channel_list, Sample )
    self.channels_H = em_utilities.get_channelNames( "H", channel_list, Sample )

self.__drawPlots( SampleName )

```

```

def __drawPlots(self, SampleName):

    fraction = self.fractions[self.fractionName]
    G0 = fraction['GroupGateName'].name() #Ohne Gate
    G2 = fraction['ScatterGate'].name() #Target Population
    G3 = fraction['SingletGate'].name() #Singlet Gate
    G4 = fraction['Donor'].name()
    G5 = fraction['Acceptor'].name()
    G6 = fraction['FRET'].name()

    # legend_M = "$textblocks.FretCalculation.Fret(sample,
    '%s', %f ).getMedians( '%s' )$" %( em_version, self.alpha, self.fractionName )
    legend_M = createMedianTable( SampleName, self.fractions[self.fractionName],
self.channels_A )

    Plot1 = [ DOTPLOT, G0, self.channels_A['FSC'], self.channels_A['SSC'], { 'edit' :
False, 'populations' : (G0,G2) }, HIDDENONE ]
    Plot2 = [ DOTPLOT, G0, self.channels_A['FSC'], self.channels_H['FSC'], { 'edit' :
False, 'populations' : (G2,) }, HIDDENONE ]
    Plot3 = [ DOTPLOT, G3, self.channels_A['VioBlue'], self.channels_A['VioGreen'], { 'edit' :
False, 'populations' : (G3,) }, HIDDENONE ]
    Plot4 = [ DOTPLOT, G3, self.channels_A['FITC'], self.channels_A['VioGreen'], { 'edit' :
False, 'populations' : (G3,) }, HIDDENONE ]
    Plot5 = [ HISTOGRAM, G4, self.channels_A['VioBlue'], None, { 'edit' : False,
'populations' : (G4,) }, HIDEOTHER ]
    Plot6 = [ HISTOGRAM, G5, self.channels_A['FITC'], None, { 'edit' : False,
'populations' : (G5,) }, HIDEOTHER ]
    Plot7 = [ HISTOGRAM, G6, self.channels_A['VioGreen'], None, { 'edit' : False,
'populations' : (G6,) }, HIDEOTHER ]

    ScriptTextTable = [ SCRIPTTEXT, SampleName, legend_M, (), EDITVIEWOFF ]

    PageDesc = [ Plot1, Plot2, Plot3, Plot4, Plot5, Plot6, ScriptTextTable, Plot7 ]

    Plots = basisEasyPageTemplate.BasisEasyPlotTemplate( self )
    Plots._drawPlots( PageDesc, "view8b" )

    Hist1 = self.plots()[4]
    Hist2 = self.plots()[5]
    Hist3 = self.plots()[6]
    Hist1.setTableFeatures([self.channels_A['VioBlue']])
    Hist1.setTableFeatureFuncs(['Median'])
    Hist2.setTableFeatures([self.channels_A['FITC']])
    Hist2.setTableFeatureFuncs(['Median'])
    Hist3.setTableFeatures([self.channels_A['VioGreen']])
    Hist3.setTableFeatureFuncs(['Median'])

```

```

for plot in self.plots():
    plot.setTableRegionFuncs( ["Path", "%-#"] )

self._mainFrame( ).setSave( Config.SB_Analysis )

```

```
class FRETAnalysePage4( basisEasyPage.BaseEasyPage ):
```

```

def __init__( self, MainFrame, SampleName, alpha, fractions, fractionName ):
    basisEasyPage.BaseEasyPage.__init__( self, MainFrame, "FRETAnalysePage4" )
    self.fraction = fractions[fractionName]
    self.__drawPlots()

```

```
def __drawPlots(self):
```

```

    G1 = self.fraction['Double positives'].name()
    G2 = self.fraction['Target Population'].name()
    G3 = self.fraction['Singlet Population'].name()

```

```

    Plot1 = [ HISTOGRAM, G3, 'FRET',    None, EDITVIEWOFF, HIDENONE ]
    Plot2 = [ DENSITYPLOT, G1, 'FSC-A',  'SSC-A', EDITVIEWOFF, HIDENONE ]
    Plot3 = [ DOTPLOT,    G2, 'FSC-A',  'FSC-H', EDITVIEWOFF, HIDENONE ]
    Plot4 = [ HISTOGRAM, G3, 'Donor',    None, EDITVIEWOFF, HIDEOTHER ]
    Plot5 = [ HISTOGRAM, G3, 'Acceptor', None, EDITVIEWOFF, HIDEOTHER ]
    Plot6 = [ HISTOGRAM, G3, 'FRETchannel', None, EDITVIEWOFF, HIDEOTHER ]

```

```
PageDesc = [ Plot1, Plot2, Plot3, Plot4, Plot5, Plot6 ]
```

```

Plots = basisEasyPageTemplate.BasisEasyPlotTemplate( self )
Plots._drawPlots( PageDesc, "view6a" )

```

```

for plot in self.plots():
    plot.setTableRegionFuncs( ["Path", "%-#"] )

```

```
self._mainFrame( ).setSave( Config.SB_Analysis )
```

```
class FRETAnalysePageFRETonly( basisEasyPage.BaseEasyPage ):
```

```

def __init__( self, MainFrame, SampleName, alpha, fractions, fractionName ):
    basisEasyPage.BaseEasyPage.__init__( self, MainFrame, "FRETAnalysePage3" )
    # self.mySample = App.sample(SampleName)
    self.fractions = fractions
    self.fractionName = fractionName
    self.alpha = alpha
    sample = App.sample( SampleName )
    self.channels_A = em_utilities.get_channelNames( "A", channel_list, sample )
    self.channels_H = em_utilities.get_channelNames( "H", channel_list, sample )

```

```

self.__drawPlots( SampleName )

def __drawPlots(self, SampleName ):

    fraction = self.fractions["VioGreen_FRET"]
    G0_FR = fraction['GroupGateName'].name() #Ohne Gate
    G2_FR = fraction['ScatterGate'].name() #Target Population
    G3_FR = fraction['SingletGate'].name() #Singlet Gate
    G4_FR = fraction['Donor'].name()
    G5_FR = fraction['Acceptor'].name()

    legend = createIntensitiesTableFRET( SampleName, self.fractions, self.channels_A )
    legend += "<p></p>"
    legend += createResultsTableFRET( SampleName, self.fractions, self.alpha,
self.channels_A )
    legend += createExportFRET( SampleName, self.fractions, self.alpha, self.channels_A )

    Plot1 = [ DOTPLOT, G0_FR, self.channels_A['FSC'], self.channels_A['SSC'], { 'edit' :
False, 'populations' : (G0_FR,G2_FR) }, HIDENONE ]
    Plot2 = [ DOTPLOT, G2_FR, self.channels_A['FSC'], self.channels_H['FSC'], { 'edit' :
False, 'populations' : (G2_FR,G3_FR) }, HIDENONE ]
    Plot3 = [ DOTPLOT, G3_FR, self.channels_A['VioBlue'], self.channels_A['VioGreen'],
{ 'edit' : False, 'populations' : (G3_FR,) }, HIDENONE ]
    Plot4 = [ DOTPLOT, G3_FR, self.channels_A['FITC'], self.channels_A['VioGreen'],
{ 'edit' : False, 'populations' : (G3_FR,) }, HIDENONE ]

    Table = [ SCRIPTTEXT, SampleName, legend, (), EDITVIEWOFF ]

    PageDesc = [ Plot1, Plot2, Plot3, Table, Plot4 ]

    Plots = basisEasyPageTemplate.BasisEasyPlotTemplate( self )
    Plots.__drawPlots( PageDesc, "view6b" )

    for plot in self.plots():
        plot.setTableRegionFuncs( ["Path","%-%#"] )

    self.__mainFrame( ).setSave( Config.SB_Analysis )

#####
#####

#####
#####
#-----
# Main analysis algorithmic
#-----
def __analyseFRET( SampleName, pv ):

```

```

Sample = App.sample( SampleName )
Sample.removeSubPopulations()
Sample.createGroupRegions()
Fractions = __retrieveFractions( SampleName )
channels_A = em_utilities.get_channelNames( 'A', channel_list, Sample )
channels_H = em_utilities.get_channelNames( 'H', channel_list, Sample )

if "VioGreen_FRET" not in Fractions:
    return False,{}

if "Blank" in Fractions:

    FRET_Fraction = Fractions["VioGreen_FRET"]
    Blank_Fraction = Fractions["Blank"]
    Donor_Fraction = Fractions["VioBlue_Donor"]
    Acceptor_Fraction = Fractions ["FITC_Acceptor"]
    print 'GroupgateName', FRET_Fraction['GroupGateName']

    #-----
    # first run:pre-gating on target population
    #-----
    mDebug( 'log', 0, 'START pre-gating1 on target population.....' )

    Range_X = GetRange( FRET_Fraction['GroupGateName'], channels_A['VioBlue'], -1.25,
minPeak=64 )
    Range_Y = GetRange( FRET_Fraction['GroupGateName'], channels_A['FITC'], -1.25,
minPeak=64 )

    coords_Pre = basisGating._calculateCoordinates( Range_X, Range_Y )

    preGate = standardGating.applyPolygonGate( FRET_Fraction['GroupGateName'],
coords_Pre,
                                channels_A['VioBlue'], channels_A['FITC'], grey, "PreGate1" )
    FRET_Fraction['PreGate'] = preGate

    pv.setProgress(1)

    #-----
    #Gating on Target Population
    #-----
    mDebug( 'log', 0, 'START gating on target population.....' )

    scatterGate = CreateEllipseGate( FRET_Fraction['PreGate'],
FRET_Fraction['GroupGateName'],
                                channels_A['FSC'], channels_A['SSC'], purple, 'ScatterGate' )

if scatterGate == None:

```



```

    raise em_utilities.AnalysisException( "Failed to create ScatterGate", Fractions )

    FRET_Fraction['ScatterGate'] = scatterGate
    copyGateToOtherFractions( Fractions, "VioGreen_FRET", scatterGate, "ScatterGate",
'GroupGateName' )

    pv.setProgress(2)

    #-----
    # Gating on SINGLETS
    #-----
    mDebug( 'log', 0, 'START gating on singlets.....' )

    singletGate = standardGating.calculateSingletGate( FRET_Fraction['ScatterGate'],
channels_A['FSC'],
                                channels_H['FSC'], 'SingletGate', darkblue )
    if singletGate == None:
        raise em_utilities.AnalysisException( "Failed to create singletGate", Fractions )

    FRET_Fraction['SingletGate'] = singletGate

    copyGateToOtherFractions( Fractions, "VioGreen_FRET", singletGate, "SingletGate",
"ScatterGate" )

    #-----
    # Gating on DONOR: S1
    #-----
    mDebug( 'log', 0, 'START gating on donor positive population.....' )

    DonorRegion = CreateSGate( Donor_Fraction['SingletGate'], channels_A['VioBlue'],
channels_A['VioGreen'], red, "S1")
    Donor_Fraction['Donor'] = DonorRegion

    FRETRegion = CreateSGate( FRET_Fraction['SingletGate'], channels_A['VioBlue'],
channels_A['VioGreen'], red, "S1")
    FRET_Fraction['Donor'] = FRETRegion

    BlankRegion = CreateWholeRange( Blank_Fraction['SingletGate'], red,
channels_A['VioBlue'] )
    Blank_Fraction['Donor']= BlankRegion

    AcceptorRegion = CreateWholeRange( Acceptor_Fraction['SingletGate'], red,
channels_A['VioBlue'] )
    Acceptor_Fraction['Donor'] = AcceptorRegion

    pv.setProgress(3)

    #-----

```

```

# Gating on ACCEPTOR
#-----
mDebug( 'log', 0, 'START gating on acceptor positive population.....' )

BlankRegion = CreateWholeRange( Blank_Fraction['SingletGate'], lightblue,
channels_A['FITC'] )
Blank_Fraction['Acceptor'] = BlankRegion

DonorRegion = CreateWholeRange( Donor_Fraction['SingletGate'], lightblue,
channels_A['FITC'] )
Donor_Fraction['Acceptor'] = DonorRegion

AcceptorRegion = CreateSGate( Acceptor_Fraction['SingletGate'], channels_A['FITC'],
channels_A['VioGreen'],
lightblue, "S2")
Acceptor_Fraction['Acceptor'] = AcceptorRegion

FRETRegion = CreateSGate( FRET_Fraction['SingletGate'], channels_A['FITC'],
channels_A['VioGreen'],
lightblue, "S2")
FRET_Fraction['Acceptor'] = FRETRegion

pv.setProgress(4)

#-----
# Gating on FRET
#-----
mDebug( 'log', 0, 'START Gating on FRET positive population.....' )

BlankRegion = CreateWholeRange( Blank_Fraction['SingletGate'], green,
channels_A['VioGreen'] )
Blank_Fraction['FRET'] = BlankRegion

DonorRegion = CreateWholeRange( Donor_Fraction['Donor'], green,
channels_A['VioGreen'] )
Donor_Fraction['FRET'] = DonorRegion

AcceptorRegion = CreateWholeRange( Acceptor_Fraction['SingletGate'], green,
channels_A['VioGreen'] )
Acceptor_Fraction['FRET'] = AcceptorRegion

FRETRegion = CreateWholeRange( FRET_Fraction['Donor'], green,
channels_A['VioGreen'] )
FRET_Fraction['FRET'] = FRETRegion

pv.setProgress(5)

return True,Fractions

```

```

else:
    FRET_Fraction = Fractions["VioGreen_FRET"]
    print 'GroupgateName', FRET_Fraction['GroupGateName']
    #-----
    # first run:pre-gating on target population
    #-----
    mDebug( 'log', 0, 'START pre-gating1 on target population.....' )

    Range_X = GetRange( FRET_Fraction['GroupGateName'], channels_A['VioBlue'], -1.25,
minPeak=64 )
    Range_Y = GetRange( FRET_Fraction['GroupGateName'], channels_A['FITC'], -1.25,
minPeak=64 )

    coords_Pre = basisGating._calculateCoordinates( Range_X, Range_Y )

    preGate = standardGating.applyPolygonGate( FRET_Fraction['GroupGateName'],
coords_Pre,
                                channels_A['VioBlue'], channels_A['FITC'], grey, "PreGate1" )
    FRET_Fraction['PreGate'] = preGate

    pv.setProgress(1)

    #-----
    #Gating on Target Population
    #-----
    mDebug( 'log', 0, 'START gating on target population.....' )

    scatterGate = CreateEllipseGate( FRET_Fraction['PreGate'],
FRET_Fraction['GroupGateName'],
                                channels_A['FSC'], channels_A['SSC'], purple, 'ScatterGate' )

    if scatterGate == None:
        raise em_utilities.AnalysisException( "Failed to create ScatterGate", Fractions )

    FRET_Fraction['ScatterGate'] = scatterGate
    copyGateToOtherFractions( Fractions, "VioGreen_FRET", scatterGate, "ScatterGate",
'GroupGateName' )

    pv.setProgress(2)

    #-----
    # Gating on SINGLETS
    #-----
    mDebug( 'log', 0, 'START gating on singlets.....' )

    singletGate = standardGating.calculateSingletGate( FRET_Fraction['ScatterGate'],
channels_A['FSC'],

```

```

                                channels_H['FSC'], 'SingletGate', darkblue )
if singletGate == None:
    raise em_utilities.AnalysisException( "Failed to create singletGate", Fractions )

FRET_Fraction['SingletGate'] = singletGate

copyGateToOtherFractions( Fractions, "VioGreen_FRET", singletGate, "SingletGate",
"ScatterGate" )

#-----
# Gating on DONOR: S1
#-----
mDebug( 'log', 0, 'START gating on donor positive population.....' )

FRETRegion = CreateSGate( FRET_Fraction['SingletGate'], channels_A['VioBlue'],
channels_A['VioGreen'], red, "S1")
FRET_Fraction['Donor'] = FRETRegion

pv.setProgress(3)

#-----
# Gating on ACCEPTOR
#-----
mDebug( 'log', 0, 'START gating on acceptor positive population.....' )

FRETRegion = CreateSGate( FRET_Fraction['SingletGate'], channels_A['FITC'],
channels_A['VioGreen'],
                        lightblue, "S2")
FRET_Fraction['Acceptor'] = FRETRegion

pv.setProgress(4)

#-----
# Gating on FRET
#-----
mDebug( 'log', 0, 'START Gating on FRET positive population.....' )

FRETRegion = CreateWholeRange( FRET_Fraction['Donor'], green,
channels_A['VioGreen'] )
FRET_Fraction['FRET'] = FRETRegion
pv.setProgress(5)

return True,Fractions

def __analyseFRET2( SampleName, pv, Fractions ):
```

```

Sample = App.sample( SampleName )
CoordsPreGate = Fractions['VioGreen_FRET']['PreGate'].points()
CoordsSingletGate = Fractions['VioGreen_FRET']['SingletGate'].points()

FRET_Fraction = {}
gateName = "Double positives"
Pop1 = standardGating.applyPolygonGate( Sample, CoordsPreGate, 'Donor', 'Acceptor',
grey, gateName )
FRET_Fraction[gateName] = Pop1

gateName = "Target Population"
Pop2 = CreateEllipseGate( Sample, Pop1, 'FSC-A', 'SSC-A', purple, gateName )

if Pop2==None:
    raise Exception( 'Failed to create TargetPopulation' )

FRET_Fraction[gateName] = Pop2

gateName = "Singlet Population"
Pop3 = standardGating.applyPolygonGate( Pop2, CoordsSingletGate, 'FSC-A', 'FSC-H',
darkblue, gateName )
FRET_Fraction[gateName] = Pop3

pv.setProgress( 8 )

Fractions['FRET'] = FRET_Fraction

return Fractions

#####
#####
#-----
# Gating-Helper Functions
#-----
def __retrieveFractions( sampleName ):
    allGroups = defaultGroups()
    mySample = App.sample( sampleName)
    groupInfo = mySample.groupInfo()
    print 'Groupinfo:', groupInfo
    # mDebug( 'log', 0, "groupInfo:",groupInfo )
    fractions = {}

print 'Bin hie kurz vor schleife'
try:
    grouplist = dict([(str(v), k) for k, v in groupInfo.items()])
    print grouplist
    groupstring = ''.join(grouplist)
    if True:

```

```

if groupstring.find('Blank') >= 1:
    print 'TRUE', groupstring
    for fk,fv in groupInfo.items():
        # mDebug( 'log', 0, "__retrieveFractions:", fk,fv )
        GroupNameFromSample =fv[1]
        for groupName in allGroups.values():
            if GroupNameFromSample== groupName:
                if GroupNameFromSample in fractions:
                    pass
                groupGateName = sampleName + '\\G'+str(fk)
                fractions[ GroupNameFromSample ] = { 'GroupNum' : fk, 'GroupGateName' :
App.sample(groupGateName) }
except:
    fractions[ 'VioGreen_FRET' ] = { 'GroupNum' : 1, 'GroupGateName' : mySample }
    print 'bin in else schleife'

print 'Bin wieder raus', fractions

return fractions

def _applyHistogramGate( ParentPop, Range, Channel, color ):
    # sample = App.sample( ParentPop )
    # print "applyHistogramGate:", Channel, Range
    region = ParentPop.createMarker( Channel,(int(Range[0]), int(256)), (int(Range[1]),
int(256)) )
    region.setRegionColor( color )
    return region

def copyGateToOtherFractions( fractions, targetFraction, targetSample, name, basename ):
    #-----
    # copy region to other fractions
    #-----
    for key,fraction in fractions.iteritems():
        if key == targetFraction:
            continue
        try:
            copyGateToFraction( fraction, targetSample, name, basename )
        except:
            raise em_utilities.AnalysisException( "Failed to link gate to %s" % (key), fractions )

def copyGateToFraction( fraction, targetSample, name, basename ):
    #-----
    # copy region to given fraction
    #-----
    BasePopulation = fraction[basename]
    #mDebug( 'log', 0, 'letzter Name von ', key, BaseRegionName )
    #mDebug( 'log', 0, basename, BasePopulation.name() )
    success = BasePopulation.linkToRegion( targetSample.region() )

```

```
if not success:
```

```
    raise Exception( "Failed to link gate to" )
```

```
NewRegionName = BasePopulation.subPopulations( False )[-1]
```

```
#mDebug( 'log', 0, NewRegionName )
```

```
fraction[name] = App.sample( NewRegionName )
```

```
def getPeakWithSDCorrection(Histogram, factor):
```

```
    Peak = Histogram.mean + Histogram.SD * factor
```

```
    return Peak
```

```
def CreateHistGate( ParentPop, color, Channel ):
```

```
    Range = GetSplit( ParentPop, Channel, -1.25, minPeak=64 )
```

```
    region = _applyHistogramGate( ParentPop, Range, Channel, color )
```

```
    return region
```

```
def GetRange( ParentPop, Channel, factor, minPeak=False ):
```

```
    print "GetRange called", Channel, factor
```

```
    Histogram = standardGating.PrepareHistogram( ParentPop, Channel )
```

```
    Histogram.calcStat()
```

```
    Peak = getPeakWithSDCorrection( Histogram, factor )
```

```
    Range = ( 2*Peak, 512 )
```

```
    return Range
```

```
def GetSplit( ParentPop, Channel, factor, minPeak=False ):
```

```
    Histogram = standardGating.PrepareHistogram( ParentPop, Channel )
```

```
    Histogram.calcStat()
```

```
    #Peak = 2 * getPeakWithSDCorrection( Histogram, factor )
```

```
    #Peak = 2* standardGating.CalculateSplit( Histogram )
```

```
    #print PEAK, 'Peak'
```

```
    minima = Histogram._getLocalMinima()
```

```
    if len(minima)>2 :
```

```
        Peak = Histogram._getOptimalSplit(3.5)
```

```
        if Peak != None:
```

```
            Peak = Peak[1]
```

```
            print Channel, ': OPTIMAL SPLIT'
```

```
        else:
```

```
            Peak = Histogram._getPossibleSplit(0, 0.5 )
```

```
            print Channel, ': POSSIBLE SPLIT'
```

```
    #~ if Peak > 240:
```

```
        #~ Peak = 2 * getPeakWithSDCorrection( Histogram, factor )
```

```
        #~ print 'PEAK WITH SD CORRECTION'
```

```

else:
    print Channel, ": No BiModal distribution!", factor
    Peak = getPeakWithSDCorrection( Histogram, factor )

Range = ( 2*Peak, 512 )

return Range

def CreateWholeRange( ParentPop, color, Channel ):
    # print "CreateWholeRange:", ParentPop, color, Channel
    Range = (1, 510)
    region = _applyHistogramGate( ParentPop, Range, Channel, color )
    return region

def CreateSGate( ParentPop, Channel1, Channel2, Color, Name="" ):
    region = CreateEllipseGate( ParentPop, ParentPop, Channel1, Channel2, Color, Name )
    return region

def CreateEllipseGate( TestPop, ParentPop, Channel1, Channel2, Color, Name="" ):

    __test = basisGating.py22DStatsSample( TestPop.name(), Channel1, Channel2 )

    if __test.isOK():
        coordinates = __test.ellipse(2)
        region = standardGating.applyEllipticGate( ParentPop, coordinates, Channel1, Channel2,
Color )
        if Name != "":
            region.setName( Name )
        return region

    return None

#-----
# ScripText Bausteine
#-----
def getStatisticScriptText( pop, topName, func, channel='FSC' ):
    #mDebug( 'log', 0, 'getStatisticScriptText:', topName, pop, func, channel )
    pop_desc = em_utilities.getPopScriptText( topName, pop )
    script_text_part = '%s.statistic("%s").%s()' % ( pop_desc, channel, func )
    return script_text_part

def makeScriptTextPart( part, precision ):
    if precision != "":
        precision = "%" + precision + " %"
    script_text = '$$' + precision + part + '$$'
    return script_text

```



```

def createTableHeader( title, columns, version=False):
    title_text = "<table cellspacing='-1' cellpadding='0'"
    title_text += "<tr align='left'"
    title_text += "<th><h3><u>%s</u></h3></th>" % title
    for i in xrange( 2, columns ):
        title_text += "<th></th>"
    if version:
        title_text += "<td align='right'>%s</td>" % version
    else:
        title_text += "<th></th>"
    title_text += "</tr>"

    title_text += em_utilities.html_emptyLine( columns )

    return title_text

def getMedianScriptTextParts( fraction, sampleName, channels_A ):
    median = {
        "Donor" : getStatisticScriptText( fraction['Donor'].name(), sampleName, 'median',
channels_A['VioBlue'] ),
        "Acceptor" : getStatisticScriptText( fraction['Acceptor'].name(), sampleName, 'median',
channels_A['FITC'] ),
        "FRET" : getStatisticScriptText( fraction['FRET'].name(), sampleName, 'median',
channels_A['VioGreen'] )
    }
    return median

def getIntensityScriptTexts( fraction, blank_fraction, sampleName, channels_A ):
    medians = getMedianScriptTextParts( fraction, sampleName, channels_A )
    median_blank = getMedianScriptTextParts( blank_fraction, sampleName, channels_A )
    intensity = {}
    for elm in ('Donor', 'Acceptor', 'FRET'):
        intensity[elm] = medians[elm] + '-' + median_blank[elm]
    return intensity

def getIntensityScriptTextsFRET( fraction, sampleName, channels_A ):
    medians = getMedianScriptTextParts( fraction, sampleName, channels_A )
    intensity = {}
#-----
    file = open("FRETintensityFile.cal", "r")
    contents = file.read()
    print "FRET FILE:", contents
    lastLine = contents.split("\n")[-2]
    finalstring = lastLine.replace("}" , "");
    #Splitting the string based on , we get key value pairs
    list = finalstring.split(",")
    print "List is:", list

```

```

ImportDict = {}
for elements in list:
    print "elements:", elements
    if ":" in elements:
        #Get Key Value pairs separately to store in dictionary
        keyvalue = elements.split(":")
        #Replacing the single quotes in the leading.
        m= keyvalue[0].strip('\')
        m = m.replace("\'", "'")
        ImportDict[m] = keyvalue[1].strip("\')

print ImportDict
file.close()

median_blank = {
    'Donor' : ImportDict["VioBlue"],
    'FRET': ImportDict["VioGreen"],
    'Acceptor': ImportDict["FITC"]}
print "median_blank", median_blank
#-----
for elm in ('Donor', 'Acceptor', 'FRET'):
    intensity[elm] = '( %s - %s)' %(medians[elm], median_blank[elm])

return intensity

def getCrossTalkScriptTexts( fractions, sampleName, channels_A ):

    crossTalk = {}
    Donor_Intensity = getIntensityScriptTexts( fractions['VioBlue_Donor'], fractions['Blank'],
sampleName, channels_A )
    crossTalk['S3m'] = '( %s ) / ( %s )' %( Donor_Intensity['Acceptor'],
Donor_Intensity['Donor'] )
    crossTalk['S1m'] = '( %s ) / ( %s )' %( Donor_Intensity['FRET'], Donor_Intensity['Donor'] )

    Acceptor_Intensity = getIntensityScriptTexts( fractions['FITC_Acceptor'], fractions['Blank'],
sampleName, channels_A )
    crossTalk['S2m'] = '( %s ) / ( %s )' %( Acceptor_Intensity['FRET'],
Acceptor_Intensity['Acceptor'] )
    crossTalk['S4m'] = '( %s ) / ( %s )' %( Acceptor_Intensity['Donor'],
Acceptor_Intensity['Acceptor'] )

    return crossTalk

def getCrossTalkScriptTextsFRET( fractions, sampleName, channels_A ):

    file = open("FRETintensityFile.cal", "r")
    contents = file.read()

```

```

lastLine = contents.split("\n")[-2]
finalstring = lastLine.replace("}", "");
#Splitting the string based on , we get key value pairs
list = finalstring.split(",")

ImportDict = {}
for elements in list:
    print "elements:", elements
    if "." in elements:
        keyvalue = elements.split(":")
        #Get Key Value pairs separately to store in dictionary
        #Replacing the single quotes in the leading.
        m= keyvalue[0].strip("\'")
        m = m.replace("\'", "")
        ImportDict[m] = keyvalue[1].strip("\'")
file.close()
# Crosstalk values
crossTalk = {}
crossTalk['S1m'] = float(ImportDict['S1m'])
crossTalk['S2m'] = float(ImportDict['S2m'])

return crossTalk

def getFinalScriptTexts( scripttext_dict, precision, extension=False ):
    for key,value in scripttext_dict.items():
        if extension:
            scripttext_dict[key] = "<#$$setvar( '%s', %s )$$>" % ( key, value )
            scripttext_dict[key] += "<#$$sample.createExtension('FRET').storeValue( '%s',
var['%s'] )$$>" % ( key, key )
            scripttext_dict[key] += makeScriptTextPart( "var['%s']" % ( key ), '.3f' )
        else:
            scripttext_dict[key] = makeScriptTextPart( value, precision )

    return scripttext_dict

def table_row( values ):
    """Return a table row"""
    line = "<tr align='left'>"
    for i, elm in enumerate(values) :
        if i<len(values)-1:
            line += "<td>%s</td>" % elm
        else:
            line += "<td align='right'>%s</td>" % elm
    line += "</tr>"
    return line

#-----

```

ScripText Tabellen

#-----

def createIntensitiesTable(sampleName, fractions, channels_A):

 resultTab = createTableHeader("Intensities (Median)", 4, version=em_version)

 resultTab += "<tr align='left'>" \

 "<th> Sample</th>" \

 "<th>Donor</th>" \

 "<th>Acceptor</th>" \

 "<th align='right'>FRET</th>" \

 "</tr>"

 resultTab += em_utilities.html_line(4)

 table_list = {

 "Unlabeled" : getFinalScriptTexts(getMedianScriptTextParts(fractions['Blank'], sampleName, channels_A), '.3f', extension=True),

 "Donor only" :

 getFinalScriptTexts(getMedianScriptTextParts(fractions['VioBlue_Donor'], sampleName, channels_A), '.3f'),

 "Acceptor only" :

 getFinalScriptTexts(getMedianScriptTextParts(fractions['FITC_Acceptor'], sampleName, channels_A), '.3f'),

 "FRET" :

 getFinalScriptTexts(getMedianScriptTextParts(fractions['VioGreen_FRET'], sampleName, channels_A), '.3f')

 }

 for name in ('Unlabeled', 'Donor only', 'Acceptor only', 'FRET'):

 entry = table_list[name]

 resultTab += table_row((name, entry['Donor'], entry['Acceptor'], entry['FRET']))

 resultTab += "</table>"

 return resultTab

def createIntensitiesTableFRET(sampleName, fractions, channels_A):

 resultTab = createTableHeader("Intensities (Median)", 4, version=em_version)

 resultTab += "<tr align='left'>" \

 "<th> Sample</th>" \

 "<th>Donor</th>" \

 "<th>Acceptor</th>" \

 "<th align='right'>FRET</th>" \

 "</tr>"

 resultTab += em_utilities.html_line(4)

 table_list = {

```

    "FRET"      :
getFinalScriptTexts( getMedianScriptTextParts( fractions['VioGreen_FRET'], sampleName,
channels_A ), '.3f' )
}

entry = table_list['FRET']
resultTab += table_row( ( 'FRET', entry['Donor'], entry['Acceptor'], entry['FRET'] ) )
resultTab += "</table>"
return resultTab

def createBackGroundTable( sampleName, fractions, channels_A ):

    columns = 4
    resultTab = createTableHeader( "Background subtraction", columns )
    resultTab += "<tr align='left'>" \
        "<th> Sample</th>" \
        "<th>Donor</th>" \
        "<th>Acceptor</th>" \
        "<th align='right'>FRET</th>" \
        "</tr>"
    resultTab += em_utilities.html_line( columns )

    table_list = {
        "Donor only" : getFinalScriptTexts( getIntensityScriptTexts( fractions['VioBlue_Donor'],
fractions['Blank'], sampleName, channels_A ), '.3f' ),
        "Acceptor only" : getFinalScriptTexts( getIntensityScriptTexts( fractions['FITC_Acceptor'],
fractions['Blank'], sampleName, channels_A ), '.3f' ),
        "FRET"      : getFinalScriptTexts( getIntensityScriptTexts( fractions['VioGreen_FRET'],
fractions['Blank'], sampleName, channels_A ), '.3f' ),
    }

    for name in ('Donor only', 'Acceptor only', 'FRET'):
        entry = table_list[name]
        resultTab += table_row( ( name, entry['Donor'], entry['Acceptor'], entry['FRET'] ) )

    resultTab += '</table>'

    return resultTab

def createResultsTableFRET( sampleName, fractions, alphaFactor, channels_A ):

    FRET_Intensity = getIntensityScriptTextsFRET( fractions['VioGreen_FRET'], sampleName,
channels_A )
    crossTalk      = getCrossTalkScriptTextsFRET( fractions, sampleName, channels_A )

    stepFRET = '( %s - ( %s )*( %s ) - ( %s )*( %s ) ) / ( %s )' %(
        FRET_Intensity['FRET'], FRET_Intensity['Donor'], crossTalk['S1m'],
        FRET_Intensity['Acceptor'], crossTalk['S2m'], FRET_Intensity['Donor']

```

)

```

A_FRET = '( %s ) / %f ' %( stepFRET, alphaFactor)
FRETE = '( %s ) / ( 1 + %s )' %( A_FRET, A_FRET )
FRETE = makeScriptTextPart( FRETE, '.3f' )
columns = 2
resultTab = createTableHeader( "Results", columns )
resultTab += "<tr align='left'>" \
    "<th></th>" \
    "<th align='right'>Value</th></tr>"
resultTab += em_utilities.html_line( columns )

alphaFactor = '%.3f' % alphaFactor
resultTab += table_row( ('alpha factor', alphaFactor) )
resultTab += em_utilities.html_emptyLine( columns )
resultTab += table_row( ("FRET efficiency median", FRETE ) )
resultTab += "</table>"

return resultTab

```

```
def createExportFRET( sampleName, fractions, alphaFactor, channels_A ):
```

```

#-----
file = open("FRETintensityFile.cal", "r")
contents = file.read()
lastLine = contents.split("\n")[-2]
finalstring = lastLine.replace("}" , "");
#Splitting the string based on , we get key value pairs
list = finalstring.split(",")
ImportDict = {}
for elements in list:
    print "elements:", elements
    if ":" in elements:
        keyvalue = elements.split(":")
        m= keyvalue[0].strip("\")
        m = m.replace("\", ")
        ImportDict[m] = keyvalue[1].strip("\")
print ImportDict
file.close()

median_blankExp = {
    'Donor' : float(ImportDict["VioBlue"]),
    'FRET': float(ImportDict["VioGreen"]),
    'Acceptor': float(ImportDict["FITC"])}

#-----
mediansExp = {}
mediansExp['Donor'] = fractions['VioGreen_FRET']['Donor'].statistic("V1-A").median()

```

```

mediansExp['Acceptor'] = fractions['VioGreen_FRET']['Acceptor'].statistic("B1-A").median()
mediansExp['FRET'] = fractions['VioGreen_FRET']['FRET'].statistic("V2-A").median()
intensityExp = {}
for elm in ('Donor', 'Acceptor', 'FRET'):
    intensityExp[elm] = (mediansExp[elm] - median_blankExp[elm])

#-----
crossTalk    = getCrossTalkScriptTextsFRET( fractions, sampleName, channels_A )

stepFRETEExp = (intensityExp['FRET'] - intensityExp['Donor'] * crossTalk['S1m'] -
    intensityExp['Acceptor'] * crossTalk['S2m']) / intensityExp['Donor']

A_FRETEExp = stepFRETEExp / float(alphaFactor)
FRETEExp = A_FRETEExp / ( 1 + A_FRETEExp )
print 'FRET for export:', FRETEExp
FRETE = "%.3f" % FRETEExp

Sample = App.sample( sampleName )
Extension = Sample.createExtension("FRET")
Extension.storeValue("FRETE", FRETE )
return u' '

def createCrosstalkTable( sampleName, fractions, channels_A ):

    columns = 2
    resultTab = createTableHeader( "Cross Talk", columns )
    resultTab += "<tr align='left'>" \
        "<th></th>" \
        "<th align='right'>Value</th>" \
        "</tr>"
    resultTab += em_utilities.html_line( columns )

    crossTalkParts = getCrossTalkScriptTexts( fractions, sampleName, channels_A )
    crossTalk = getFinalScriptTexts( crossTalkParts, '.3f', extension=True )

    for name in ('S1m', 'S3m', 'S2m', 'S4m'):
        entry = crossTalk[name]
        resultTab += table_row( ( name, entry ) )

    resultTab += "</table>"

    return resultTab

def createResultsTable( sampleName, fractions, alphaFactor, channels_A ):

    FRET_Intensity = getIntensityScriptTexts( fractions['VioGreen_FRET'], fractions['Blank'],
sampleName, channels_A )
    crossTalk    = getCrossTalkScriptTexts( fractions, sampleName, channels_A )

```

```

stepFRET = '( %s - ( %s )*( %s ) - ( %s )*( %s ) ) / ( %s )' %(
    FRET_Intensity['FRET'], FRET_Intensity['Donor'], crossTalk['S1m'],
    FRET_Intensity['Acceptor'], crossTalk['S2m'], FRET_Intensity['Donor']
)
A_FRET = '( %s ) / %f ' %( stepFRET, alphaFactor)
FRETE = '( %s ) / ( 1 + %s )' %( A_FRET, A_FRET )
FRETE = makeScriptTextPart( FRETE, '.3f' )

#TODO: write FRETE in extension
Sample = App.sample( sampleName )
Extension = Sample.createExtension("FRET")
Extension.storeValue("FRETE", FRETE )

columns = 2
resultTab = createTableHeader( "Results", columns )
resultTab += "<tr align='left'>" \
    "<th></th>" \
    "<th align='right'>Value</th></tr>"
resultTab += em_utilities.html_line( columns )

alphaFactor = '%.3f' % alphaFactor
resultTab += table_row( ('alpha factor', alphaFactor) )
resultTab += em_utilities.html_emptyLine( columns )
resultTab += table_row( ("FRET efficiency median", FRETE ) )

resultTab += "</table>"

return resultTab

def createMedianTable( sampleName, fraction, channels_A ):

    columns = 2
    resultTab = createTableHeader( "Median Intensities", columns )
    resultTab += "<tr align='left'>" \
        "<th>Population</th>" \
        "<th align='right'>Median</th>" \
        "</tr>"
    resultTab += em_utilities.html_line( columns )

    medians = getFinalScriptTexts( getMedianScriptTextParts( fraction, sampleName,
channels_A ), '.3f' )

    for entry in ('Donor', 'Acceptor', 'FRET'):
        resultTab += table_row( (entry, medians[entry]) )

    resultTab += "</table>"

```



```

return resultTab

#####
#####
#-----
# Main interface to analyse data from app
#-----
def viewPage( SampleName ):
    analyseSample( SampleName )

def analyseSample( SampleName ):
    def createPage( SampleName, PageType, alpha, __Fractions, FractionName=None ):
        PageManager = basisEasyPageManager.singleton( )
        Page = PageManager.appendPage( PageType, ( SampleName, alpha, __Fractions,
FractionName ) )
        Page.showPage( )

    mDebug( 'log', 0, 'analyse ...' )

    pv = em_utilities.cfgProgView('Analyzing data...','FRET_MultiSample', 8)

    # Create Gating
    try:
        success, Fractions = __analyseFRET( SampleName, pv )
        mDebug( 'log', 0, "Done Analysis:", success )

    except em_utilities.AnalysisException, e:
        mDebug( 'log', 0, "Error while analyzing %s %s ..." %( SampleName, e.message ) )
        mDebug( 'log', 0, str(e.message) )
        import traceback
        traceback.print_exc()
        Fractions = e.createdGates
        success = False

    except Exception, e:
        mDebug( 'log', 0, 'Error while analyzing %s %s ...'%( SampleName, e ) )
        mDebug( 'log', 0, str(e) )
        import traceback
        traceback.print_exc()
        success = False
        Fractions = {}

    if success == False:

        em_utilities.hideProgView( )
        Script.critical("FRET analysis error", "Failed to analyse data %s ..." %( SampleName ) )

    else:

```

try:

```
Sample = App.sample( SampleName )
channels_A = em_utilities.get_channelNames( "A", channel_list, Sample )
channels_H = em_utilities.get_channelNames( "H", channel_list, Sample )

# Get alpha
# Create Pages
# keylist: List with predefined order containing all possible Fractions
keylist = [ 'Blank', 'VioBlue_Donor', 'FITC_Acceptor', 'VioGreen_FRET' ]
for key in keylist:
    if key not in Fractions.keys(): keylist.remove( key )
# mDebug( 'log', 0, 'sortierte Liste der gemessenen Fraktionen', keylist )

if 'Blank' in keylist:

    print'BLANK is in fraction, running controls'

    alpha = getAlphaFromDescription( Sample )
    mDebug( 'log', 0, "Found alpha:", alpha )

    for fractionName in keylist:
        createPage( SampleName, FRETAnalysePage1, alpha, Fractions, fractionName )

    createPage( SampleName, FRETAnalysePage2, alpha, Fractions )
    createPage( SampleName, FRETAnalysePage3, alpha, Fractions )

    pv.setProgress( 6 )

    # Create new mqd file with FRET-Channel
    Extension = Sample.createExtension("FRET")
    Extension.storeValue("alpha factor", alpha )
    # Extension.storeValue("Fractions", str(Fractions))
    FretSample = CreateFretEfficiencySampleFile( SampleName, Fractions, channels_A,
channels_H )
    pv.setProgress( 7 )

    Fractions = __analyseFRET2( FretSample, pv, Fractions )
    createPage( FretSample, FRETAnalysePage4, alpha, Fractions, 'FRET' )

else:
    print 'FRET Sample only'

    alpha = getAlphaFromCSV( Sample )
    mDebug( 'log', 0, "Found alpha:", alpha )
    createPage( SampleName, FRETAnalysePageFRETOnly, alpha, Fractions )
    pv.setProgress( 6 )
```

```

    em_utilities.hideProgView( )

except Exception, e:
    em_utilities.hideProgView()
    mDebug( 'log', 0, e )
    import traceback
    traceback.print_exc()

def analyseSamplePS( SampleName):
    #variabels = ["SampleID", "Param1", "Param2", "Param3"]
    # wenn nur eine variable:
    variabels = ["FRET Efficiency", "Calib-Date"]
    sample = App.sample( SampleName )
    Ext = sample.createExtension("FRET")
    FRETE = Ext.getValue("FRETE")

    file = open("FRETintensityFile.cal", "r")
    contents = file.read()
    print "FRET FILE:", contents
    lastLine = contents.split("\n")[-2]
    finalstring = lastLine.replace("}" , "");
    #Splitting the string based on , we get key value pairs
    list = finalstring.split(",")
    print "List is:", list

    ImportDict = {}
    for elements in list:
        print "elements:", elements
        if ":" in elements:
            #Get Key Value pairs separately to store in dictionary
            keyvalue = elements.split(":", 1)
            #Replacing the single quotes in the leading.
            m= keyvalue[0].strip("\'")
            m = m.replace("\'", "")
            ImportDict[m] = keyvalue[1].strip("\'")
    file.close()
    CalibTime = ImportDict['time']
    #FRETE = 12

    values = [FRETE, CalibTime ]
    status = True

    return status, variabels, values

#-----

```

```

# Functions for FRET-Calculation
#-----
def getAlphaFromDescription( sample ):
    description = sample.description( sample.DescriptionPatient )

    alpha = 0.2 # default value for alpha
    # this will be used, in case it cannot be determined from the description

    description = description.replace( ",", "." )
    try:
        alpha = float( description )
    except:
        re_pattern = '(?i)alpha *=* *([0-9]+[.]?[0-9]*)'
        m = re.search( re_pattern, description )
        if m:
            alpha = float( m.group( 1 ) )
    return alpha

def getAlphaFromCSV( sample ):

    alpha = 0.3533 # default value for alpha

    file = open("FRETintensityFile.cal", "r")
    contents = file.read()
    print "FRET FILE:", contents
    lastLine = contents.split("\n")[-2]
    finalstring = lastLine.replace("}" , "");
    #Splitting the string based on , we get key value pairs
    list = finalstring.split(",")
    print "List is:", list

    ImportDict ={}
    for elements in list:
        print "elements:", elements
        if ":" in elements:
            #Get Key Value pairs separately to store in dictionary
            keyvalue = elements.split(":")
            #Replacing the single quotes in the leading.
            m= keyvalue[0].strip("\'")
            m = m.replace("\'", "")
            ImportDict[m] = keyvalue[1].strip("\'")
    file.close()
    alpha = float(ImportDict['alphaFactor'])
    return alpha

def CreateFretEfficiencySampleFile( SampleName, Fractions, channels_A, channels_H ):

    # Check, if to be created file is already loaded

```

```

# unload first, to avoid problems at overwriting it
NewSampleName = SampleName + 'FRET'
sample = App.sample( NewSampleName )
if sample:
    if App.isAnalysisMode():
        App.setAnalysisMode( False )
        App.removeSample( sample )

sample = App.sample(SampleName)
sampleFileName = sample.filename()
dataDir = os.path.dirname( sampleFileName )
FRET_FileName = dataDir + '\\ ' + NewSampleName + '.mqd'

#START calculate new FRET file by cell analysis file

# Get stored values from Extension of analyzed file
Ext = sample.createExtension("FRET")

# Background Values in all FRET channels
BG = {
    'VioBlue': Ext.getValue("Donor"),
    'VioGreen': Ext.getValue("FRET"),
    'FITC': Ext.getValue("Acceptor")
}
# Crosstalk values
S1m = Ext.getValue("S1m")
S2m = Ext.getValue("S2m")

#TODO: maybe write CSV here with all data
#test in print
#possibly easier than single values
print 'BG values---:', BG

alphaFactor = Ext.getValue("alpha factor")
file = open("FRETIntensityFile.cal", "a")
#sep = ";"
sep = ","
file.write("time:" + str(time.ctime()) + sep)

myList = []
myList2 = []
myList.append(BG)
valueDict = {}
valueDict["S1m"] = S1m
valueDict["S2m"] = S2m
valueDict["alphaFactor"] = alphaFactor
myList2.append(valueDict)

```

```

for entry in myList:
    myLine = ""
    for key,value in entry.items():
        myLine += ("""+ key + "":")
        myLine += (str(value)+sep)
file.write(myLine)

for entry2 in myList2:
    myLine2 = ""
    for key,value in entry2.items():
        # myLine2 += (key + sep)
        #myLine2 += (str(value)+sep)
        myLine2 += ("""+ key + "":")
        myLine2 += (str(value)+sep)
file.write(myLine2)
file.write("\n")
file.close()

# Set New Features for FRET_Analyse
Features = mq.Features(0)

Features.appendFeature( SetFeature( "FRET-Efficiency", "FRET",    "FRET-Efficiency",
150.0, 0.0, 100.0, mq.Feature.Linear, mq.Feature.Linear) )
Features.appendFeature( SetFeature( "FSC-A",    "FSC-A",    "FSC-A",    1000.0,
0.0, 1000.0, mq.Feature.Linear, mq.Feature.Linear) )
Features.appendFeature( SetFeature( "SSC-A",    "SSC-A",    "SSC-A",    1000.0,
0.0, 1000.0, mq.Feature.Linear, mq.Feature.Linear) )
Features.appendFeature( SetFeature( "FSC-H",    "FSC-H",    "FSC-H",    1000.0,
0.0, 1000.0, mq.Feature.Linear, mq.Feature.Linear) )
Features.appendFeature( SetFeature( "VioBlue-A", "Donor",    "VioBlue-A",
1000.0, 0.01, 1000.0, mq.Feature.Linear, mq.Feature.Logarithmic ) )
Features.appendFeature( SetFeature( "FITC-A",    "Acceptor", "FITC-A",    1000.0,
0.01, 1000.0, mq.Feature.Linear, mq.Feature.Logarithmic ) )
Features.appendFeature( SetFeature( "VioGreen-A", "FRETchannel", "VioGreen-A",
1000.0, 0.01, 1000.0, mq.Feature.Linear, mq.Feature.Logarithmic ) )

FRET_fraction = Fractions['VioGreen_FRET']['GroupGateName']
group_count = FRET_fraction.eventCount()

# create new mqdFile with additional channels for FRET calculations
FRET_File = mq.MqdWriter()
if not FRET_File.create( FRET_FileName, Features, group_count ):
    raise Exception( "Failed to create destination file" )

# get old mqdFileInfo, in order to retrieve meta info to store to new file
filename = sample.filename()
OldFileInfo = mq.MqdFileInfo( filename )

```

```

channelLookup = createChannelLookup( OldFileInfo )

for event_index in xrange( group_count ):
    event = CalcFretEfficiency( event_index, channelLookup, BG, S1m, S2m, alphaFactor,
FRET_fraction, channels_A, channels_H )
    FRET_File.append( event )

# retrieve remaining stuff from old file and finalize it
FRET_File.setDeviceSettings( OldFileInfo.deviceSettings() )
FRET_File.setViewPage( OldFileInfo.viewPage() )
FRET_File.setExtension( OldFileInfo.extension() )
FRET_File.finalize()

if not App.load( FRET_FileName ):
    raise Exception( "Failed to load destination file" )

return NewSampleName

def CalcFretEfficiency( event_index, channelLookup, BG, S1m, S2m, alphaFactor,
FRET_fraction, channels_A, channels_H ):
    # get Background corrected event-values for VioBlue, VioGreen and FITC parameter:
    newValues = {}
    for channelName in ( 'VioBlue', 'VioGreen', 'FITC' ):
        LookUp = channelLookup[ channels_A[ channelName ] ]
        param_index = LookUp['index']
        old_value = FRET_fraction.value( event_index, param_index )
        newValues[ channelName ] = old_value * LookUp['scaleMax'] - BG[channelName]
    #TDODO: write CSV with channel LookUp
    # print values
    #use param_index se in print results

    #Calculation of FRET efficiency
    stepFRET = ( newValues['VioGreen'] - newValues['VioBlue'] * S1m - newValues['FITC'] *
S2m ) / newValues['VioBlue']
    A_FRET = stepFRET / alphaFactor
    fretEff = A_FRET / ( 1 + A_FRET )

    # re-Normalize corrected Fluorescence-values
    VioBlue = newValues['VioBlue'] / channelLookup[ channels_A['VioBlue'] ]['scaleMax']
    FITC = newValues['FITC'] / channelLookup[ channels_A['FITC'] ]['scaleMax']
    VioGreen = newValues['VioGreen'] / channelLookup[ channels_A['VioGreen'] ]['scaleMax']

    # get event Index for Scatter Parameter:
    # Index_SSC = channelLookup[ channels['SSC'] ]['index']
    # Index_FSC = channelLookup[ channels['FSC'] ]['index']
    for channelName in ( 'SSC', 'FSC' ):
        LookUp = channelLookup[ channels_A[channelName] ]

```

```

newValues[ channelName ] = FRET_fraction.value( event_index, LookUp['index'] )

LookUp = channelLookUp[ channels_H['FSC'] ]
newValues[ 'FSC-H' ] = FRET_fraction.value( event_index, LookUp['index'] )

# return new event
return fretEff, newValues['FSC'], newValues['SSC'], newValues['FSC-H'], VioBlue, FITC,
VioGreen

def SetFeature( userDefName, name, param, maxRange, minScale, maxScale, RangeType,
ScaleType ):
    #mDebug( 'log', 0, "setFeature: ", userDefName )
    Feature = mq.Feature()
    Feature.setUserdefName( userDefName )
    Feature.setBaseInfo( name, param, 0, 4 )
    Feature.setDataRange(0.0, maxRange, RangeType )
    Feature.setScale(minScale, maxScale, ScaleType )
    Feature.setFactor(1.0)
    Feature.setGain(100)
    return Feature

def createChannelLookup( OldFile ):
    eventsize = OldFile.features().count()
    channelLookUp = {}
    for i in xrange( 1, eventsize ):
        feature = OldFile.features().feature( i )
        channelLookUp[ feature.name() ] = { 'index' : i, 'scaleMax' : feature.scaleMax() }
    return channelLookUp

#-----
# Main interface to get a acquisition page
#-----
def getAcqPage( ):
    PageManager = basisEasyPageManager.singleton( )
    Page = PageManager.appendPage( FRETAcquisitionPage )
    Page.showPage( )

def getAcqProcObject( ):
    return FRETExpressProzessor( )

class FRETExpressProzessor( basisExpressMode.ExpressProzessor ):
    def __init__( self ):
        basisExpressMode.ExpressProzessor.__init__( self )

    def prolog( self ):
        # get current IS
        IS = mq.getCurrentInstrumentSettings()

```



```

# copy and store for restoring after measurement
self.mCurInstSetting = mq.deepCopyInstrumentSetting( IS )
# this is necessary, so that epilog can be done, even though prolog was not finished
properly

# check for FL7 instrument; and stop here; EM Analysis needs VioGreen channel and
thus
# is not compatible to FL7 instruments
if IS.profileName()[0] == "FL7":
    self.setState( basisExpressMode.CSTATE.ERROR )
    message = "Expressmode " + em_name + " not compatible with your
Instrument.<BR>"
    message += "You need a MQ10 or VYB instrument to run this expressmode."
    Script.showMessage( em_name, "<H3 align=center >" + message + "</H3>",
( "Abort", ) )
    return

# set fluorescence channels to 'log5'
for channel in IS.channels():
    if channel.isFluorescence():
        IS.channel( channel.name() ).setMode( 'log5' )

IS.enableCompensation( False )

# enable modified IS
mq.takeInstrumentSettingsAsCurrent( IS )

basisExpressMode.ExpressProzessor.prolog( self )

def epilog( self ):
    # reset IS to settings as found in prolog
    mq.takeInstrumentSettingsAsCurrent( self.mCurInstSetting )
    return basisExpressMode.ExpressProzessor.epilog( self )

#####
#####
#-----
# Main call
#-----
def run( ):

    FileName = Script.getOpenFileName( "", "Open FRET_MultiSample-file for analysis",
"*.mqd", "*.mqd" )
    if FileName != "" and FileName != None:
        em_utilities.loadFCSFile( FileName )
        Temp = FileName.strip(".mqd").split("/")
        Sample = Temp[-1]

```

```
analyseSample( Sample )  
  
# for sn in samples...  
  
def pause( ):  
    pass  
  
def stop( ):  
    pass
```

9.2 The FRET Express Mode Post Paser Script

```
import os
import time
from expressModes import basisEasyPage
from expressModes import basisGating
from expressModes import basisEasyPageTemplate
from expressModes import basisEasyPageManager
from expressModes.app.mq.express.Analysis import FRETexportData_testloops
import utilities
import basisCalibration
import mq
from profiles import hardware as hardwareProfiles

from __main__ import App
from __main__ import Script
from __main__ import Config

def run():
    print "Test"

    inputPath =
"C:/Users/kerstinv/Desktop/BerlinToAnalyze/P161202A1P4013/P161202A1P4013_"
    files = []
    date = "_2016-12-05.0001.mqd"
    letterlist = ["A", "B", "C", "D", "E", "F", "G", "H", "I", "J", "K", "L", "M", "N", "O", "P"]
    letterlistControls = ["E", "F"]
    # for i in xrange(3,19,1): #Files from 1 to 6
    #     number =str(i)
    #     #print number
    #     longNumber = ""
    #     for j in xrange(4-len(number)):
    #         longNumber += "0"
    #     longNumber +=number
    #     #print longNumber
    #     file = inputPath+longNumber+".mqd"
    #     files.append(file)
    #     print 'File:', file

    for x in letterlist:
        for y in xrange (21,23):
            number =str(y)

            #     newNumber = number
            print x, number
            file = inputPath + x + number + date
```

```

files.append(file)
print 'File:', file

#print files

header = "Results from analysis using EM 'FRET'\n\n"
header += "SampleName\tSampleID\tDescription\tStartTime\tEventCount\tStatus"

lines = ""

firstSample = True

for sample in files:

    sampleName = sample.split("/")[-1][0:-4]
    print "post processing of:", sampleName

    # Apply express-mode to sample
    Sample = App.sample( sampleName )
    ExpInfo = Sample.experiment()
    if ExpInfo == None:
        ExpInfo = "None"
    print "Exp Info:", ExpInfo
    FileInfo = mq.MqdFileInfo( Sample.filename() )
    features = FileInfo.features()

    StartTime      = GetStartTimeText( features )
    DescriptionOfSample = mq.ISampleExperimentInfo.description( ExpInfo )[0]
    SampleID       = ".join(mq.ISampleExperimentInfo.sampleId( ExpInfo )[0])
    EventCount     = str(Sample.eventCount())

    FRETEXportData_testloops.analyseSample(sampleName)
    status, variables, values = FRETEXportData_testloops.analyseSamplePS(sampleName)

    if firstSample:
        # Open output-file
        outputPath = "C:/Users/kerstinv/Desktop/ExportFiles_"
        fullPath = outputPath + sampleName + "_FRET" + ".csv"
        file = open(fullPath, "w")

        # Complete header
        for variable in variables:
            header += "\t" + str(variable)
        header += "\n"

    firstSample = False

```

```
# Create single line
line = sampleName
line += "\t" + SampleID
line += "\t" + DescriptionOfSample
line += "\t" + StartTime
line += "\t" + EventCount

line += "\t" + str(status)
for value in values:
    line += "\t" + str(value)
line += "\n"

# Transfer single line to all lines
lines += line
print lines

file.write(header)
file.write(lines)
file.close()
print 'file is written'
```



```
def GetStartTimeText( features ):
    return features.startDate() + " " + features.startTime()
```